



Open Sea Operating Experience to Reduce Wave Energy Costs

Deliverable D5.3

Uncertainty in Wave Energy Converter Power Performance Assessment

Lead Beneficiary	TECNALIA
Delivery date	2019-05-30
Dissemination level	Public
Status	Approved
Version	1.0
Keywords	Uncertainty, Yield prediction, Short time scale assessment, Power matrix dimensionality, LCOE



This project has received funding from the European Union's Horizon 2020 research and innovation programme under grant agreement No 654444

Disclaimer

This Deliverable reflects only the author's views and the Agency is not responsible for any use that may be made of the information contained therein

Document Information

Grant Agreement Number	654444
Project Acronym	OPERA
Work Package	WP5
Task(s)	T5.3, T5.4
Deliverable	D5.3
Title	Uncertainty in Wave Energy Converter Power Performance Assessment
Author(s)	Joannès Berque (TECNALIA), Pablo Ruiz Minguela (TECNALIA), David Crooks (UEDIN), Florent Thiebaud (UCC).
File Name	OPERA_D5.3_Uncertainty in WEC power performance assessment_TECNALIA_20190529_v1.2.docx

Change Record

Revision	Date	Description	Reviewer
0.1	11/12/2018	Initial outline	WP5 partners
0.2	14/03/2019	Partial draft	WP5 partners
0.5	20/05/2019	First complete draft	UEDIN, UCC
0.9	28/05/2019	Final draft for peer-review	Pablo Ruiz-Minguela
1.0	30/05/2019	Final version for EC	EC

EXECUTIVE SUMMARY

The Horizon 2020 OPERA Project greatly increased the set of open-sea operating data publicly available for wave energy research and development. This document reports on the application of the Technical Specifications (TS) of the International Electrotechnical Commission (IEC) to open-sea data collected in the project. Emphasis is on practical implication for Wave Energy Converter (WEC) developers and experts working with the IEC technical specifications or other normative processes.

Some of the most relevant findings may be summarised as follows.

- The IEC-TS provided a highly valuable coherent framework for the analysis of open-sea performance data in OPERA
- The evaluation of uncertainty as per IEC-TS/62600-100 and IEC-TS/62600-102 is one aspect where users identify a need for more guidance in the TS
- While more data would be needed to confirm, there are indications that an additional dimension of spectral bandwidth may increase accuracy of yield prediction at a second site at least in some cases
- The use of performance data in samples shorter than the 20 minutes required in the TS may be highly valuable to make best use of expensive at-sea test time. However, certain issues such as sample variability must be checked in detail
- More data is needed to provide reliable recommendations on yield prediction for scaled prototypes

TABLE OF CONTENTS

EXECUTIVE SUMMARY	3
TABLE OF CONTENTS	4
LIST OF FIGURES	6
LIST OF TABLES	8
ABBREVIATIONS, ACRONYMS AND SYMBOLS.....	9
1. INTRODUCTION	10
2. UNCERTAINTIES IN YIELD PREDICTION FROM APPLYING TS100 IN OPERA OPEN-SEA CAMPAIGNS.....	12
2.1 Overview of TS100 methodology and application	12
2.2 review of uncertainty components and methodology	14
2.3 Challenges and uncertainties in the application of TS100	16
2.4 Issues for consideration by the IEC group of experts	17
3. UNCERTAINTIES IN WAVE ENERGY CONVERTER YIELD PREDICTION AT A PROSPECTIVE DEPLOYMENT SITE.....	18
3.1 TS102 Procedure	18
3.1.1 TS102 guidance on description of WEC	19
3.1.2 TS102 guidance on description of deployment sites	20
3.1.3 TS102 guidance on Presentation of power performance information recorded at location 1.....	29
3.1.4 TS102 guidance on mapping information from location 1 to location 2 and an evaluation of spectral bandwidth as an additional matrix dimension	32
3.1.5 Additional aspects covered in TS102	41
3.2 Discussion on the application of TS102 and uncertainty	42
3.3 Implications for LCOE modelling and business case development.....	44
3.4 Recommendations for TC114.....	45
4. PERFORMANCE ASSESSMENT USING SHORT SAMPLES	46
4.1 SUMMARY AND MAIN RESULTS	46
4.2 INTRODUCTION AND OBJECTIVES	48
4.2.1 potential interest of power assessment at finer time-scales	48
4.2.2 Technical issues with power assessment at FINER time-scales.....	50

4.3 MEASUREMENTS AVAILABLE	50
4.3.1 Bimep	51
4.3.2 Mutriku.....	51
4.4 PROPAGATION TIME FROM PRESSURE SENSOR TO OWC CHAMBERS.....	54
4.4.1 Propagation time from linear wave theory	54
4.4.2 Propagation time from time-lagged cross correlation	55
4.4.3 Manual identification of individual wave signals.....	56
4.5 WAVE STATISTICS FOR RECORDS OF LESS THAN 20 MINUTES	59
4.5.1 Spectral significant wave height	60
4.5.2 Energy period	63
4.5.3 Scatter diagrams obtained	66
4.5.4 Significance of differences in scatter diagrams obtained	70
4.6 PLANT OPERATING DATA WITH SHORT SAMPLES	71
4.7 POWER MATRICES.....	73
4.8 IMPACT ON ENERGY PRODUCTION ESTIMATES.....	75
4.9 SAMPLE DURATION AND DISPERSION IN PERFORMANCE DATA.....	80
4.9.1 Mutriku data	80
4.9.2 Bimep data	83
4.10 SAMPLE DURATION AND TESTING TIME NEEDED.....	83
4.11 CAUSES OF THE HIGH SCATTER IN PERFORMANCE DATA	87
4.11.1 Effect of tides	88
4.11.2 Effect of variation of wave height and period across a cell	89
4.11.3 Capture length matrix and reduction in intra-cell variability	91
4.11.4 Example of detail of intra-cell variability	93
4.12 SUMMARY AND PRACTICAL IMPLICATIONS.....	96
4.12.1 issues of potential interest to the IEC group of experts	96
4.12.2 Summary for WEC developers	97
5. YIELD PREDICTION FOR SCALED PROTOTYPES FROM OPEN-SEA TESTING.....	100
6. REFERENCES	102

LIST OF FIGURES

Figure 1: IDOM's MARMOK-A5 device deployed at BiMEP	19
Figure 2: WEC mooring arrangement [3]	20
Figure 3: Chart of the BiMEP site [5]	22
Figure 4: Diagram of EMEC's wave test sites [6]	22
Figure 5: BiMEP directional Rose plot	23
Figure 6: EMEC directional rose plot	23
Figure 7: BiMEP scatter diagram (corresponding to power measurements)	24
Figure 8: EMEC scatter diagram	25
Figure 9: Comparison of BiMEP and EMEC resource, presentation of available data and applicable complementation methods	26
Figure 10: BiMEP and EMEC Probability of exceedance	27
Figure 11: BiMEP Joint probability distribution	28
Figure 12: EMEC joint probability distribution	28
Figure 13: WEC (CA 1) mean normalised Electrical power matrix (percentage of overall power from each sea state)	30
Figure 14: WEC (CA 1) Mean normalised CL matrix - scaled for presentation	30
Figure 15: WEC (CA 1) Max normalised CL MATRIX - SCALED FOR PRESENTATION	31
Figure 16: WEC (CA 1) Min normalised CL matrix - scaled for presentation	31
Figure 17: WEC (CA 1) Standard deviation CL matrix - scaled for presentation	31
Figure 18: WEC (CA 1) number of recordings	32
Figure 19: Normalised capture length plotted against each of the bandwidth parameter tested for fixed H_{m0} (0.5 M to 1.0 M) and T_E (7 s to 8 s)	35
Figure 20: Normalised capture length plotted against ϵ_0 for fixed H_{m0} (0.5 M to 1.0 M) and T_E (7 s to 8 s)	36
Figure 21: Diagram of increasing dimensionality of capture length matrix	37
Figure 22: Percentage of normalised power with the bandwidth ranges for fixed H_{m0} (0.5 m to 1.0 m) and T_e (7 s to 8 s) and number of sea states represented in each bandwidth range	37
Figure 23: Percentage of all sea states recorded within presented bandwidths	38
Figure 24: BiMEP - CA1 – Annual Energy content of different bandwidth ranges and comparison of MAEP calculated when considering bandwidth with conventional MAEP method	38
Figure 25: BiMEP - CA2 – Annual Energy content of different bandwidth ranges and comparison of MAEP calculated when considering bandwidth with conventional MAEP method	39
Figure 26: EMEC - CA1 – Annual Energy content of different bandwidth ranges and comparison of MAEP calculated when considering bandwidth with conventional MAEP method	39

Figure 27: EMEC - CA2 – Annual Energy content of different bandwidth ranges and comparison of MAEP calculated when considering bandwidth with conventional MAEP method.....	40
Figure 28: Indidcation of bin mismatch and average normalised power for bandwidth ranges (WEC operating at EMEC under CA1).....	40
Figure 29: Sensitivity spider plot for LCOE [13].....	45
Figure 30: An example of high peak to average power output at mutriku	49
Figure 31: position of the wave instrument upwave the plant	52
Figure 32: a view of the seabed near the pressure sensor upwave of mutriku (From: CDA)..	53
Figure 33: Bathymetry upwave the mutriku plant.....	55
Figure 34: Time-lagged cross correlations between wave signal and plant operating data ...	57
Figure 35: Example of matching wave data to plant data	58
Figure 36: Other example of matching of wave and plant data	59
Figure 37: H_{m0} vs. $H_{1/3}$ for 1-hour and 5-minute samples	61
Figure 38: Time series of significant heights for various sample durations.....	62
Figure 39: Example of resolution problem with 16 DOF spectra in short samples	64
Figure 40: Energy period obtained for the record and zoom on end March	65
Figure 41: Energy period vs. mean upcrossing period of third of highest waves	66
Figure 42: Time series of turbine 13 power output averaged over various sample durations	72
Figure 43: Time series of power output for the storm and mean regime cells	86
Figure 44: Convergence in mean with the number of samples	87
Figure 45: Convergence to the mean when requiring one-hour spacing	88
Figure 46: Tidal height and Turbine 13 power for the storm and mean regime cells	89
Figure 47: Effect of change in H_{m0} across one cell on turbine 13 output	90
Figure 48: Correlation of mean power to zero-upcrossing period within the storm cell	91
Figure 49: Wave and plant data for energetic storm cell sample.....	94
Figure 50: Wave and plant data for low energy storm cell sample	95

LIST OF TABLES

Table 1: Scatter diagram of hourly sea-states at pressure sensor.....	67
Table 2: Scatter diagram of 5-minutes sea-states (8 DOF)	67
Table 3: Scatter diagram from the BiMEP reference buoy	67
Table 4: scatter diagram of 5-minute sea-states at sensor (16DOF)	68
Table 5: scatter diagram of 30 minutes sea-states at sensor	69
Table 6: Scatter diagram of 15-minutes sea-states at sensor.....	69
Table 7: Scatter diagram of 10-minute sea-states at sensor	69
Table 8: relative difference between the 1-hour and 5-minute scatter diagrams	70
Table 9: Relative differences of scatter diagram of 3-hourly and hourly sea-states.....	71
Table 10: Relative differences of scatter diagrams of half-hourly and hourly sea-states	71
Table 11: 1-hour samples power matrix	74
Table 12: 5-minute samples power matrix	74
Table 13: 30-minute samples power matrix	76
Table 14: 15-minute samples power matrix	76
Table 15: 10-minute samples power matrix	76
Table 16: Energy production (MWh) with the 1-hour power matrix and scatter diagram	77
Table 17: Energy production from the 5-minute power matrix and scatter diagram	77
Table 18: Energy production in BiMEP using power matrix of 1-hour samples	78
Table 19: Energy production in BiMEP with power matrix of 5-minute samples.....	78
Table 20: AEP (MWh) with 1-hour power matrix and 5-minute scatter diagram	79
Table 21: Standard deviation over mean value for cells of the 1-hour power matrix	81
Table 22: Ratio of samples standard deviations, 5-minute to 1-hour matrix.....	81
Table 23: rms error on cells of 1-hour power matrix if normally distributed.....	82
Table 24: ratio of rms error on mean of 5-min to 1-hour power matrices.....	82
Table 25: 1-hour samples Standard deviations over mean value, ocean tec marmok	84
Table 26: Marmok, Ratio of 20-minute over 1-hour samples standard deviation	84
Table 27: Marmok, ratio of 3-hour to 1-hour samples standard deviations	84
Table 28: Turbine 13 output normalised by deepwater energy flux (5-minute samples).....	93
Table 29: ratio of standard deviation to that in power matrix cells, 5-minute samples	93

ABBREVIATIONS, ACRONYMS AND SYMBOLS

AEP	Annual Energy Production.
BiMEP	Biscay Marine Energy Platform, a test and operating site for floating Wave Energy Converters and other ocean energy-related studies.
CDA	Commercial Diving Activity, a Bilbao-based marine contractor.
EMEC	European Marine Energy Centre, a test and operating site for marine energy.
EVE	Ente Vasco de Energía.
H_s	Significant wave height.
IEC	International Electrotechnical Commission. IEC is active in advancing technical specifications and standards for wave energy.
OWC	Oscillating Water Column.
T_e	Energy period.
WEC	Wave Energy Converter.
WP	Work Package, usually referring to work packages of H2020 OPERA.

1. INTRODUCTION

Uncertainty on the power performance of WECs greatly limits financing opportunities for projects and increases cost of capital for existing ones. One of the central objectives of at-sea testing of a Wave Energy Converter (WEC) is to demonstrably assess power performance, along with real operating costs, to facilitate the evaluation of further project opportunities with a particular type of device. This performance assessment is a basic input to evaluate potential revenues and cost of energy for wave energy.

At-sea testing is expensive. In addition to the cost of engineering and manufacturing a seaworthy prototype, the testing itself includes berth renting, installation, maintenance and decommissioning and may well cost developers about the same order as the prototype itself. For this reason, financing at-sea testing has been and remains a central challenge for many promising concepts of WEC. Open-sea testing must therefore be used as effectively as possible to assess power performance.

This deliverable reports on the experience gained in the H2020 OPERA project on power performance assessment using new open-sea operating data. The report is formatted to facilitate the sharing of experience with developers planning open-sea testing or post-processing available data. Also, it reports experience of relevance to technical specifications of power performance for WECs. In particular: IEC-TS/62600-100, on power performance assessment, and IEC-TS/62600-102, on yield prediction in a second location.

Section 2 reports considerations on uncertainty in WEC power performance assessment using the methodology in IEC-TS/62600-100. This includes experience from the OPERA and other projects.

Section 3 reports on the application of IEC-TS/62600-102 to the particular case of using open-sea testing results from the BiMEP site in the Bay of Biscay to evaluate power production at EMEC in the North of Scotland. Site conditions at the two locations are analysed and differences identified which may most impact the evaluation of power production at EMEC from BiMEP at-sea testing data. The applicability and gains in yield prediction from adding dimensions (in addition to H_s and T_e) to the power matrix or tensor is analysed in detail in the case of various metrics of spectral bandwidth. A discussion is also provided on how these uncertainties may impact the cost of energy and business case for WEC project.

Section 4 reports an assessment of how using shorter samples of open-sea performance data may yield more accurate estimates of power production. The conditions under which this can be the case, and some of the technical issues that emerge when using samples shorter than the 20 minutes recommended by IEC/TS62600-100 are identified. The analysis focusses on performance data from the Mutriku commercial wave power plant in the Basque Country, Spain. There appears to be important potential benefits in using shorter samples of power

performance, in terms of increasing the number of samples and the area of the (H_s , T_e) space that is explored. Defining meaningful wave statistics shorter than 20 minutes and decorrelating successive short samples are some of the key issues that must be addressed. Some methods that appear to work for this particular dataset are proposed. Besides, some points of potential interest to the IEC Group of Experts working on technical specifications relating to power performance assessment of WECs are proposed.

Finally, Section 5 discusses the prediction of yield for scaled prototypes. General aspects and limitations to commonly used scaling laws are discussed.

2. UNCERTAINTIES IN YIELD PREDICTION FROM APPLYING TS100 IN OPERA OPEN-SEA CAMPAIGNS

This section analyses uncertainty in the WEC yield prediction from applying TS100 recommendations based on the results from OPERA sea trials and performance analysis carried out in the project. It includes comments on TS100 methodology on uncertainty analysis and suggestions to improve power performance assessment.

2.1 Overview of TS100 methodology and application

In TS100, uncertainty analysis is mentioned in two locations:

- TS100 - Section 7.4. Metocean Data. This section is about wave data only and refers to a list of wave parameters in TS100 - Section 5.2.1.
- TS100 - Annex C, Evaluation of Uncertainty. This annex mainly describes the various parameters to be taken into account.

A more detailed review of these sections is provided below.

TS100 - Section 7.4. Metocean Data:

- Measure and record all parameters believed to have an influence on power production
- Awareness of any correlation between power and a specific parameter should be sought and reported. It shall be recorded and calculated
- List included in 5.2.1
 - Spectral shape
 - Directionality of waves
 - Directional frequency spectrum
 - Water depth including tidal effect
 - Tidal and marine current, direction and velocity
 - Wind speed and direction
 - Density of water
 - Occurrence and thickness of ice
- Minimum requirement: H_{m0} , T_e and wave energy flux (J) shall be calculated using the measured wave data.
- The accuracy of the calculated parameters shall be given, according to the uncertainty estimation defined by ISO/IEC Guide 98-1 and ISO/IEC Guide 98-3
- Directly measured parameters will be expressed with indication of absolute error. Specifications on the type, location, calibration, and accuracy of the measurement instrument shall be given.

TS100 - Annex C, Evaluation of Uncertainty:

Two types of uncertainty categories, all expressed as standard deviations and are denoted standard uncertainty:

- A: the magnitude of which can be deduced from measurements
- B: estimated by other means

Uncertainty analysis:

- Power matrix, determined by the measured and normalised values of electrical power production and sea state parameters, and the estimate annual energy production.
- As a minimum, H_s and T_e shall be considered as measurands. Uncertainties in measurements are converted to uncertainties in these measurands by means of sensitivity factors
- Table C.1. contains a minimum list of uncertainty components that shall be included in the uncertainty analysis.
- Where category A uncertainties are used, the measurement and analysis methods shall be described.
- Where category B uncertainties are used, the means by which the standard deviation has been determined shall be described

Table C.1 – List of uncertainty components

Measured/model parameter	Uncertainty component	Uncertainty category ^a
Significant wave height	Wave measuring instrument/model calibration	B
	Influence of moorings and/or other local effects on WMI	B
	Data acquisition system (e.g. sampling rate, windowing)	B
	Directional spectral analysis	B
	Variability of significant wave height	A
Energy period	Wave measuring instrument/model calibration	B
	Influence of moorings and/or other local effects on WMI	B
	Data acquisition system (e.g. sampling rate, windowing)	B
	Directional spectral analysis	B
	Strength of marine currents	B
	Variability of energy period	A
Wave power density	Water depth	A / B
	Water density	A / B
Electrical power	Current transformers	B
	Voltage transformers	B
	Power transducer or power measurement device	B
	Data acquisition system	B
	Variability of electrical power	A
^a according to ISO/IEC Guide 98-1:2009 and ISO/IEC Guide 98-3:2008.		

2.2 REVIEW OF UNCERTAINTY COMPONENTS AND METHODOLOGY

Energy yield prediction in TS100 is based on the scatter diagram at the WEC location, using H_s and T_e inputs, corresponding wave energy flux and the average electrical power of the device at the centre of each bins of the scatter diagram. While this method is commonly used, there are significant uncertainties in its application including measurement of H_s and T_e but also due to variations observed in the WEC electrical power capture length for similar values of H_s and T_e . This is acknowledged in TS100 and was review in the OPERA project, which also includes the analysis of other parameters influencing the power matrix and energy yield

It is therefore understood that uncertainty in power performance assessment of WEC and energy yield is difficult to assess fully for all types of device. It is influenced by several parameters; some are still being investigated in research projects. This section comments uncertainty components described in TS100 and suggests additional parameters with discussions and results from work carried out in the OPERA project. Table ?? comments on the

TS100 uncertainty components:

Measured / model parameter	Uncertainty component	Comments
Significant wave height (Hs) And Energy Period (Te)	Wave measuring instrument/model calibration	Pre-calibration required and uncertainty parameters to be used in this analysis should be described in TS100
	Influence of mooring and/or other local effects on WMI	Difficult to assess, this cannot be done before deployment and no standard method is defined in TS100.
	Data acquisition system (e.g Sampling rate, windowing)	A minimum of 1Hz is mentioned in TS100 but there is no information on suggested uncertainty when this condition is fulfilled.
	Directional spectral analysis	This does not affect the Hs or Tp at a given location but may affect the WEC performance. It should be in the "Measured parameter" list when required
	Variability of significant wave height and energy period	TS100 should include a description of how this influences the estimation of Hs or Te.
Wave energy density	Water depth	This can be measured to a high level of accuracy and is used in the calculation of energy density but there is no information on how to estimate its impact on uncertainty
	Water density	This can be measured or estimated to a high level of accuracy and is used in the calculation of energy density but there is no information on how to estimate its impact on uncertainty
Electrical power	Current Transformer	When power is measured at the grid connection point, as recommended in TS100, this is not relevant
	Voltage transformer	When power is measured at the grid connection point, as recommended in TS100, this is not relevant
	Power transducer or power measurement device	Pre-calibration required
	Data acquisition system	Pre-calibration required to estimate uncertainty
	Variability of electrical power	Need explanation on how this affects the power time series

As mentioned in table ??? significant information is missing in order to assess uncertainty of the measured parameters. This includes details on the uncertainty components, how

uncertainty should be assessed for each component and how this affects uncertainty of the measured parameter. Additional components could be useful:

- Significant wave height and energy period:
 - o Transferring data from the location of measurement to the location of the WEC
- Wave energy density:
 - o H_s and T_e should be mentioned in the list of uncertainty components.
- Electrical power:
 - o No suggestion

These three measured parameters are used to determine the wave scatter diagram, capture length matrix and the power matrix of a specific WEC at a given location. While this is a common practice, there is ongoing discussions and research on this method accuracy as this is neglecting important factors that can affect the WEC performance. TS100 does not discuss this point and only recommends calculating the standard deviation of the capture length in each cell. Analysis carried out in the OPERA project show large variability of the intra-cell capture length.

TS100 does not mention year to year variation in the wave scatter diagram. It recommends the use of at least 10 years of data which in some cases is not possible and does not define uncertainty based on this data.

2.3 Challenges and uncertainties in the application of TS100

All information found in the document merely provides a list of parameters and suggest expressing results in standard deviation. There is no detail or discussion on how to assess uncertainty which are necessary to ensure all project carries out a similar analysis.

Two references are mentioned, ISO/IEC Guide 98-1 and ISO/IEC Guide 98-3. Relevant information from those documents should be summarised in TS100.

Based on work carried out in the OPERA project, large uncertainties were highlighted in the power performance results and energy yield when calculated using the TS100 methodology and it is unclear how to handle this uncertainty on a standardised method. Several parameters were highlighted, spectral shape, wave data, sample duration, moorings, etc. and uncertainties 10-20 % on some results were observed. This shows the importance to improve power performance characterisation in the future, following future research studies and publications

2.4 Issues for consideration by the IEC group of experts

There is no section dedicated on uncertainty analysis in TS100, therefore a review of the document structure on uncertainty of power performance results and energy yield is recommended. In the core part of the document, this is mentioned in section 7.4 for wave parameters only. More details are provided in Annex C which includes all uncertainty parameters, up to power performance and energy yield. It is suggested to introduce uncertainty either in other relevant sections or in one new section for all type of measurements and calculations carried out following TS100.

3. UNCERTAINTIES IN WAVE ENERGY CONVERTER YIELD PREDICTION AT A PROSPECTIVE DEPLOYMENT SITE

This section reports on the inherent uncertainty that remains when applying IEC TS 62600-102 [1] (TS102) to estimate the performance of a WEC at a prospective deployment site. The observations presented in this section relate to T5.4 of the H2020 project: Improvement of yield prediction modelling at multiple sites, and scales. T5.4 brings together resource information provided by IDOM and EMEC.

TS102 is part of the *Marine energy - Wave, tidal and other water current converters* series and entitled *Part 102: Wave energy converter power performance assessment at a second location using measured assessment data*. It presents a method of estimating the power performance of a Wave Energy Converter (WEC) at a second location (location 2) based on power performance measurements recorded at a primary location (location 1). It is expected that the power performance measurements recorded at the original site should be carried out in accordance with IEC TS 62600-100:100 (TS100) [2].

This section outlines the steps of the TS102 procedure and an application of that procedure (Section 3.1), a discussion on its implementation (Section 3.2) the implementations of TS102 for LCOE analysis and business case development (Section 3.3) and recommendations for IEC TS114 (Section 3.4).

3.1 TS102 PROCEDURE

This section outlines an application of TS 102 based on information gathered during the OPERA project, namely: normalised power performance measurements recorded at the Biscay Marine Energy Platform S. A. (BiMEP, location 1) along with the corresponding sea state measurements and sea state measurements recorded at and by European Marine Energy Centre (EMEC, location 2).

TS102 discretizes its methodology into eleven steps. Steps 1 to 11 are summarised in sections 0 to 3.1.5 (*italicised in grey*) along with a presentation of the application based on the information gathered in the OPERA project. Sections 0 to 3.1.5 present: how the WEC(s) under investigation should be described; how locations 1 and 2 should be assessed; how WEC power performance at location 1 should be presented; aspects related to mapping data from location 1 to location 2, including an investigation to higher matrix dimensions and; additional aspects covered by TS102 but not covered in this application.

3.1.1 TS102 GUIDANCE ON DESCRIPTION OF WEC

1. *Describe the WEC under investigation (that which has been deployed at the primary location and which will be deployed at the second location):*
 - a. *Operational principle,*
 - b. *Geometry and dimensions,*
 - c. *Mass properties,*
 - d. *PTO system and*
 - e. *Mooring arrangement.*

Comment based on present application

The WEC under investigation is IDOM's MARMOK-A-5 WEC, see Figure 1. It is a point absorber with an Oscillating Water Column (OWC) Power Take-Off (PTO) [3]. The WEC is a spar buoy type design and has a diameter of 5 m where it pierces the water's surface. The buoy is scaled in diameter relative to the planned commercial device. The WEC has a draft of 35 m, this is not scaled relative to the planned commercial device. The device tested during the OPERA project has a generating capacity roughly 1/10th of the planned commercial device.



FIGURE 1: IDOM'S MARMOK-A5 DEVICE DEPLOYED AT BIMEP

During the OPERA project, the WEC was deployed at the BiMEP (location 1) on two separate occasions. The data recorded and used in this study was obtained during the first deployment of the device. During that deployment, the WEC was fitted with a Wells turbine for a PTO and the mooring arrangement was in the form of a square around the device, see Figure 2. During the second deployment, a number of innovations were tested to determine how they impacted the device's Levelised Cost of Energy (LCOE), namely: an improved WEC control program, a bi-radial turbine instead of the Wells turbine and an elastomeric tether, replacing the conventional mooring lines in the original mooring arrangement. The impact these innovations have on LCOE will be reported in a further OPERA deliverable - D7.3 Tracking metrics for wave energy technology performance.

3.1.2 TS102 GUIDANCE ON DESCRIPTION OF DEPLOYMENT SITES

2. *Assess the characteristics of the study's two wave resources (Analysis of the wave resources should be based on IEC TS 62600-101 [4] (TS101)).*
 - a. *Prepare a site description according to section 6 of TS101,*
 - b. *Present maps,*
 - c. *Geometric coordinates,*
 - d. *Water depths,*
 - e. *General descriptions of:*
 - i. *Shoreline geometry and bathymetry,*
 - ii. *Prevailing wave and wind conditions and*
 - iii. *Typical tidal range and currents.*
 - f. *Directional rose plots,*

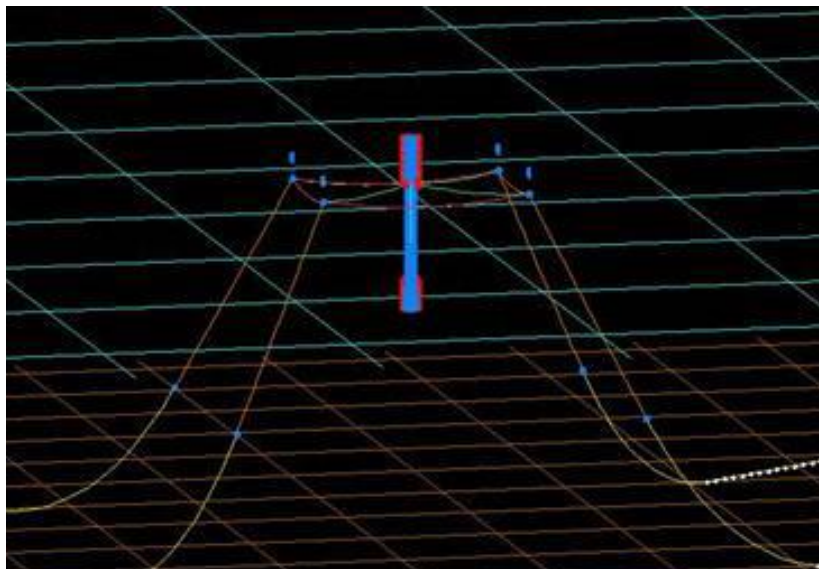


FIGURE 2: WEC MOORING ARRANGEMENT [3]

- g. Scatter tables and plots,*
 - h. Exceedance and persistence plots and*
 - i. Joint probability analysis tables.*
 - 3. Undertake a quality assurance study on the new capture length matrix for application at location 2.*
 - a. Label empty bins as 'undefined.'*
 - b. Label bins in which the data is known to be inaccurate as 'underpopulated,' or if there are less than 3 data records.*

Comment based on present application

As stated, the two wave resources used for this application of TS102 are BiMEP, the deployment location of the MARMOK-A-5 WEC, and EMEC at Orkney. Both locations are test areas for WECs. Figure 3 is a chart showing the WEC test areas at BiMEP and Figure 4 is a diagram showing the wave test sites at EMEC.

A formal application of TS102 would require a site description to be prepared according to TS101. Such a description would include details on site: area, bathymetry, wave resource and wind resource. A site description of this detail is deemed not necessary for this application of TS102 since the purpose is to evaluate TS102 and not for the actual deployment of the WEC at a prospective location. However, it should be noted that the parameters that TS101 recommends will impact on the power performance of a WEC.

Further general details that TS102 requests in a formal application but are not required for this review include descriptions of shoreline geography, bathymetry, prevailing wind conditions and typical tidal information. As highlighted in the preceding paragraph, these parameters will have an impact on WEC power performance, however they are not the focus of this review.

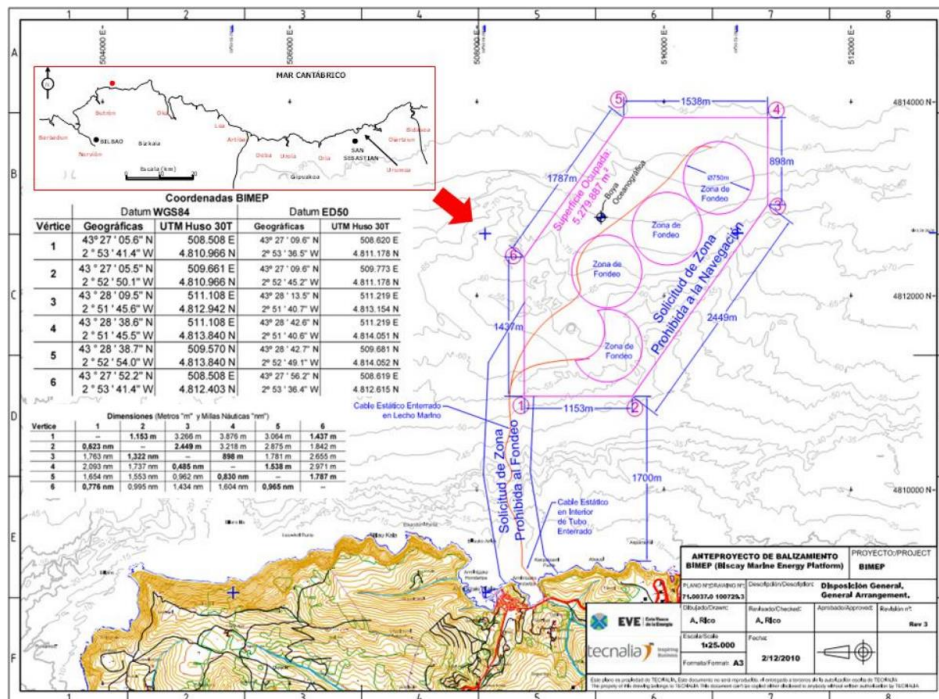


FIGURE 3: CHART OF THE BIMEP SITE [5]

WAVE TEST SITE

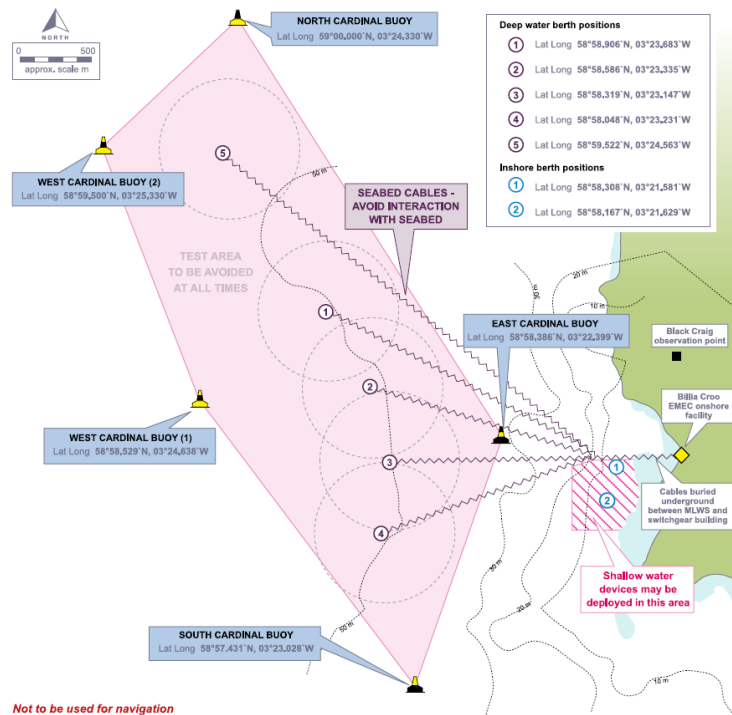


FIGURE 4: DIAGRAM OF EMEC'S WAVE TEST SITES [6]

Figure 5 and Figure 6 are directional rose plots indicating the mean direction of oncoming sea states to the Wave Measurements Instruments (WMIs) at BiMEP and EMEC respectively. Figure 5 indicates that the majority of sea states approach the BiMEP WMI from the North West with fewer sea states approaching from the West and North of the site. Figure 6 indicates that the majority of sea states approach the EMEC WMI from the West with sea states also approaching the WMI from the North West and North.

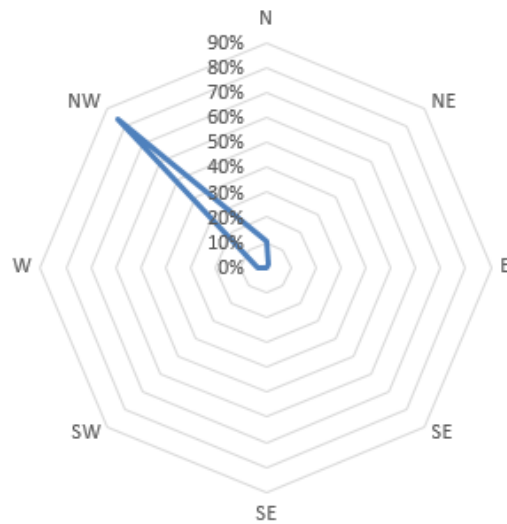


FIGURE 5: BIMEP DIRECTIONAL ROSE PLOT

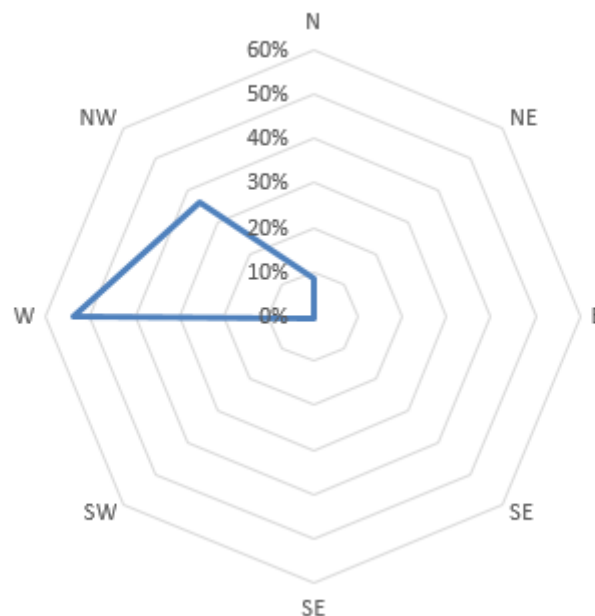


FIGURE 6: EMEC DIRECTIONAL ROSE PLOT

Figure 7 and Figure 8 are the BiMEP and EMEC scatter diagrams and tables respectively. These are discretised by H_{m0} and T_e as in other TSs in the 62600 wave series. H_{m0} bins have a range

of 0.5 m and the numbers presented alongside the vertical axes of the scatter, joint probability distribution, normalised power and Capture Length (CL) matrices and diagrams are the midpoints of the ranges. T_e bins have a range of 1 s and the numbers presented alongside the horizontal axis of the aforementioned matrices and diagrams are the midpoints of the ranges.

Note, the scatter diagram presented in Figure 7 reflects the sea states that were recorded during periods of power measurement. The numbers in each *bin* indicate the number of sea states that occurred with H_{m0} and T_e characteristics that fell within the ranges associated with that bin. The data presented in Figure 7 was recorded during a period that spanned from the beginning of March to the end of June 2017. Although there are limitations associated with using such a limited data set, it is sufficient for this analysis of TS102. The data presented in Figure 8 represents a recording period spanning from January 2015 to December 2017.

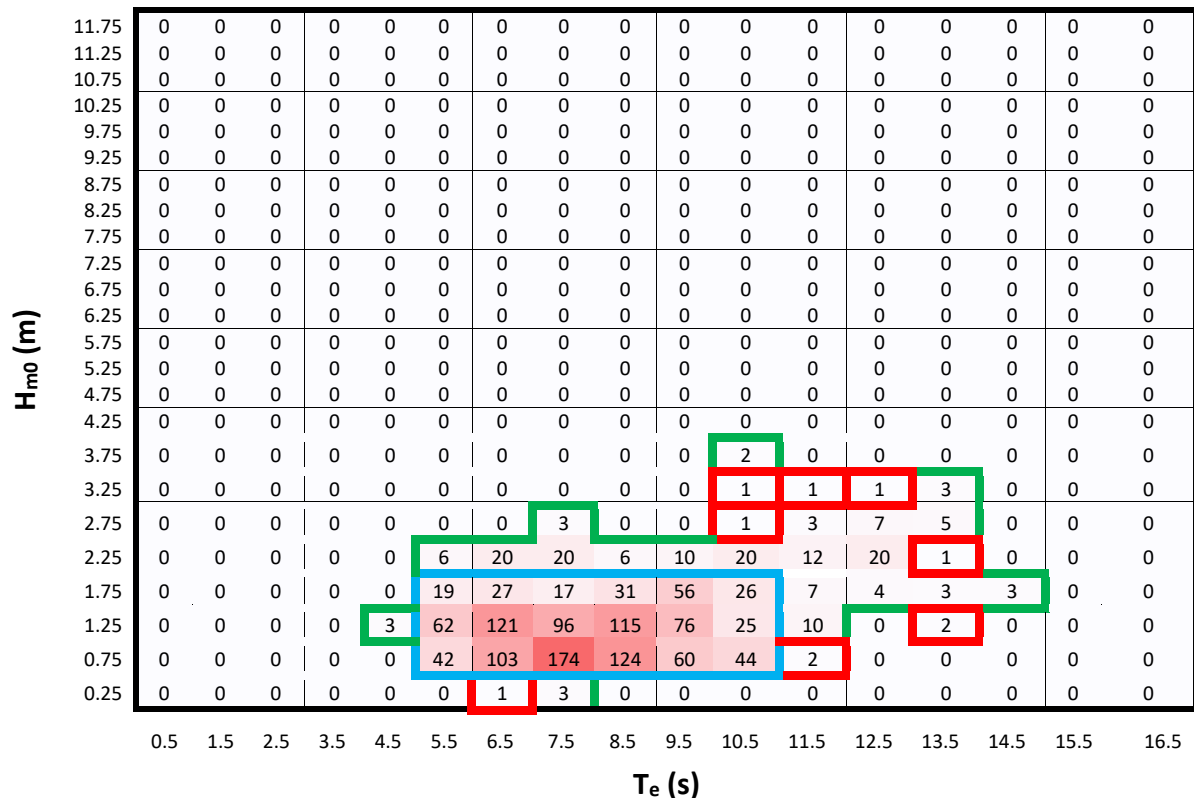


FIGURE 7: BIMEP SCATTER DIAGRAM (CORRESPONDING TO POWER MEASUREMENTS)

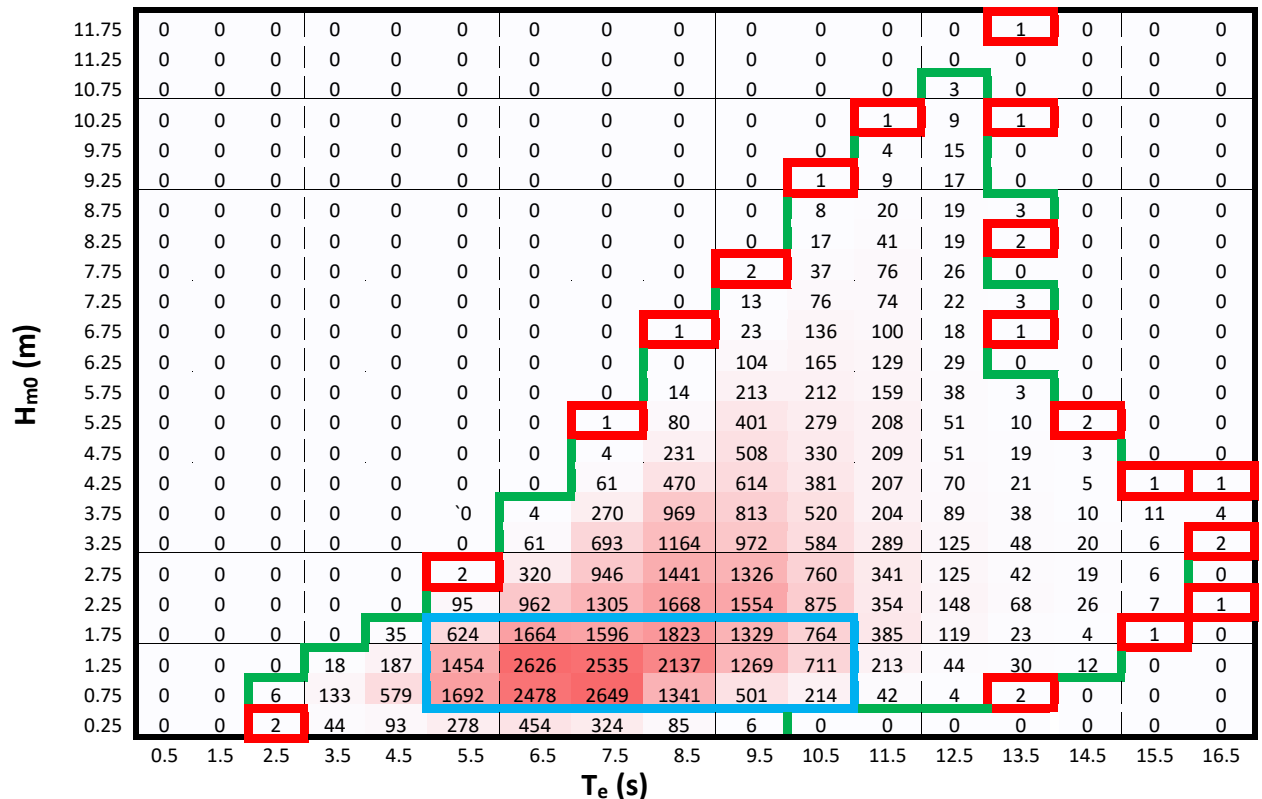


FIGURE 8: EMEC SCATTER DIAGRAM

In both Figure 7 and Figure 8, the green border surrounds the area within which sea states were recorded. The red border surrounds cells in which less than 3 sea states were recorded, TS 102 indicates that these cells have to be identified and listed as ‘underpopulated.’ Cells with zero recordings within an area of interest, such as a device’s operating envelope, need to be identified and listed as ‘undefined.’ Underpopulated and undefined cells need to be filled with complimentary data from either data fitting or numerical or physical modelling.

Defining the cells as either underpopulated or undefined is part of the quality assurance step of the TS 102 procedure.

Figure 9 is the EMEC scatter diagram but with different regions highlighted for explanation. The blue shaded cells indicate the overlap of the BiMEP scatter diagram (associated with the power measurements) with the EMEC diagram. The orange border indicates a theoretical MARMOK-A-5 operating envelope. The green and yellow shaded cells indicate the bins, either underpopulated or undefined, for which complimentary data would need to be generated to represent how the MARMOK-A-5 device would behave at EMEC. The green shaded cells are those for which data fitting techniques, either interpolation or extrapolation, could be used.

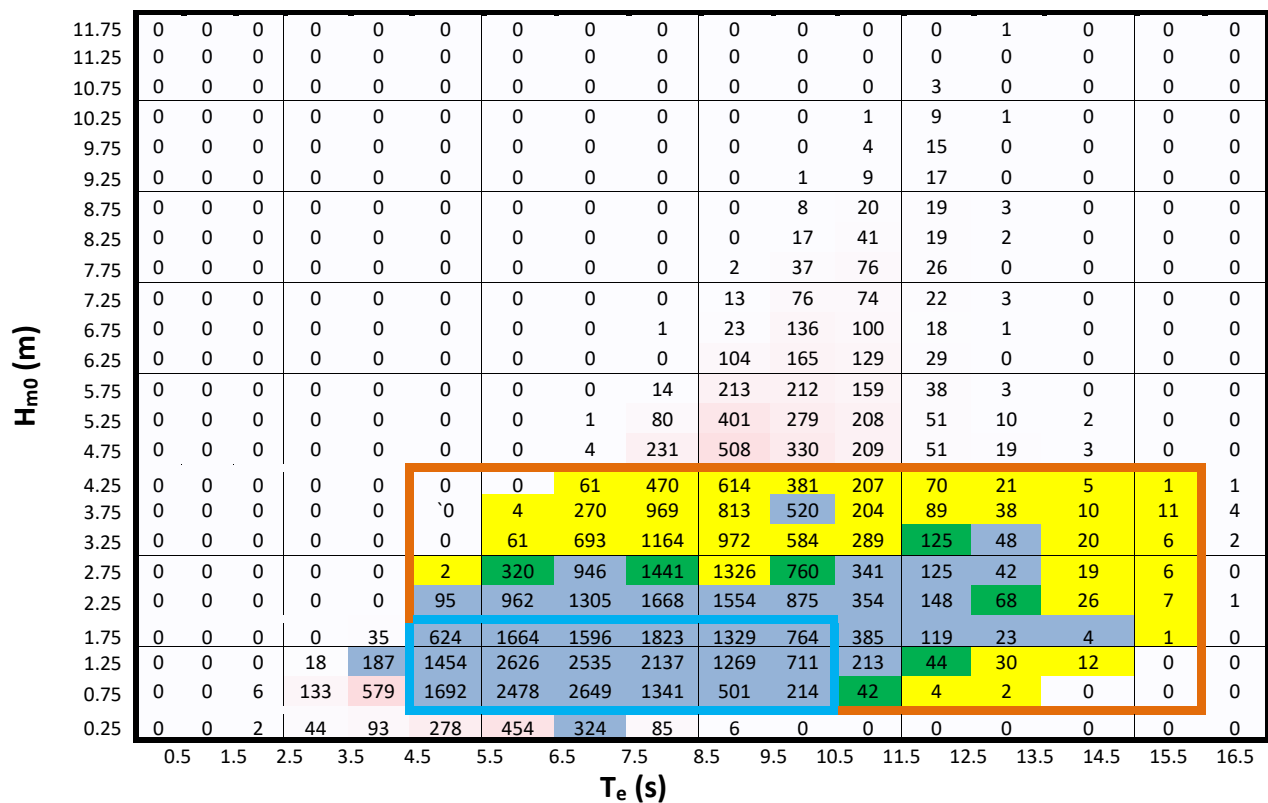


FIGURE 9: COMPARISON OF BIMEP AND EMEC RESOURCE, PRESENTATION OF AVAILABLE DATA AND APPLICABLE COMPLEMENTATION METHODS

The yellow shaded cells are those which would require either physical or numerical data. Since physical or numerical data isn't available, a smaller pseudo operating envelope was selected for the purpose of applying TS102. This smaller operating envelope isn't a true operating envelope of the MARMOK-A-5 device. The smaller operating envelope is identified in the scatter, joint probability distribution (Figure 11 and Figure 12), normalised power (Figure 13) and CL diagrams/figures (Figure 14 to Figure 18) by a light blue border. The smaller operating envelope was chosen because sea states were recorded for each of the bins contained within it at both BiMEP and EMEC. The pseudo smaller operating envelope ranges from a T_e of 4 s to 11 s and H_{m0} of 0.5 m to 2 m.

With regards to the number of sea states within the smaller operating envelope, 88% of all the sea states recorded at BiMEP fall within the smaller operating envelope. 50% of the sea states recorded at EMEC fall within the smaller operating envelope. IDOM envisage the commercial MARMOK-A-5 operating envelope to range from a T_e of 4 s to 16 s and H_{m0} of 0.5 m to 4.5 m.

Figure 10 is a wave energy flux probability of occurrence plot for both BiMEP and EMEC. A larger data set was used in the generation of the BiMEP curve shown in Figure 10, spanning from December 2016 to October 2017. This larger data set was used because the exceedance curve, which is representative of the site, is unrelated to the power performance measurements and therefore an independent and larger data set could be used to present the characteristics of the site. The exceedance curves plotted for EMEC represent two periods spanning from December to October within the three years of data available.

Figure 10 indicates that, in general, EMEC has a greater wave energy flux than BiMEP. In general, the probability that wave energy flux will be greater than a given level is greater at EMEC than it is at BiMEP.

Figure 11 and Figure 12 are joint probability distributions; BiMEP and EMEC respectively.

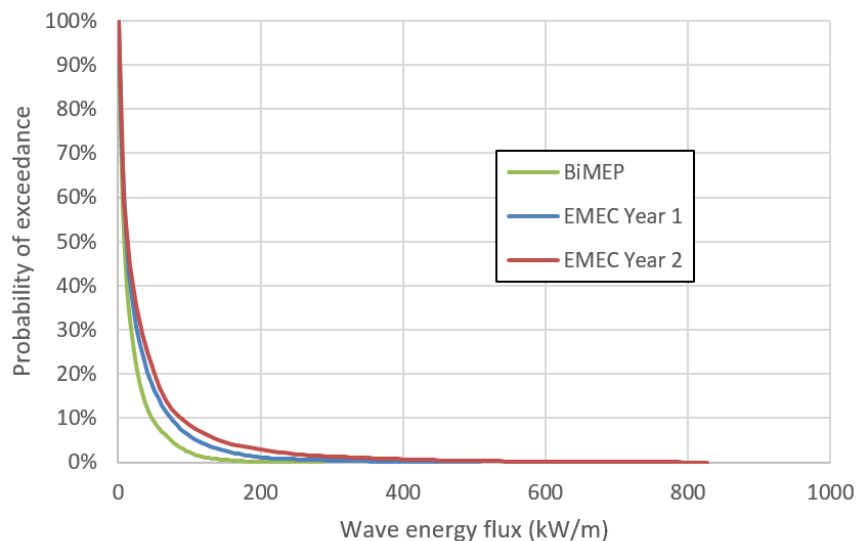


FIGURE 10: BIMEP AND EMEC PROBABILITY OF EXCEEDANCE

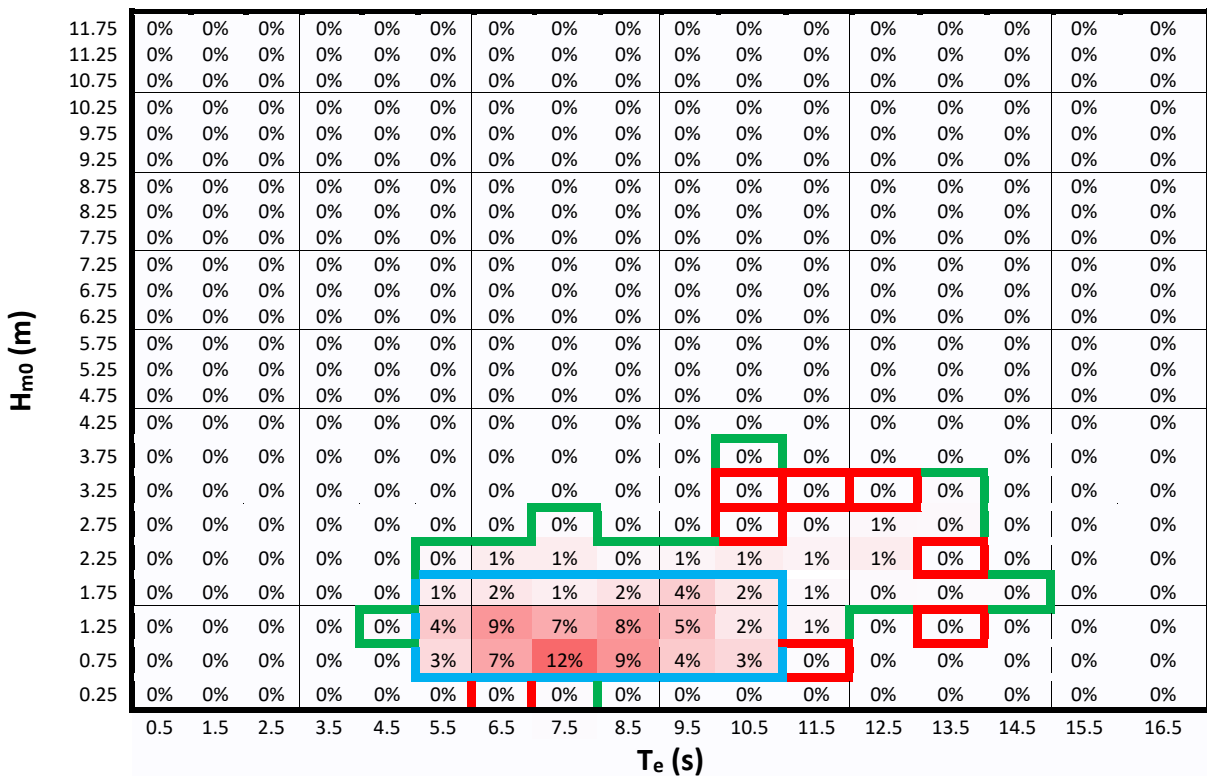


FIGURE 11: BIMEP JOINT PROBABILITY DISTRIBUTION

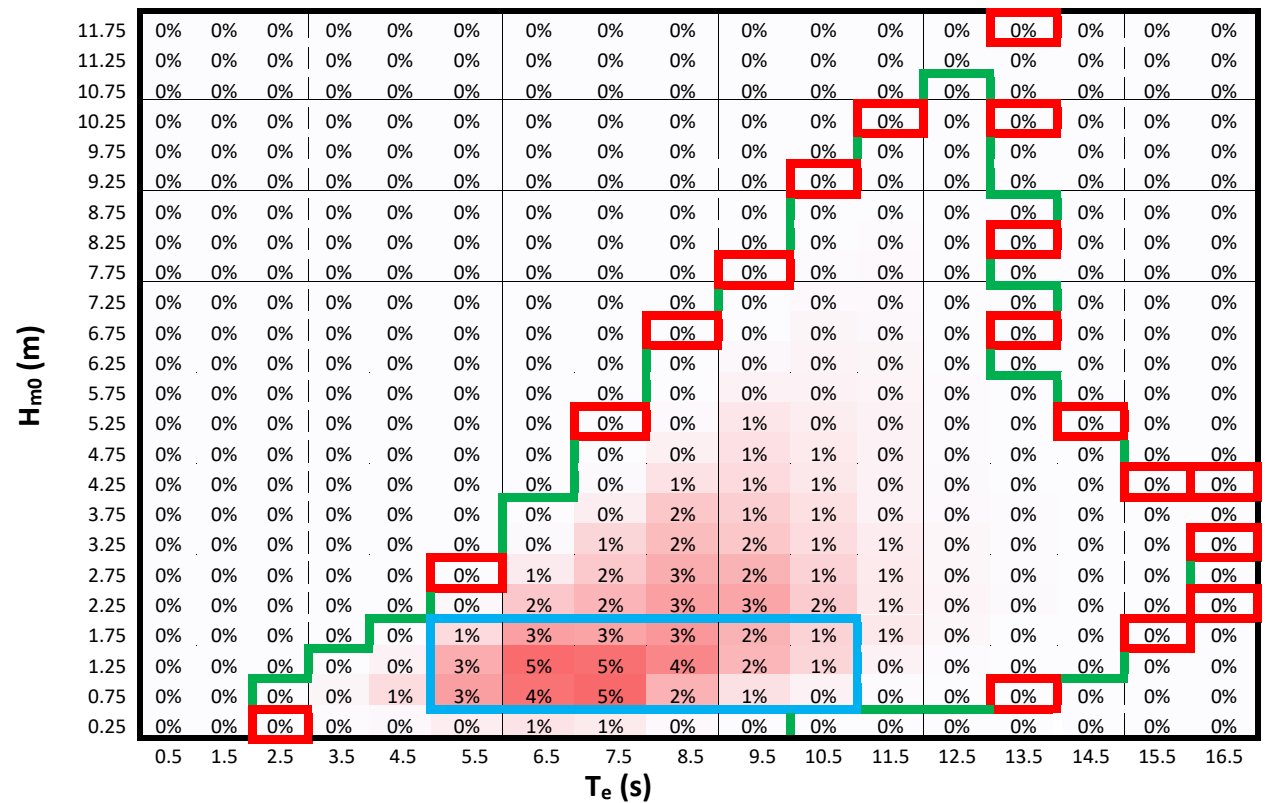


FIGURE 12: EMEC JOINT PROBABILITY DISTRIBUTION

These plots are similar to the scatter diagrams except that they are in terms of the percentage chance that a specific sea state with a particular H_{m0} and T_e characteristics would occur.

3.1.3 TS102 GUIDANCE ON PRESENTATION OF POWER PERFORMANCE INFORMATION RECORDED AT LOCATION 1

4. Calculate the WEC power capture at location 1 and the resulting Capture Length (CL) matrix based on TS100. Present:
 - a. An electrical power matrix,
 - b. a mean CL matrix,
 - c. a max CL matrix,
 - d. a min CL matrix,
 - e. a standard deviation of CL matrix,
 - f. A number of recordings matrix and
 - g. If possible (optional) absorbed power and PTO efficiency matrices.

Comment based on present application

Figure 13 to Figure 18 present the information that TS102 requests in terms of the power performance of the WEC at location 1, except for absorbed power and PTO efficiency matrices; items 4.a to 4.f.

Figure 13 isn't strictly an electrical power matrix since a normalised power matrix was provided for analysis. Figure 13 instead presents the percentages of the overall normalised power that originates in each of the H_{m0} and T_e bins. Further to this, power performance information was provided for the WEC when operating under two different control algorithms. In this report they will be referred to as CA1 and CA2. It isn't clear what the characteristics are of the two different control algorithms, however, it is understood that they have different impacts on the power performance of the WEC. Unless otherwise stated, the data presented here is that which was recorded when the WEC was operating with CA1.

Figure 14 presents the mean CL of the WEC for each of the sea states recorded. Both TS100 and TS102 recommend that CL be used in the presentation of normalised power performance because it is less sensitive to sea-state parameters and therefore less affected to the approach followed to bin sea states. CL is calculated through equation (1),

$$L = \frac{P}{J}, \quad (1)$$

In which P is the WEC power measurement and J is the wave energy flux which is calculated through equation (2).

$$J = \rho g \sum_i S_i c_{gi} \Delta f \quad (2)$$

ρ in equation (2) is water density, g is acceleration due to gravity, S_i is a particular sea state's spectra at the i^{th} frequency component, c_{gi} is the group velocity of the i^{th} frequency component and Δf is the frequency step of the sea state's spectra.

The normalised power matrix provided for analysis yielded normalised CL values with an excessive number of decimal places. The values presented in Figure 14 to Figure 17 were scaled for ease of presentation.

Figure 14 presents the mean normalised CLs calculated using the normalised power performance measurements recorded in each of the sea state bins. Figure 15 presents the maximum normalised CLs calculated using the normalised power performance measurements recorded in each of the sea state bins.

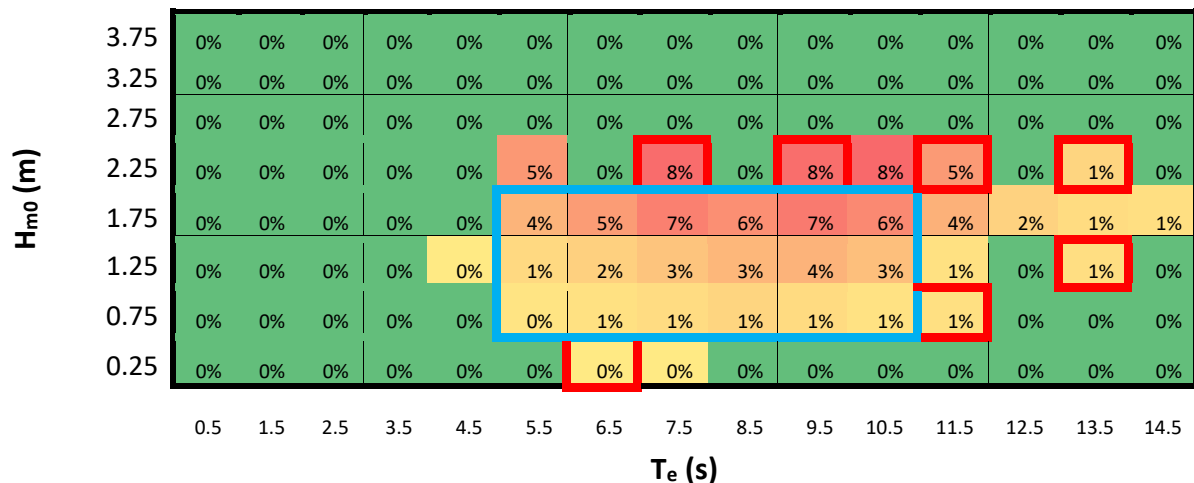


FIGURE 13: WEC (CA 1) MEAN NORMALISED ELECTRICAL POWER MATRIX (PERCENTAGE OF OVERALL POWER FROM EACH SEA STATE)

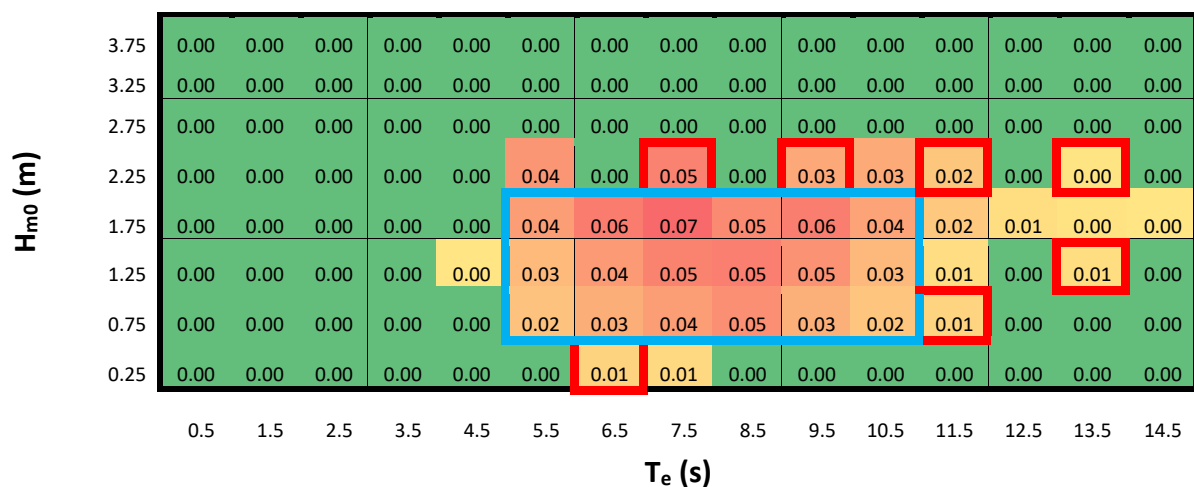


FIGURE 14: WEC (CA 1) MEAN NORMALISED CL MATRIX - SCALED FOR PRESENTATION

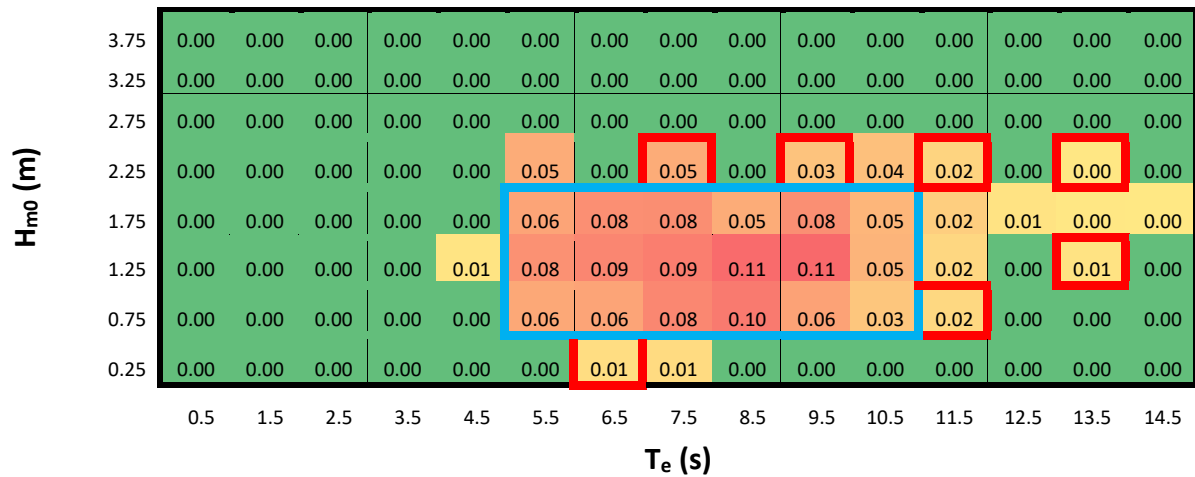


FIGURE 15: WEC (CA 1) MAX NORMALISED CL MATRIX - SCALED FOR PRESENTATION

Figure 16 presents the minimum CLs calculated using the normalised power performance measurements recorded in each of the sea state bins. Figure 17 presents the standard deviation of the CLs calculated for each of the sea state bins. Figure 18 indicates the number of power recordings that were obtained for each of the sea state bins.

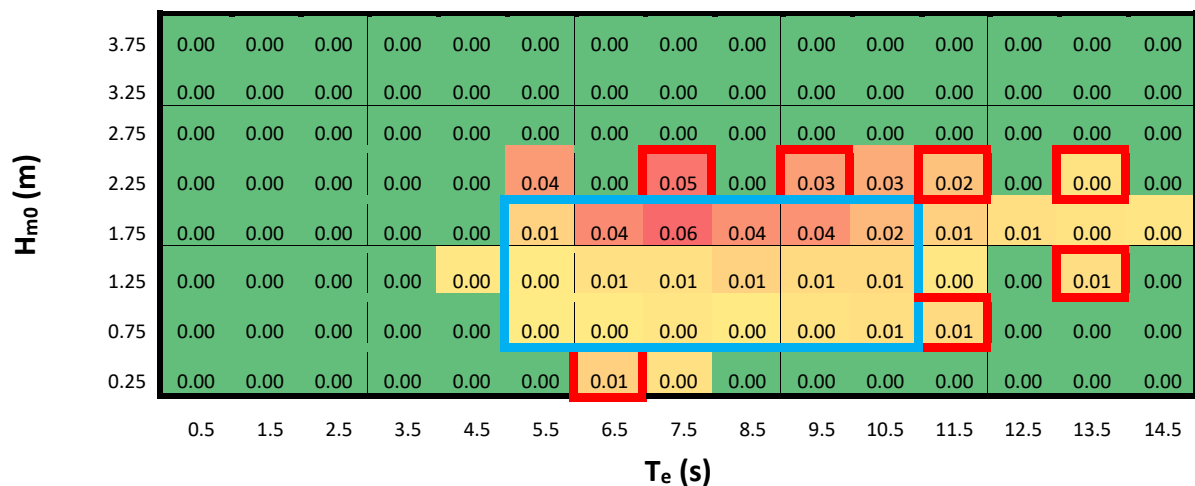


FIGURE 16: WEC (CA 1) MIN NORMALISED CL MATRIX - SCALED FOR PRESENTATION

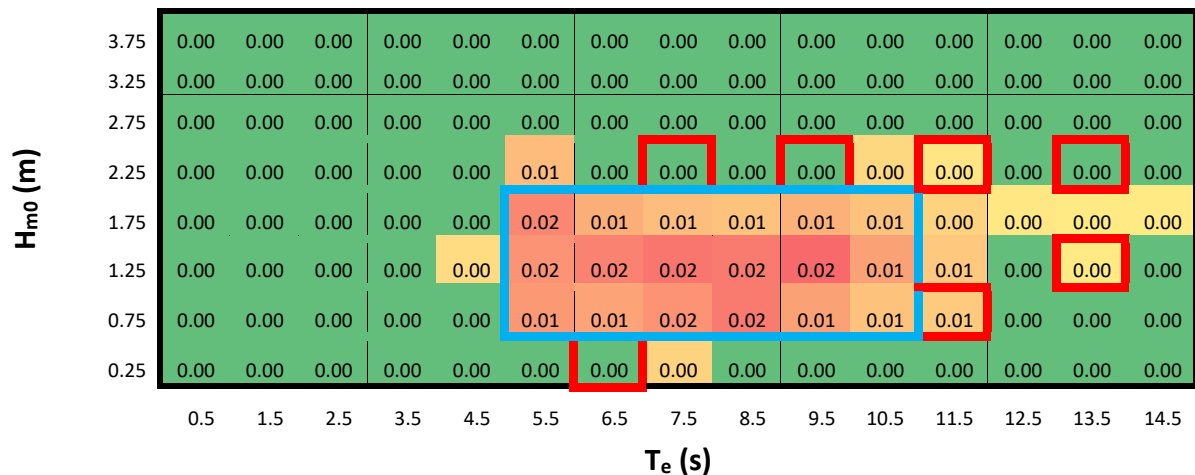


FIGURE 17: WEC (CA 1) STANDARD DEVIATION CL MATRIX - SCALED FOR PRESEFOR PRESENTATION

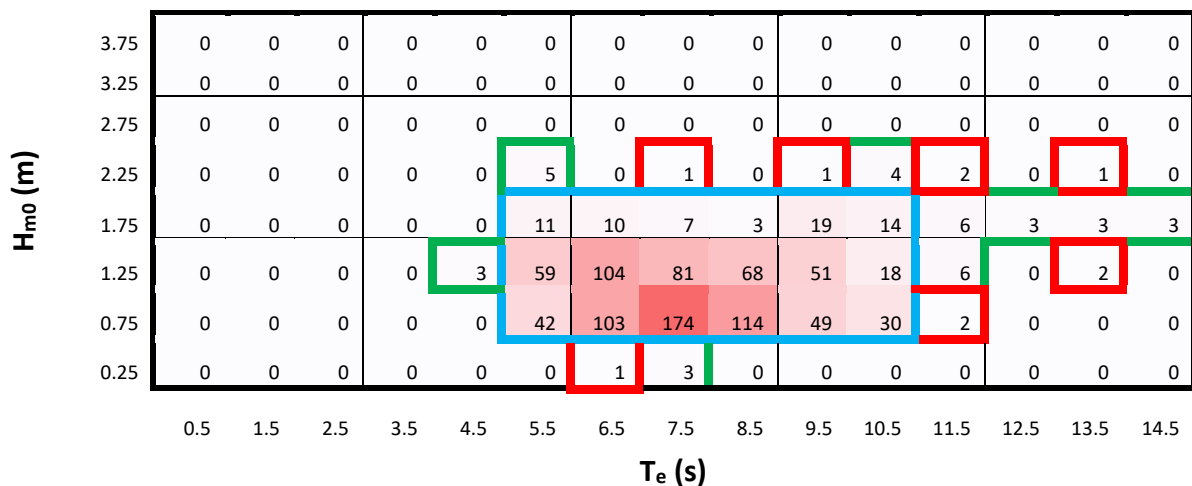


FIGURE 18: WEC (CA 1) NUMBER OF RECORDINGS

3.1.4 TS102 GUIDANCE ON MAPPING INFORMATION FROM LOCATION 1 TO LOCATION 2 AND AN EVALUATION OF SPECTRAL BANDWIDTH AS AN ADDITIONAL MATRIX DIMENSION

5. Compare the CL matrix obtained for location 1 with the scatter diagram of location 2. Complement the CL matrix with validated numerical model or physical data, to fill undefined or underpopulated cells, so as to cover the range of sea states present at the second location within the WEC's operational envelope.
 - a. Capture length matrix requirements are set out in TS100. Where required, to reduced variability in capture length in the bins, expand the dimensionality of the matrix
 - b. Need to appreciate the sensitivity of the WEC to:
 - i. Water depth,
 - ii. Wave direction,
 - iii. Spectral shape and directional spreading,
 - iv. Water current and
 - v. Tidal range.
 - c. If inclusion of a third dimension modifies MAEP by more than 10% then the third dimension should be included.
 - d. Complement through:
 - i. Data fitting or
 - ii. Numerical or physical modelling.
 - e. Cells containing complemented data should be clearly identified (use the method with least uncertainty).
 - f. When using a data fitting approach, you can't use complementation data.

- g. *When using a numerical model, the shape of the spectra used should be representative of range observed within the bin.*
 - h. *Physical modelling should be based on International Towing Tank Conference (ITTC) Recommended Guidelines 7.5-02-07-03.7.*
 - i. *The model used shall be a scale model of the WEC deployed at location 2. The PTO's characteristics need to be reported and the means of representing need to be documented and justified.*
6. *Validate the [numerical model used to compliment location 1's capture length matrix] with data from location 1.*
- a. *TS102 outlines the minimum requirements for validation:*
 - i. *Minimum of 10 bins should be used in the validation; 3 model runs each (bins selected should be justified). Use either observed wave conditions as input or representative wave conditions,*
 - ii. *Need to present the percentage error between the measured and modelled capture length for each of the 10 validation bins,*
 - iii. *Need to present the percentage error between the measured and model MAEP (based only on the validation bins) and*
 - iv. *Need to account for conversion losses within the PTO. For a physical model, record absorbed power then scale appropriately then apply PTO efficiencies.*
7. *Calculate Mean Annual Energy Production (MAEP) at location 2 using the complimented capture length matrix and location 2's resource matrix.*
- a. *Use either the standard or alternative methods described in TS100.*
8. *Clearly present the MAEP that was calculated at location 2 through the different methods of obtaining capture length values: measured at location 1, interpolated/extrapolated and numerically estimated or experimentally measured.*

Comment based on present application

Section 3.1.2, and in particular Figure 9, compare the coverage of the CL matrix produced for BiMEP (location 1) with the scatter diagram for EMEC (location 2). Figure 9 also indicates the bins that would require complementary data, both through data fitting and modelling results, were this application to consider the MARMOK-A-5's full theoretical operating envelope. Section 3.1.2 also notes how, since physical and numerical model data isn't available, in this application of TS102, a smaller pseudo operating envelope was used. Since each of the bins within the smaller pseudo operating envelope had information obtained from more than 3 sea states, no complementary data was required. It is recommended that further studies, with access to either physical or numerical modelling results, should apply TS102 to test the procedure more completely.

With regards to testing increasing the dimensionality of the matrices, in this application of TS102, four bandwidth parameters were investigated to determine if any correlation existed between them and the variability in power performance observed in the sea state bins. Bandwidth was investigated since the other higher dimension parameters suggested by TS102 (5.b.i to 5.b.v) were either considered to be less likely to have a significant effect on the WEC's performance or similar information was not available for both BiMEP and EMEC. The bandwidth parameters are shown in equations (3a) to (3d).

$$\varepsilon_0 = \sqrt{\frac{m_0 m_{-2}}{m_{-1}^2} - 1} \quad (3a)$$

$$\varepsilon_1 = \sqrt{\frac{m_1 m_{-1}}{m_0^2} - 1} \quad (3b)$$

$$\varepsilon_2 = \sqrt{\frac{m_0 m_2}{m_1^2} - 1} \quad (3c)$$

$$\varepsilon_4 = \sqrt{1 - \frac{m_2^2}{m_0 m_4}} \quad (3d)$$

m_n in equations (3a) to (3d) is the n^{th} mode of the recorded sea states energy spectra.

The bandwidth parameters tested are as follows:

- Broadness parameter (ε_0) [7],
- Bandwidth parameter (ε_1) [8],
- Narrowness parameter (ε_2) [9] and
- Broadness factor (ε_4) [10]

The references listed alongside the parameters are believed to be the originators of the parameters. A number of studies and reports have compiled and reviewed these parameters and their effects on WEC performance, of particular note is [11].

Figure 19 is a plot of normalised CL against bandwidth for each of the recorded sea states that fell within the most populated bin of the WEC's power matrix when it was operating under CA1 at BiMEP; H_{m0} ranging from 0.5 m to 1.0 m and T_e ranging from 7 s to 8 s. In total, 174 sea states that were recorded for the most populated bin. The coefficient of variation of normalised CL, which is a relative measure of the standard deviation and calculated as the standard deviation as a percentage of the mean, is 40%. Each of the bandwidth parameters considered are presented by different colours and shapes and their respective coefficients of variation are presented in the legend. Based on Figure 19, little clear relationship exists between normalised CL and bandwidth for the bandwidth parameters tested.

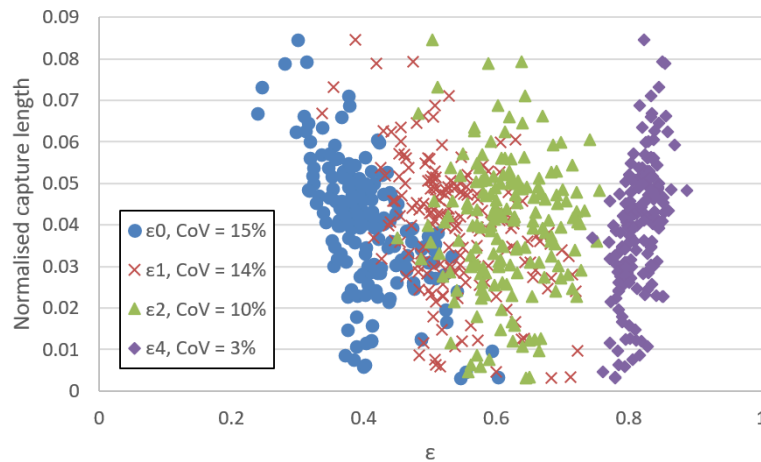


FIGURE 19: NORMALISED CAPTURE LENGTH PLOTTED AGAINST EACH OF THE BANDWIDTH PARAMETER TESTED FOR FIXED H_{m0} (0.5 M TO 1.0 M) AND T_e (7 S TO 8 S)

However, of the bandwidth parameters tested, it is recommended that further investigation should be carried out to determine what relationship exists between CL and the broadness parameter, ϵ_0 . It varied the most out of the parameters tested and has the benefit of being calculated with lower order moments [12].

Figure 20 plots normalised CL against ϵ_0 . The data is discretised by wave steepness, different marker colours and shapes. Wave steepness ($H_{m0}/\lambda(T_e)$) is a nondimensional parameter which is a function of both H_{m0} and T_e ($\lambda \propto T_e$). Presenting it on Figure 20 enables a review of whether the variability of normalised CL within the bin is a result of higher resolution changes in H_{m0} and T_e , i.e. greater resolution than the standard 0.5 m discretisation of H_{m0} and 1 s discretisation of T_e . Figure 20 indicates that variability in normalised CL is not clearly related to higher resolution steps in H_{m0} and T_e , i.e. it is not clear that the variability in normalised CL is related to changes in wave steepness.

As a high level investigation into the relationship between normalised CL and ϵ_0 , linear trend lines are presented on Figure 20 along with their equations and respective coefficients of determination. Five trend lines are presented, corresponding to the five wave steepnesses. A linear trend line was produced for the bin's full dataset which had a coefficient of determination (R^2) of 0.376. The coefficient of determination was only improved by 3% when increasing the complexity of the trend line to a second order polynomial.

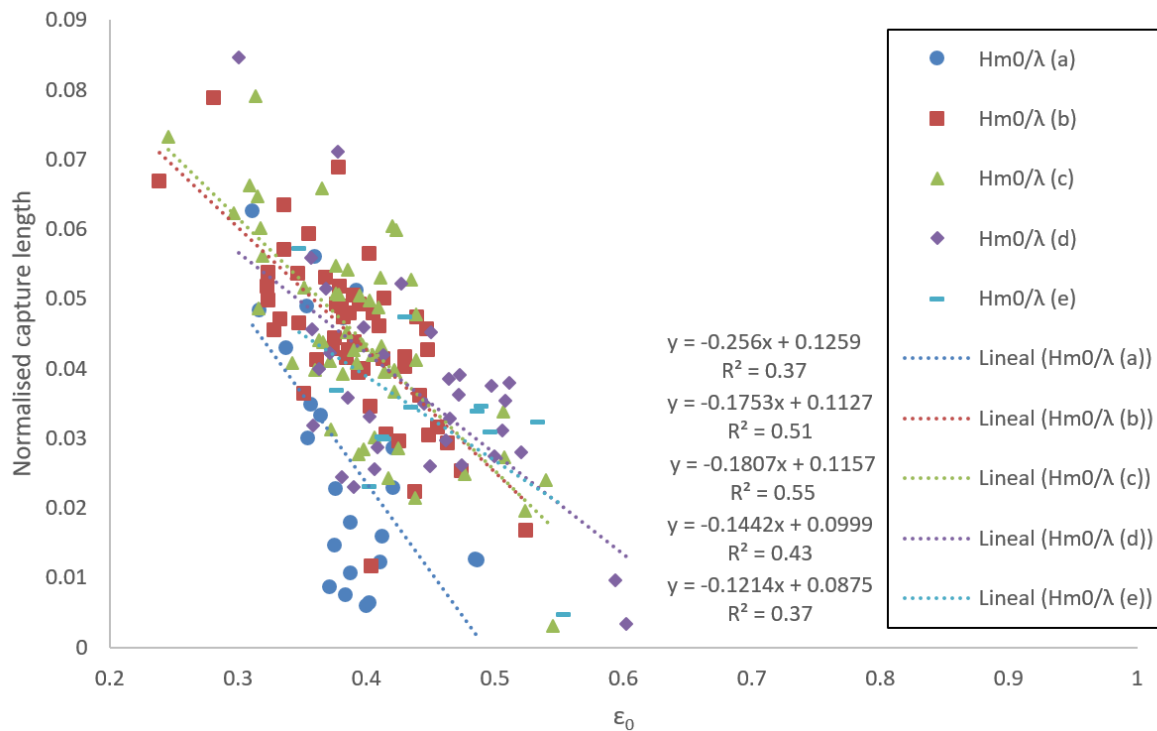


FIGURE 20: NORMALISED CAPTURE LENGTH PLOTTED AGAINST ϵ_0 FOR FIXED H_{m0} (0.5 M TO 1.0 M) AND T_e (7 S TO 8 S)

Although each of the trend lines for each of the steepness bins have low coefficients of determination (less than 0.55), the equations suggest that CL reduces with increasing ϵ_0 .

Figure 21 depicts how the dimensionality of any of the matrices presented thus far can be increased; in this case the dimensionality of a mean normalised CL matrix. Each of the 'sheets' in Figure 21, along the ϵ_x axis, present mean normalised CL matrices, discretised by H_{m0} and T_e , for a range of bandwidth values. To observe how considering the additional bandwidth parameters impacts calculated Mean Annual Energy Production (MAEP) required the generation of similar higher dimension power and occurrence matrices.

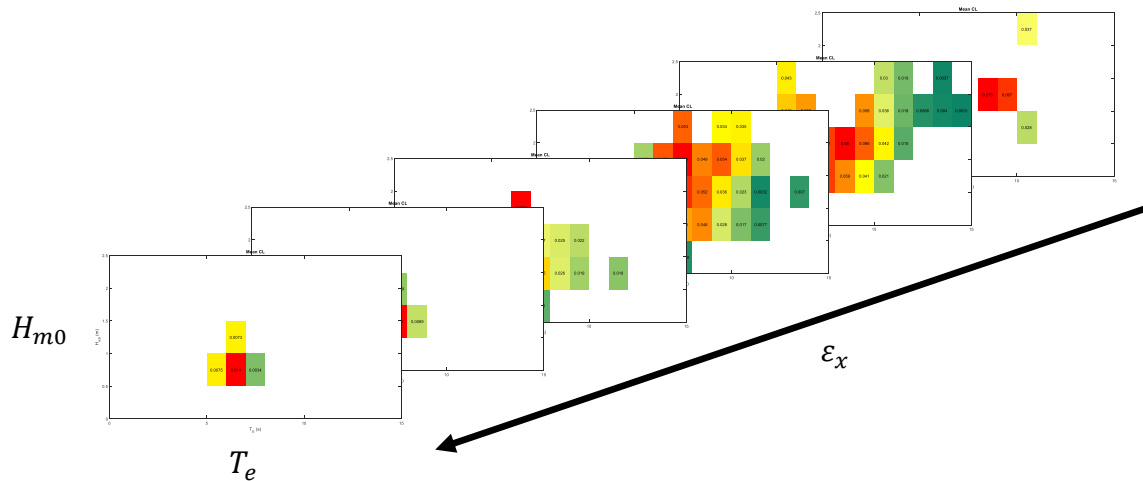


FIGURE 21: DIAGRAM OF INCREASING DIMENSIONALITY OF CAPTURE LENGTH MATRIX

Figure 22 shows the average normalised power performance contained in each bandwidth range, in the form of the percentage of overall power, for each of the bandwidth parameters tested. It also presents the number of sea states represented in each bandwidth range. Note, the results presented in Figure 22 were recorded at BiMEP with the WEC operating under CA1.

Figure 23 indicates the bandwidth ranges within which the all the sea states were recorded, for each of the bandwidth parameters tested. In general, a marginally greater spread of bandwidths was observed at EMEC. However, in only four of the bandwidth range bins (cells outlined in black) were there sea states recorded in bandwidth ranges that were only observed at EMEC.

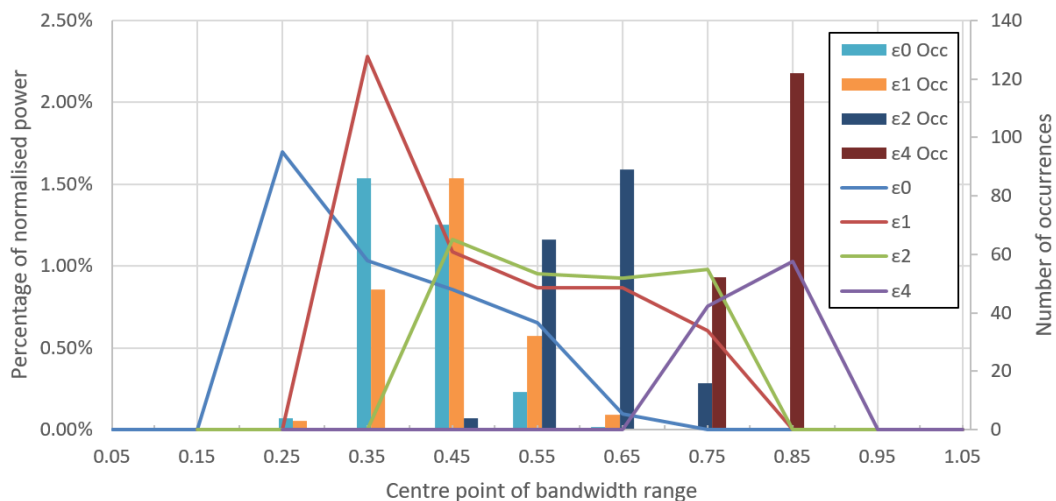


FIGURE 22: PERCENTAGE OF NORMALISED POWER WITH THE BANDWIDTH RANGES FOR FIXED H_{m0} (0.5 M TO 1.0 M) AND T_e (7 S TO 8 S) AND NUMBER OF SEA STATES REPRESENTED IN EACH BANDWIDTH RANGE

ϵ_0

ϵ_1

ϵ_2

ϵ_4

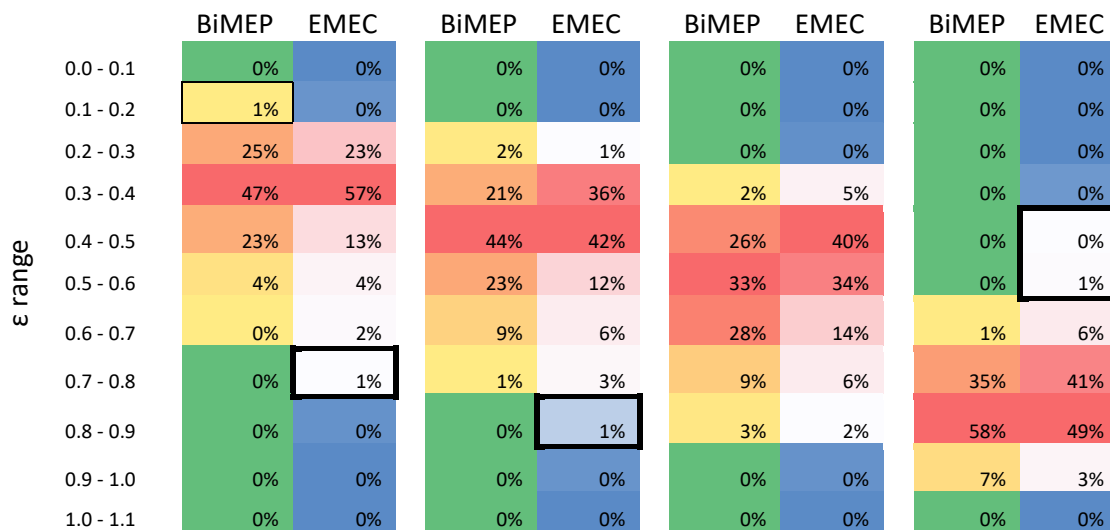


FIGURE 23: PERCENTAGE OF ALL SEA STATES RECORDED WITHIN PRESENTED BANDWIDTHS

Figure 24 to Figure 27 present the percentage of overall energy content contained in each of the bandwidth bins, for each of the bandwidth parameters tested, both the control algorithms and both deployment locations. Each of the figures also indicate how the total MAEPs calculated when considering bandwidth vary relative to MAEP calculated when disregarding bandwidth (conventional MAEP), i.e. when using only matrices discretised with H_{m0} and T_e bins. It must be stressed that Figure 26 and Figure 27 were created with the data available, and as such are missing complementary data which would be required for the $H_{m0}/T_e/\epsilon_x$ bins for which there is a mismatch in recorded performance data and EMEC resource data.

TS102 indicates that if the percentage error between the MAEP value calculated when considering bandwidth and the MAEP value calculated through the conventional method is greater than 10%, then the result obtained considering the bandwidth should be used.

Figure 24 to Figure 27 indicate that, as the bandwidth parameters progress from ϵ_0 to ϵ_4 , which roughly equates to using increasingly higher order moments to calculate the bandwidth parameters, the greater the bandwidth range containing the majority of sea states.

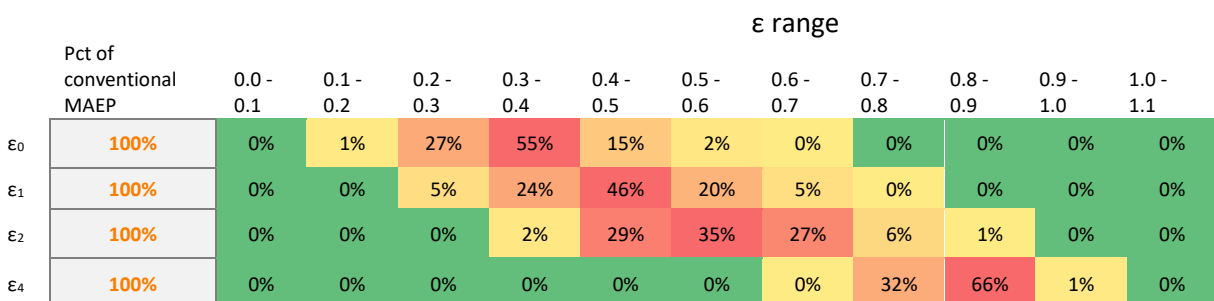


FIGURE 24: BiMEP - CA1 – ANNUAL ENERGY CONTENT OF DIFFERENT BANDWIDTH RANGES AND COMPARISON OF MAEP CALCULATED WHEN CONSIDERING BANDWIDTH WITH CONVENTIONAL MAEP METHOD

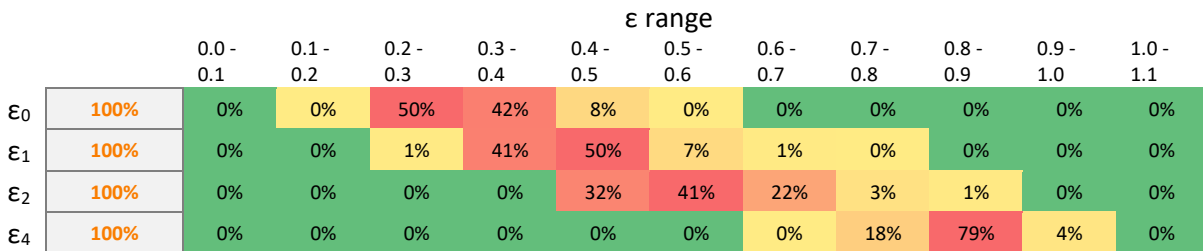


FIGURE 25: BiMEP - CA2 – ANNUAL ENERGY CONTENT OF DIFFERENT BANDWIDTH RANGES AND COMPARISON OF MAEP CALCULATED WHEN CONSIDERING BANDWIDTH WITH CONVENTIONAL MAEP METHOD

In general, the ϵ_4 parameter appears to compress the sea states to within a smaller range of bandwidths than the other parameters. This is also seen in Figure 19 and Figure 22. Figure 24 and Figure 25 present data obtained at BiMEP with the WEC operating under both CA1 and CA2 respectively.

Figure 26 and Figure 27, showing estimates for EMEC with the WEC operating under both CA1 and CA2, show that the MAEP values calculated when considering bandwidth ranged from being 82% to 89% of the MAEP values calculated through the conventional method. If these differences were observed in a formal application of TS102, the TS states that the bandwidth should be considered in the MAEP calculation.

There are a number of reasons why the MAEP values calculated when considering bandwidth have poorer agreement with the MAEP values calculated through the conventional method at EMEC, when disregarding bandwidth. To a degree, this is due to the marginally greater spread of bandwidths observed at EMEC (shown on Figure 23). However, this doesn't explain the poor agreement shown for the Narrowness parameter, ϵ_2 , (82% for CA1, and 86% for CA2) since a similar spread of bandwidth ranges were observed at both BiMEP and EMEC. As alluded to, the lower MAEPs will be due to the mismatches in recorded performance data and EMEC resource data for certain $H_{m0}/T_e/\epsilon_x$ bins. These cells of mismatch would require further complimentary data. Further to this, the greater the average bin power on a bandwidth range sheet, the greater the influence that cell mismatch would have.

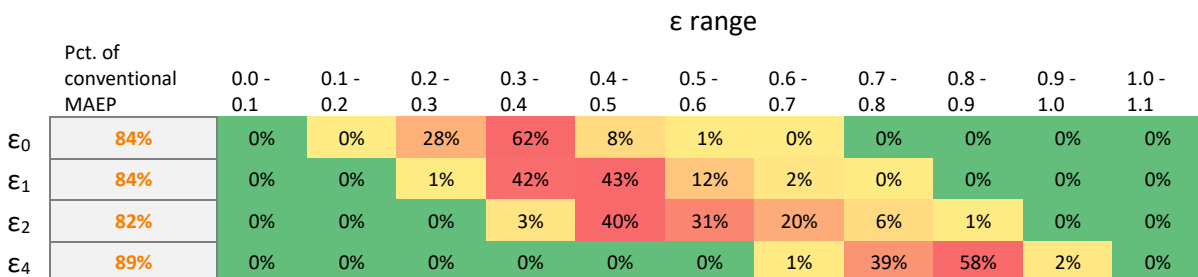


FIGURE 26: EMEC - CA1 – ANNUAL ENERGY CONTENT OF DIFFERENT BANDWIDTH RANGES AND COMPARISON OF MAEP CALCULATED WHEN CONSIDERING BANDWIDTH WITH CONVENTIONAL MAEP METHOD

ϵ range

	Pct. of conventional MAEP	0.0 - 0.1	0.1 - 0.2	0.2 - 0.3	0.3 - 0.4	0.4 - 0.5	0.5 - 0.6	0.6 - 0.7	0.7 - 0.8	0.8 - 0.9	0.9 - 1.0	1.0 - 1.1
ϵ_0	85%	0%	0%	34%	57%	9%	0%	0%	0%	0%	0%	0%
ϵ_1	82%	0%	0%	0%	43%	47%	9%	0%	0%	0%	0%	0%
ϵ_2	86%	0%	0%	0%	0%	44%	37%	16%	2%	0%	0%	0%
ϵ_4	86%	0%	0%	0%	0%	0%	0%	1%	37%	60%	2%	0%

FIGURE 27: EMEC - CA2 – ANNUAL ENERGY CONTENT OF DIFFERENT BANDWIDTH RANGES AND COMPARISON OF MAEP CALCULATED WHEN CONSIDERING BANDWIDTH WITH CONVENTIONAL MAEP METHOD

By way of example, Figure 28 indicates, in percentage terms for the WEC deployed at EMEC operating under CA1: the mismatch that can exist on each bandwidth range sheet, the average power on each bandwidth range sheet and product values to indicate the significance of the mismatches observed.

		ϵ range										
		0.0 - 0.1	0.1 - 0.2	0.2 - 0.3	0.3 - 0.4	0.4 - 0.5	0.5 - 0.6	0.6 - 0.7	0.7 - 0.8	0.8 - 0.9	0.9 - 1.0	1.0 - 1.1
ϵ_0	Mismatch	0%	11%	7%	0%	13%	20%	22%	20%	6%	0%	0%
	Average power	0%	8%	38%	39%	12%	2%	1%	0%	0%	0%	0%
	Product	0%	16%	47%	0%	27%	8%	2%	0%	0%	0%	0%
ϵ_1	Mismatch	0%	0%	22%	2%	3%	3%	14%	22%	22%	10%	0%
	Average power	0%	0%	11%	34%	28%	21%	5%	1%	0%	0%	0%
	Product	0%	0%	45%	10%	17%	13%	12%	3%	0%	0%	0%
ϵ_2	Mismatch	0%	0%	13%	29%	10%	6%	10%	6%	16%	10%	0%
	Average power	0%	0%	0%	9%	28%	29%	21%	10%	2%	0%	0%
	Product	0%	0%	0%	26%	26%	18%	19%	6%	4%	0%	0%
ϵ_4	Mismatch	0%	0%	0%	0%	8%	12%	28%	28%	12%	12%	0%
	Average power	0%	0%	0%	0%	0%	0%	1%	32%	54%	14%	0%
	Product	0%	0%	0%	0%	0%	0%	1%	52%	38%	10%	0%

FIGURE 28: INDICATION OF BIN MISMATCH AND AVERAGE NORMALISED POWER FOR BANDWIDTH RANGES (WEC OPERATING AT EMEC UNDER CA1)

3.1.5 ADDITIONAL ASPECTS COVERED IN TS102

9. *Estimate the uncertainty in the MAEP calculated at location 2.*
 - a. *Some of this is indicated by the percentage of the MAEP calculated using measured cells from location 1; the more measured cells there are the more the estimate of MAEP is based on real data and it indicates that the device is operating in conditions similar to those observed at location 1.*
 - b. *Uncertainty is due to:*
 - i. *The quality of the performance and wave data at location 1,*
 - ii. *The quality of the wave resource data at location 2 and*
 - iii. *The accuracy and quality of the complementary data.*
10. *Outline proposed WEC changes that would be actioned to optimise its performance at location 2.*
 - c. *Need to document:*
 - i. *Description of the change,*
 - ii. *Purpose of the change and*
 - iii. *Impact of the change.*
11. *Evaluate how the proposed changes affect the capture length using physical and/or validated numerical models. If the difference between measured (at location 1) and numerically estimated or physically measured capture length is greater than 10% then use the numerical or experimental value.*
 - d. *Can only use capture length matrix obtained using WEC1 at location 1 to characterise WEC2 if the difference in power performance is observed to be less than 10% per bin - if the difference is greater than 10% then use a numerical model result,*
 - e. *If the WEC is modified, the numerical model validation steps outlined in step 6 need to be followed for every capture length bin recorded at location 1 and*
 - f. *The difference between mean capture lengths shall be calculated for each bin and use numerical value if difference is greater than 10%.*

Comment based on present application

As highlighted, it is recommended that a similar test application of TS102 be conducted with physical and/or validated numerical model data to more fully test the methodology. Due to the approach taken in this study, calculating MAEP using a smaller pseudo operating envelope, no physical and/or validated numerical model data was used (recall it wasn't available), so it is not possible to indicate what percentage of the MAEP figure was estimated by these complimentary methods.

With regards to the quality of the data used, there is no evidence to suggest that the data recorded is of poor quality in terms of how it was recorded. The bins within the smaller pseudo

operating window contained information from at least 3 sea states or more. It isn't clear how the power performance information has been normalised and whether this has affected the quality of the analysis.

It has been clear throughout this application, that it is more than likely that a WEC's design will change when moved from location 1 to location 2. Particularly if the approach followed to select location 2 does not consider the characteristics of the WEC. TS102 describes how to account for changes to the WEC – this involves using physical and/or validated numerical model data (with the model adjusted to the WEC design for location 2) to replace measured cells if the difference in values is greater than 10%.

Finally, it should be noted that TS102 stresses the importance of transparency in the procedure.

3.2 DISCUSSION ON THE APPLICATION OF TS102 AND UNCERTAINTY

WECs will be required to operate at different deployment locations, however the approach taken to choosing deployment locations can be approached in two ways. In one approach, arbitrary locations with a high energy resources could be chosen. In the other approach, the location could be based on what is appropriate for the WEC being deployed. The former approach might require significant changes to the WEC, incurring corresponding costs, although it would be in a higher resource and therefore generate a higher income. In the latter approach, minimal changes would be required to the WEC however the income might not be as great. In the ideal scenario, both approaches could be satisfied, in which the WEC is suited to a high level of resource site. However, it is up to a project developer to determine which approach to take for the most economic deployment.

The steps outlined in TS102 guide on what to do in both approaches. TS102 acknowledges that location 2 will have different metocean conditions and that WECs might have design changes¹ for the purposes of location 2. TS102 specifies the physical tests, validated numerical model tests and/or data fitting techniques that should be conducted to compliment the performance observations from location 1 and reflect the changes that device design will have on performance. Further to this, it states that there should be an assessment of the uncertainties involved in the procedure followed.

It would be useful if TS102 provided guidance on selection of an appropriate location for WEC's deployment. For example, it could indicate a range of parameters that should be checked, and if they are within certain limits, then location 2 could be deemed to be similar

¹ Changes in dimension, geometry, PTO system, control logic and moorings system. Need to explain the change, its purpose and its impact on power performance.

to location 1, within the accuracy that can be expected from WEC power performance assessments.

In an ideal scenario, power performance measurements would be recorded at location 1 that cover all the sea states that arise at location 2. The longer the deployment period of the WEC at location 1, the greater the chance that power performance measurements would be recorded for all the sea states that occur at location 2. However, until power performance measurements are recorded, at location 1, for all the sea states that occur at location 2, complimentary data will be required. The complimentary data obtained either through data fitting or physical or validated numerical model data. In addition to this, and as discussed at the start of this section, physical or validated numerical model results should be used when accounting for changes that arise due to modifications in WEC design if the results obtained differ from measured results by more than 10%. Deferring to these approaches of generating power performance data suggests a high level of trust in values that they provide, i.e. in the case of differences being greater than 10%, the approach of generating synthetic data is preferred over the measure data. This being the case, it suggests that the data measured at location 1 might be best used to validate the physical and/or numerical models. Then the user could prefer to use those models to estimate the performance of the WEC at location 2. TS102 provides some guidance on model validation, however, perhaps this section could be further developed to provide more guidance on acceptable limits on accuracy.

With regards to the uncertainty in estimating the performance of a WEC at a prospective deployment location, TS102 highlights that the uncertainty in the estimate will be greater the more complimentary data that is used and vice versa. This has hard to assess without either physical or numerical data and actual power performance data recorded at location 2.

In addition to this, the application of TS102 presented in this deliverable attempted to determine how higher dimensions (different bandwidth parameters) could explain the variability of power performance measurements in the different sea state bins. No clear relationships were observed, except that normalised power appeared to reduce as bandwidth increased which makes sense for a point absorber type WEC. There is still uncertainty in this area and WEC developers need to identify which sea state parameters, other than H_{m0} and T_e , impact the performance of their device. Understanding these additional parameters and how they impact their devices will reduce uncertainty further.

Further to this, TS102 emphasises that additional sources of uncertainty in predictions of power performance will arise because of differences in site characteristics (bathymetry, tidal and weather conditions etc.), marine currents, wave direction and WEC modifications. The more that is understood about these factors the less uncertainty there will be.

3.3 IMPLICATIONS FOR LCOE MODELLING AND BUSINESS CASE DEVELOPMENT

Figure 29 is a sensitivity spider plot indicating how LCOE, equation (4) varies with percentage changes in different inputs.

$$LCOE = \frac{\sum_{t=0}^n \frac{CAPEX_t + OPEX_t + DECOM_t}{(1+r)^t}}{\sum_{t=0}^n \frac{MAEP_t}{(1+r)^t}} \quad (4)$$

LCOE is a well-established metric used to evaluate the economic performance of an energy generation device over its lifetime. It is comparable to the market selling price/break-even price of electricity. As shown in equation (4), LCOE is the total Capital Expenditure (CAPEX), Operational Expenditure (OPEX) and Decommissioning (DECOM) costs associated with the generation of electricity, discounted to present day values, divided by the sum of the discounted *MAEP*, also discounted. r in equation (4) is the nominal discount rate, t is time measured in years and n is the number of years a WEC, or WEC array, would be in operation.

Figure 29 indicates that MAEP (identified as *AEP (MWh)* in the Figure 29) has the greatest impact on LCOE out of all the components that go into the calculation of LCOE, highlighting the importance of being able to accurately estimate LCOE at prospective deployment locations.

In addition to the MAEP at a prospective deployment location calculated by following the method set out in TS102, the other information gathered on site characteristics is also useful for economic modelling. For example, the site resource information collated through the application of TS102 could feed into an OPEX model and the deployment site information could also feed into logistic modelling, such as activities to estimate electrical architecture costs etc.

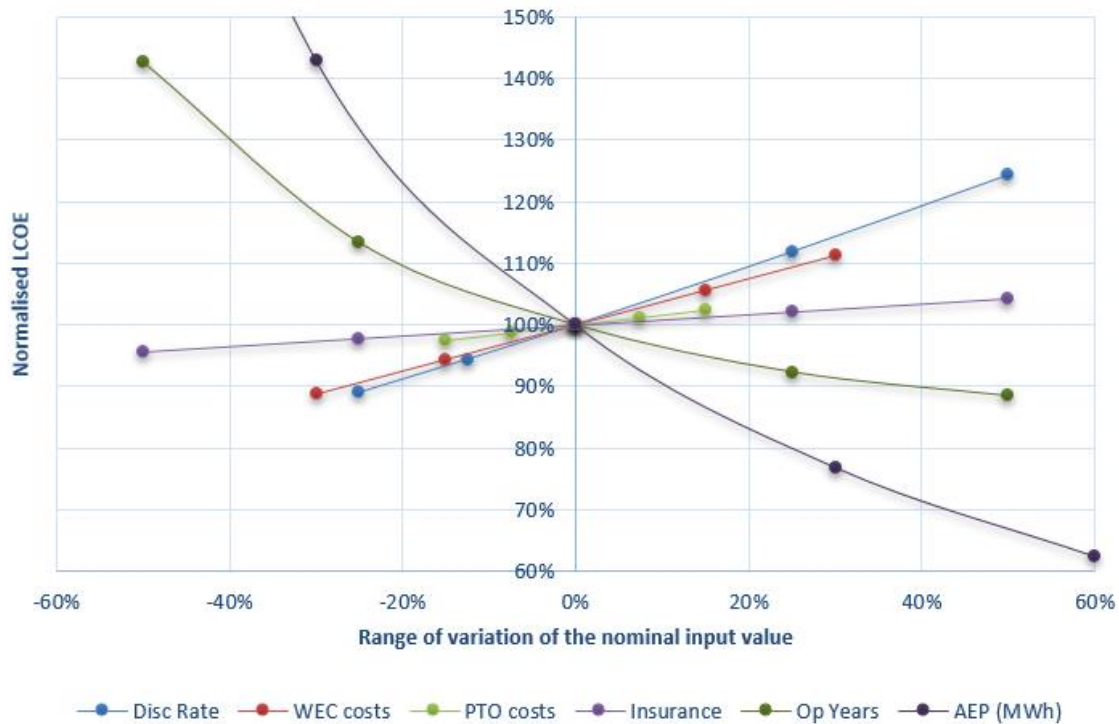


FIGURE 29: SENSITIVITY SPIDER PLOT FOR LCOE [13]

It should be noted that, due to the significant impact that MAEP has on LCOE, uncertainty in MAEP also has a significant impact on LCOE. It is clearly important that uncertainties in AEP need to be understood and reduced as much as possible.

3.4 RECOMMENDATIONS FOR TC114

Through this application of TS102, based on an early stage WEC with a limited deployment time, the following recommendations are made:

- Guidance should be provided on how to determine if a site is suited to a WEC's characteristics, i.e. advice on differences acceptable for location 2 to be considered similar to location 1.
- Consideration should be made on the applicability of this TS to early stage devices. As discussed, if performance data is limited or changes are made to the WEC, TS102 tends to suggest that users defer to the use of physical or validated numerical model data. Perhaps the TS should focus on how to ensure that models are properly validated by data recorded at location 1 so as to increase the confidence in the models that are used to estimate the performance of the WEC at a location 2.

4. PERFORMANCE ASSESSMENT USING SHORT SAMPLES

Abstract

Assessing power performance at sea is an important step in taking wave energy towards commercial projects. Open-sea testing being expensive, it is essential that it be conducted in the most efficient way. One measure of this is how accurately power production can be predicted using data from a given testing period. We report on how using sample durations ranging from three hours to five minutes affects power performance assessment. The analysis focusses on open-sea operating data from EVE's Mutriku wave power plant, a shoreline breakwater housing oscillating water columns. Results suggest that post-processing with sample duration as short as five minutes, in complement to the standard twenty minutes, can be useful to populate parts of the power matrix where longer-sample data is too sparse. This is because short-term wave statistics cover a wider range of the scatter diagram than standard, longer averaged sea-states. Shorter sampling may also enable faster assessment of various device configurations, by cycling through them in more rapid succession. This would greatly reduce testing duration and costs, but would require changes in the implementation of at-sea testing. With the dataset analysed, it appears that samples as short as five minutes still result in annual energy production estimates within the range of estimates based on standard sample durations. Difficulties that arise when using shorter samples are discussed and some methods that appear to partly resolve them for this particular dataset are presented.

4.1 SUMMARY AND MAIN RESULTS

This section reports on the use of various sample durations for power performance assessment of Wave Energy Converters (WECs). Currently IEC-TS/62600-100 specifies a minimum of 20 minutes for sample duration. Practice in metocean data analysis is to use samples no shorter than 17 minutes (1024 seconds, or 2048 samples at 2 Hz, a convenient number for spectral analysis). This would correspond typically to a record of some hundred waves. It is difficult to derive reliable statistics on waves with much less.

However, for the particular application to WEC power performance assessment, both the wave energy flux and the power output of WECs often show high peak to average ratio at time scales as short as that of one individual wave. It thus appears worthwhile to investigate how the shorter time scale response of the WEC could be related to statistics of the incoming wavefield at shorter time scales.

Power data and wave data from EVE's Mutriku wave power plant were analysed for power performance with sample duration ranging from 24 hours to 5 minutes and then down to individual waves. The Mutriku plant is a shoreline breakwater housing 18 chambers of Oscillating Water Columns (OWC), most of which are equipped with Wells Turbines of nominal

capacity of 18.5 kW. Certain results with data from IDOM/Oceantec's floating OWC operating at the Biscay Marine Energy Platform (BiMEP) are also presented.

Results indicate that for the dataset considered, sample variability actually increases significantly at shorter sample duration of power performance. There doesn't appear to be any simple way to relate power output to wave characteristics at finer time-scales that can be used to reduce scatter in power performance data.

On the other hand, it was found that this increase in sample variability may be compensated by the increase in the number of samples, so that the rms error expected in the final estimate of the mean may be significantly less when using short samples. Conditions such as independence and separation of samples may be necessary and certain methods are reported on that seem to work for this particular dataset.

No significant loss of accuracy in energy yield prediction is found from using samples as short as five minutes, in that differences are of the same order than between samples of 30 minutes, one hour and three hours – about 5%. The wider applicability of this result is difficult to assess with this dataset only. The main limitation is duration of the observing campaign, which spans less than a year, with imperfect coverage. Should robustness of yield prediction to changes in sample duration be confirmed with larger datasets and other devices, it would be valuable in reducing necessary testing duration and better assess various device configurations such as control algorithms.

Finally, another potential advantage of using short samples is that a significantly larger part of the (H_s, T_e) space can be covered. The main reason is that the scatter diagram of "sea-states" of five minutes duration covers significantly more (H_s, T_e) space than twenty-minute samples. Performance data can thus be obtained for cells of the power matrix where modelling or interpolation would normally be used. This may be particularly useful when the developer is interested in performance of their WEC in conditions that occur rarely at the test site. For example, when evaluating performance at a second location with a different wave climate. A nice feature is that this populating of more parts of the power matrix with shorter samples can be added at no cost to any post-processing analysis, in complement to, and without any modification to, the analysis of standard, twenty minutes or longer samples.

More data from Mutriku would be useful to confirm these results, and applicability to other shoreline or floating devices remains to be investigated. Considering the cost to developers of open-sea test time, and the many device configurations such as control strategies that must be evaluated during this limited period, the possibility to assess performance with shorter samples would be highly valuable to wave device developers and plant managers. This report is formatted so as to facilitate the use of this experience by developers planning or post-processing open-sea data. Some considerations of relevance to IEC technical specifications for wave energy performance assessment are also proposed.

4.2 INTRODUCTION AND OBJECTIVES

This section reports on experience using various sampling strategies to assess wave energy converter (WEC) power performance. The focus is on the impact of using various durations of samples of power performance.

The analysis reported herein was part of H2020 OPERA/T5.3: Wave-by-wave assessment of power production to reduce uncertainty in IEC/TS 62600-100. Task 5.3 (T5.3) is within WP5, which has overall goal to accelerate the establishment of appropriate practices and standards at all the levels of the supply chain for wave energy, in order to reduce uncertainty and their impact on cost of capital for projects. T5.3 investigates how uncertainty in WEC power performance assessment may be reduced by increasing the resolution at which WEC power output is related to statistics of the incoming wavefield.

4.2.1 POTENTIAL INTEREST OF POWER ASSESSMENT AT FINER TIME-SCALES

Perhaps many a visitor to the Mutriku wave power plant has noted the high peak to average ratio of the power output from turbines there. On some days, the plant may be silent for a few minutes, then, suddenly, with the arrival of a group of large waves, the water columns will oscillate loudly for a few cycles, perhaps a bit less than one minute, during which one may feel like their head is in a jet engine at take-off, before going silent again for a few minutes. Until the next wave group. Many a casual beachgoer also would have observed similar behaviour of the nearshore waves on some days, where wave agitation appears to be dominated by the contribution of groups of a few waves with relatively quiescent lulls in between.

This phenomenon, and the initial motivation for this study, may be best illustrated by the plant operating data shown in Figure 30. This is a 20-minute record of wave elevations at the pressure sensor (upper panel) and Turbine 13 power output (lower panel), on February 19th, 2018, from half past midnight to 0:50 (data sources and other specifics will be presented in the following sections). While groupiness may not be so conspicuous in the wave elevation record shown, the elevation squared (middle panel), which is more relevant for the wave energy flux, shows more pronounced grouping. Turbine 13 power output shows very marked patterns of high output sequences, which may last from 15 seconds to slightly over one minute, where power is over the turbine nominal power of 18.5 kW, followed by lulls of a few minutes where output is a few kW or less.

This behaviour is not resolved in 20-minute samples. One may be tempted, therefore, to investigate whether the turbine output on shorter time scales (during the peaks or lulls) may be usefully related to some characteristic of the incoming wavefield at the corresponding time scales (for example, a group of large waves or a peak in the elevation squared, or energy flux).

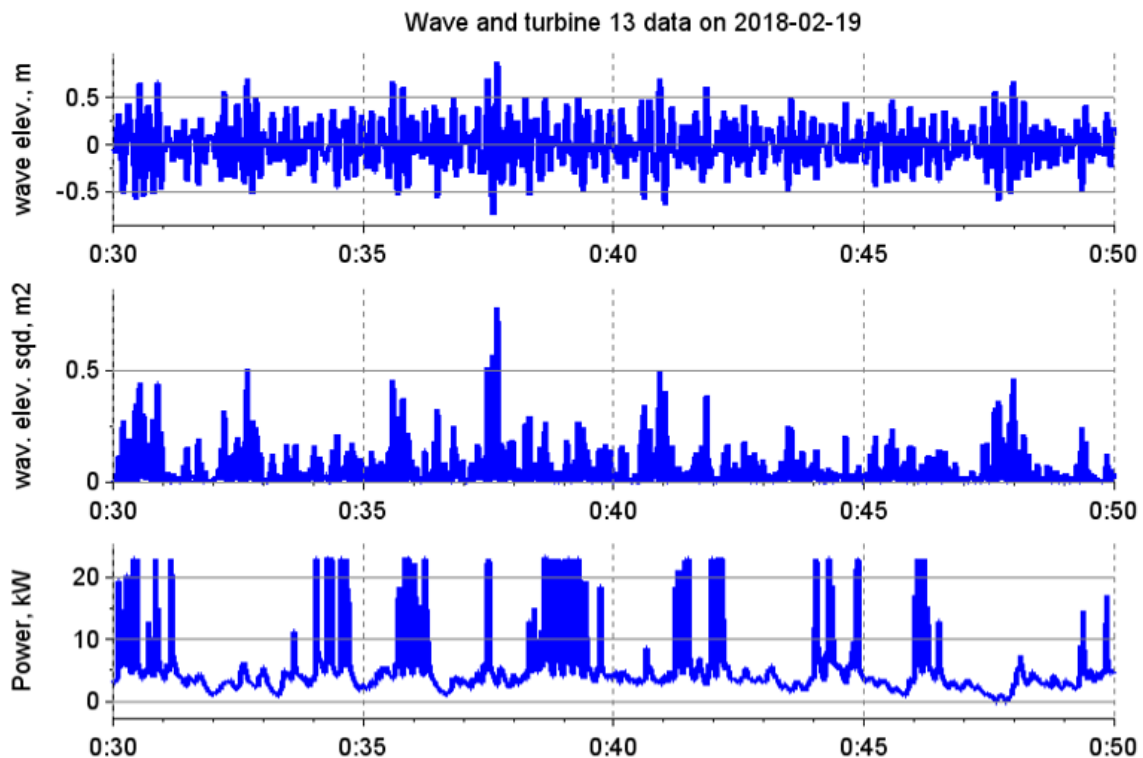


FIGURE 30: AN EXAMPLE OF HIGH PEAK TO AVERAGE POWER OUTPUT AT MUTRIKU

This is, essentially, the initial motivation to investigate plant production at short time-scales, with an objective to relate turbine output to individual waves characteristics.

Successfully relating turbine output and wave characteristics at these time scales may have valuable applications, such as:

- Better understanding and specifying how the WEC power output behaviour can be related, and predicted, by certain measurable conditions in the wavefield
- Reducing dispersion in power performance samples: could shorter individual samples of power performance better resolve the peaks/lull in power output and thereby better predict them by peaks/lull in wave power?
- Possibility to have more samples in the same testing period, which would allow for reduced error on the mean
- Possibility to populate more parts of the power matrix, since shorter sea-states are expected to show more variability (this will be shown in the following sections).

These possibilities become particularly attractive considering the high cost of testing time to developers. Another important aspect is that power output may depend on device configuration, such as control strategy. For example, in OPERA, seven control strategies were tested and compared at Mutriku, with impacts on power output of the order of 50%. In this context, the possibility to have meaningful information on power performance of a particular

device configuration with shorter samples becomes increasingly crucial for effective use of at-sea test time.

4.2.2 TECHNICAL ISSUES WITH POWER ASSESSMENT AT FINER TIME-SCALES

There is at least one obvious technical difficulty in reducing the sampling time for WEC power performance assessment. It relates to the necessary sampling time to obtain meaningful wave statistics.

Long experience with the analysis of wave records has shown that to obtain meaningful statistics on the heights and periods of waves, a minimum record length of some twenty minutes is necessary. More precisely, common practice is to use 1024 seconds (17 min and 4 seconds), which corresponds to 2048 data points sampling at 2 Hz (a power of two is best for efficiency of the fast Fourier transform (FFT) algorithm). This corresponds to some hundred waves of period 10 seconds and is a good trade-off between acceptable sampling variability and the need for a stationary sea-state (e.g., Goda 2010 [14]). For more slowly varying wavefield, such as remotely-generated swell after its initial arrival, records longer than 30 minutes are preferred. IEC-TS/62600-100, Edition 1, Clause 6.2, specifies a minimum sample duration of 20 minutes. It is noted therein that a short sampling duration can result in poor characterisation of the sea-state.

Another issue with using shorter records is the lack of frequency resolution with the spectral analysis. Wave statistics such as peak period or energy-mean period are obtained with spectral analysis. To obtain reasonable confidence intervals in spectral component estimates, common practice in oceanography is to combine FFTs on 8 sub-records, which gives 16 degrees of freedom. A 1024 seconds record divides in eight 128 sub-records, the Nyquist interval in this case results in a resolution a little worse than 2 seconds for variance at periods over 15 seconds. Coarser resolution in variables such as peak period may become a problem for many marine applications. IEC-TS/62600-100, Edition 1, Clause 7.5-a) specifies that the minimum frequency resolution for the spectral analysis of wave data is 0.015 Hz, which means sub-records of at least 66 seconds.

Section 4.4 reports on the examination of characterising the sea-state with short samples. In brief, it appears that while the aforementioned issues may be problematic for studies focussed on assessing the wave climate, their impact on the analysis of WEC power performance may be more manageable. The effectiveness of various methods used to deal with the issues outlined above is reported.

4.3 MEASUREMENTS AVAILABLE

The analysis presented in this section is focused on operating data from EVE's Mutriku shoreline wave power plant. The main reason for this focus is the availability of high-quality

datasets with little or no confidentiality requirement. However, the analysis of sample variance also includes data from Marmok, Oceantec's (now IDOM) floating WEC operating in BiMEP.

4.3.1 BIMEP

Wave measurements at BiMEP were presented in various reports from WP1. Briefly, spectral wave data is available every 20 minutes from a Triaxys particle-following buoy situated some 200 m upwave of the WEC. If needed these can be complemented by data from the bimep reference buoy, a FUGRO heave-pitch and roll buoy deployed about 1 km to the south the WEC, and several Zunibal particle-following buoys within the same distance.

Regarding power performance data, Borja de Miguel of IDOM kindly provided data of standard deviation in power outputs, normalized to mean power, for many cells of the power matrix.

4.3.2 MUTRIKU

There are many data streams from the Mutriku shoreline plant. This analysis focusses essentially on wave and plant data from two deployments in 2018: Phase II, from February to mid-April 2017, and Phase III, of which the useful data is from July to mid-August 2018.

It should be noted that the First Edition of IEC62600-100 explicitly excludes shoreline devices from its scope. Also, the data available does not comply with minimum requirements therein to evaluate annual energy production, such as at least a full-year of operating data to correctly sample seasonality. However, useful conclusions can be obtained with the data available at Mutriku on the impact of sample duration on power performance assessments.

4.3.2.1 WAVE DATA

The main source of wave data in this study is an RBR pressure sensor and data-logger installed on the seabed some 200 m upwave of the plant.

Wave instrument deployed

An RBR virtuoso pressure transducer was deployed some 200 m upwave of the wave power plant in Mutriku (Figure 31). This distance is a trade-off between representativity of the wavefield at the wave power plant, which requires proximity, and reducing the impact on measurements of the waves reflected off the breakwater at Mutriku, which can be important up to about this distance (Pedro Liria, personal communication 2018). Approximate coordinates are as follows:

Mean depth: 9.5 m

Latitude: 43°18'51.59"N

Longitude: 2°22'33.99"W

Data used in this analysis are from two deployments in 2018, Phase II (January 31 to April 18th) and Phase III (June to Mid-August).



FIGURE 31: POSITION OF THE WAVE INSTRUMENT UPWAVE THE PLANT

Processing of data

The pressure is sampled at 2 Hz. To remove tidal and non-wave signal, a 10-minute moving mean average is used. Pressure is converted to depth assuming hydrostatic balance and linear wave theory (see below considerations on the validity of this approximation) and seawater density values typical of this region and season. More details are available in the OPERA Technical Note: Processing of Bottom-Pressure Sensor Data (2018). The calculation of wave statistics from wave heights is described in Section 4.4.

Possible limitations with wave statistics from nearshore pressure sensor data

Compared to deeper water sea waves, the nearshore wavefield includes a number of phenomena which impact the analysis and interpretation of wave data. One issue is wave breaking, which occurs as far as 300 m offshore during winter in Mutriku. In general, the wavefield in the nearshore may be more non-linear, which will influence wave statistics such as significant wave height. In addition the seabed in Mutriku is highly irregular, with large rocks and other topographic features of one meter or so in scale (see Figure 32 for an example of such topographic features). Thus depth changes by some 10% over distances of a few meters,

and this could modify the wavefield in various ways such as scattering, refraction, and bottom friction.

It is expected, thus, that the wavefield upwave of Mutriku have significant variability at small spatial scales. This is confirmed by plant data, which shows that the wave climate for OWC chambers just a few meters apart can be significantly different. Clearly the wavefield at the pressure sensor 200 m upwave cannot be expected to be the same as the wavefield at the shoreline and for any particular chamber of the plant. These data are not adequate for purposes such as assessing the wave resource at the WEC location. In general, measurement of the incoming wavefield for shoreline devices is expected to include some additional complications relative to the deeper water WECs, though they may be less severe on gently sloping beaches than on an irregular coastline with rocky bottom such as that faced by the Mutriku plant.

Regarding the instrument itself, bottom-pressure measurements have long been used as a convenient and cost-effective way to analyse waves and is generally reported to be accurate to within 5% for important wave statistics [15], [16]. In the conditions of deployment at Mutriku, that include humbling plunging breakers in winter and large rocks sloshed around the seabed by these, measuring from the bottom was the only option that entered within project budget. And even then, surviving one winter was not obvious. However, it should be noted that there are issues specific to the measurement of waves with bottom-fixed pressure sensors. In OPERA deliverable D4.2 [17], Annex 8.2, João Henriques et al. discuss how, when applied to predictive control of WECs, bottom-pressure sensor data analysed with linear wave theory may result in underestimation of short-period waves. The data from the sensor appears



FIGURE 32: A VIEW OF THE SEABED NEAR THE PRESSURE SENSOR UPWAVE OF MUTRIKU (FROM: CDA)

rather consistent with this possibility, with a low occurrence of sea-states with short energy period (more details in Section 4.5.3 when discussing the scatter diagrams obtained).

After reviewing these potential limitations, it should be clarified that the wave pressure record available is quite well correlated with the plant operating data. No obvious ways have been found by which imperfection in the wave measurements should greatly impact broad conclusions on the influence of sample duration on power performance assessment of WECs.

4.3.2.2 PLANT DATA

The Mutriku plant operating data used in this analysis was provided by François-Xavier Faÿ of Tecnalia, after processing as part of investigation conducted in H2020-OPERA/WP4 (see e.g. [17]). Pressure differential, turbine rotation velocity, butterfly valve angle and power output for turbines 7, 13 and 15 are used in this analysis, with a focus on turbine 13 as it has the best coverage and may be the most directly impacted by waves measured at the pressure sensor location. WP4 and WP1 deliverables should be consulted for details of the Mutriku wave power plant instrumentation.

4.4 PROPAGATION TIME FROM PRESSURE SENSOR TO OWC CHAMBERS

To match power output time series with the incoming wavefield statistics at shorter time scales, the wave propagation time from the pressure sensor to the plant chambers must be accounted for. An initial study [18] showed promising results in relating phase lag between signal at the pressure sensor and in the OWC chamber pressure with the tidal height. This work was subsequently extended to a larger dataset but at time of writing, an unambiguous prediction method for the propagation time has not been obtained. This section reports on the methods used and technical difficulties encountered.

Attempts to predict propagation time at Mutriku in this project can be classified into three groups. The first is based on shallow water linear wave theory, relating wave group velocity to observed tidal height. The second is analysis of time-lag in the cross-correlation functions between the pressure signal at the sensor and the pressure signal in the OWC chambers. The third one is the manual identification and matching of individual wave features in the pressure signal and in plant operating data. Experience applying these three methods is reported in the following subsections.

4.4.1 PROPAGATION TIME FROM LINEAR WAVE THEORY

In water depths significantly lesser than the wavelength of ocean gravity waves, these become non-dispersive and the frequency-independent propagation velocity, in this case equal to the phase velocity, can be approximated as:

$$c_g = c_\phi = \sqrt{gD}$$

where c_g is the wave propagation velocity (or group velocity), c_ϕ is the phase velocity, g is the gravity acceleration and D is the water depth. In this approximation thus the wave velocity at some point nearshore is entirely determined by the water depth only.

Nearshore multibeam data collected in earlier projects in this area was kindly provided by Azti-Tecnalia. Figure 33 shows a colour rendition. The meter scale features discussed earlier are quite visible in this high-resolution data. A representative mean depth along the wave rays is necessarily a rather coarse approximation.

Tidal elevation are obtained from 10-minutes averages of the pressure sensor as discussed in the previous section. Inclusive of tides, mean depth at the sensor during the observed period ranges from 7.5 to 12 m. The resulting propagation time from linear wave theory range from 19.5 to 27 seconds. While it is expected that this approximation will have limited accuracy due to non-linearity in the wavefield, complex topography, changes in wave direction, etc.; it does provide a useful indicator of the expected range in propagation time.

4.4.2 PROPAGATION TIME FROM TIME-LAGGED CROSS CORRELATION

For certain pairs of signals, identifying a maximum in the time-lagged cross correlation function is a useful approach to determine a representative delay between them. This section

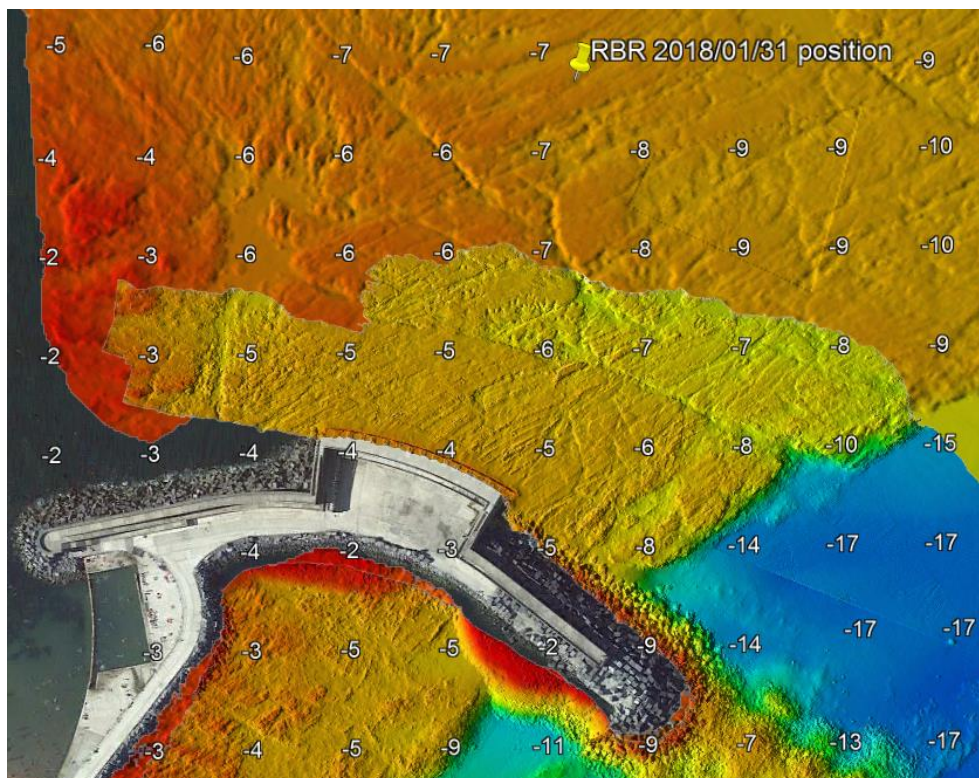


FIGURE 33: BATHYMETRY UPWAVE THE MUTRIKU PLANT

reports on the complications encountered in applying this method with the pressure sensor and plant data.

The main problem is the difficulty to distinguish between the peaks in cross-correlation that correspond to (1) the time-lag between an individual wave signal in the pressure sensor and this same wave's signal in the plant operating data, which is the peak that is required here to evaluate propagation time; or (2) those peaks that correspond instead to the correlation between successive waves. No method was found to unambiguously discriminate between those two. That the average propagation time from linear theory, at some 20 or so seconds, approximately corresponds to two wave periods is adding to the complication.

As illustration of this problem, the calculated cross-correlations between pressure sensor derived wave elevation and Turbine 13 pressure and power output for a 20-minutes sample on April 4th, 2018 are shown in Figure 34. It is apparent that while there is periodicity in the extrema in correlation, it is difficult to assign a particular peak or minimum to either the propagation time or to the periodicity in the incoming wave signal itself.

Another issue illustrated in Figure 34 is the different phase lag for the chamber pressure and power output. The turbine rotation velocity has yet other lags for its extrema (not shown). Determining which of these should be considered the relevant phase lag would necessitate a consideration of the details of excitation forces and response of the oscillating water column, generator characteristics, etc.

In summary, basic cross-correlation analysis does not appear to easily provide useful estimates of propagation time for these data. However, it is possible that more advanced analysis inclusive of the details of the chamber and generator physics would be more successful.

4.4.3 MANUAL IDENTIFICATION OF INDIVIDUAL WAVE SIGNALS

As described above, periodicity in the wave signal complicates the matching of peaks and troughs in the pressure sensor data upwave to peaks and troughs in the plant operating data and power output. However, it should be possible to identify and match individual events that are not periodic. These could be, for example, an isolated large wave or wave group, or the end/beginning of a lull or of a high-activity run in incoming waves. [18] obtained promising results with a short stretch of data from late 2016 with this approach. Apparent propagation times were well correlated to tidal heights in ways that could be well predicted by linear wave theory. Unfortunately at time of writing it was difficult to reliably obtain similar results with this dataset. This section reports on the methods applied and technical difficulties encountered.

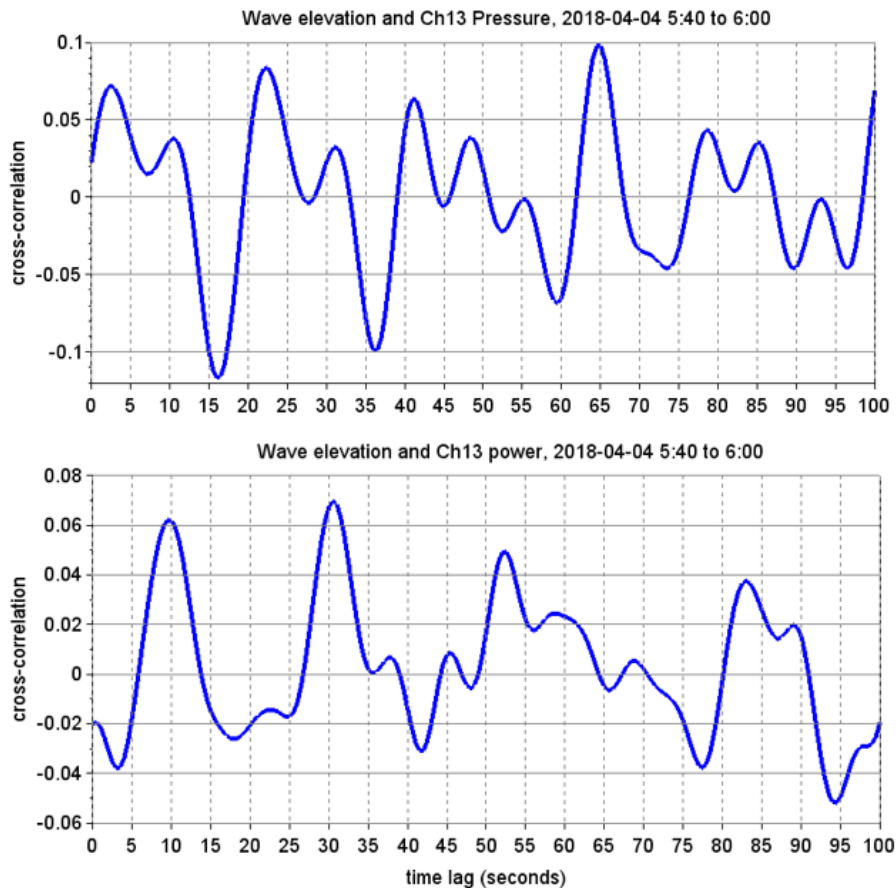


FIGURE 34: TIME-LAGGED CROSS CORRELATIONS BETWEEN WAVE SIGNAL AND PLANT OPERATING DATA

Figure 35 shows an example of matching incoming wave data to plant power output. As is often the case, it is difficult to identify clearly non-periodic features in the original wave elevation record. However, the wave elevation squared or the square of the heave velocity derived from the original time series of wave elevation, which are better indicators of the incoming wave energy flux than surface elevation, reveal pronouncedly non-periodic events. The lower two panels show an example of matching lulls before a burst in incoming wave energy and plant output; and matching peaks in the square of the heave velocity to peaks in plant outputs. In this particular case, both methods yield propagation times of about 30 seconds.

Figure 36 shows another matching, where more of the available plant data is used. In this case, turbine pressure differential or rpm exhibit strong periodicity and are thus difficult to use. Turbine power output and, again, wave heave velocity squared reveal pronounced non-periodic events. (The thin blue and green in the power graph are the outputs of Turbine 7 and Turbine 15 – showing, incidentally, how the long-crested approximation is not valid for the incoming wavefront). In this particular case the peak can be better matched than the ends of lulls, but for many cases analysed the situation was reversed.

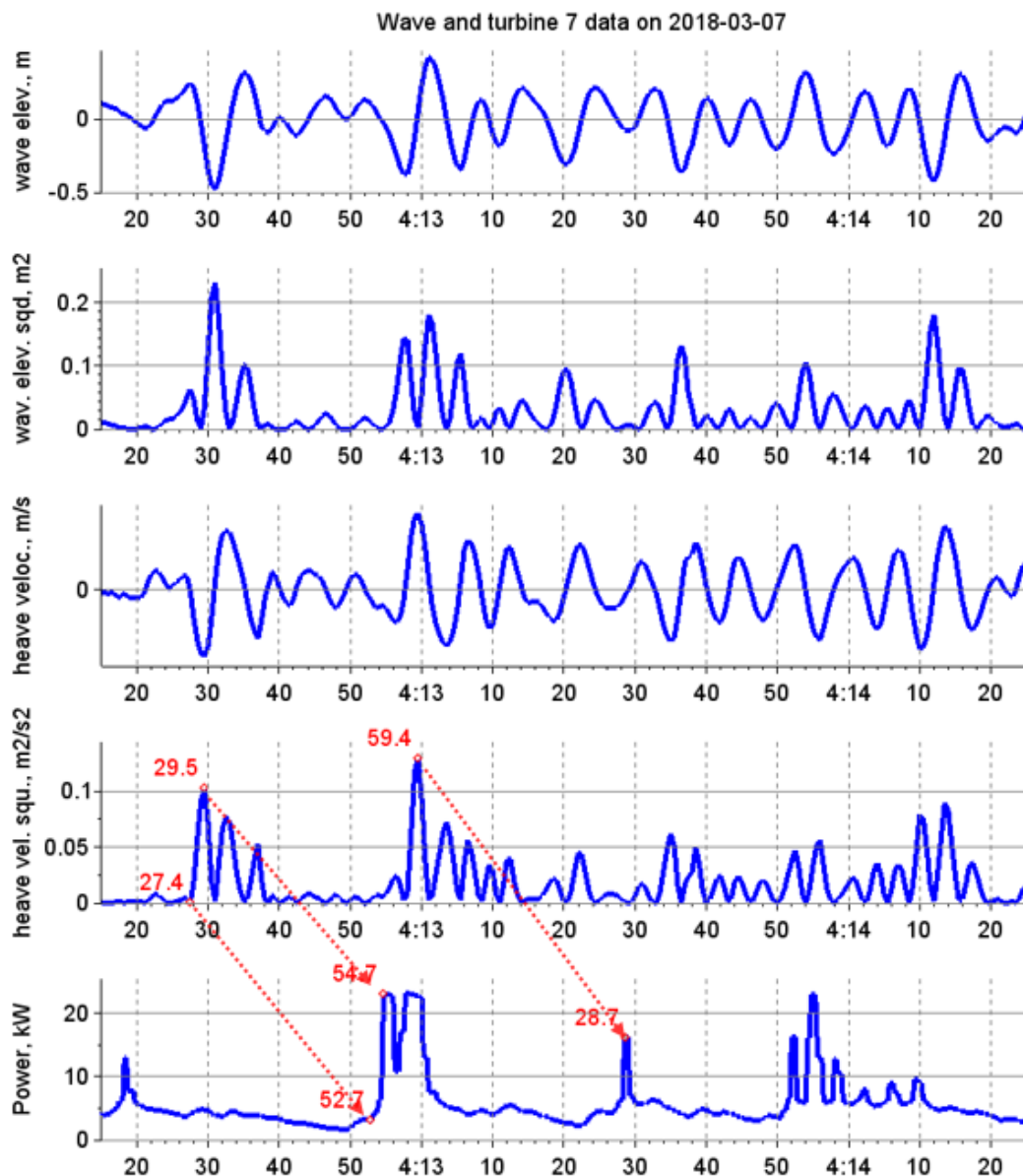


FIGURE 35: EXAMPLE OF MATCHING WAVE DATA TO PLANT DATA

This method appears to work rather well when zooming-in on short stretches of a few minutes. Specific individual wave features can be matched seemingly unambiguously to individual features in the plant response, and the lags obtained do not exhibit clear inconsistencies in other parts of the few minutes stretch. However, when considering many such cases with longer spacing in time, no coherence was found across cases in the propagation times obtained. Differences do not appear to be easily explained by tidal elevation or other measurements available.

Nonetheless, despite the scatter in the time lags, it is found that propagation time is almost always roughly within the range that is expected from linear shallow water wave theory.

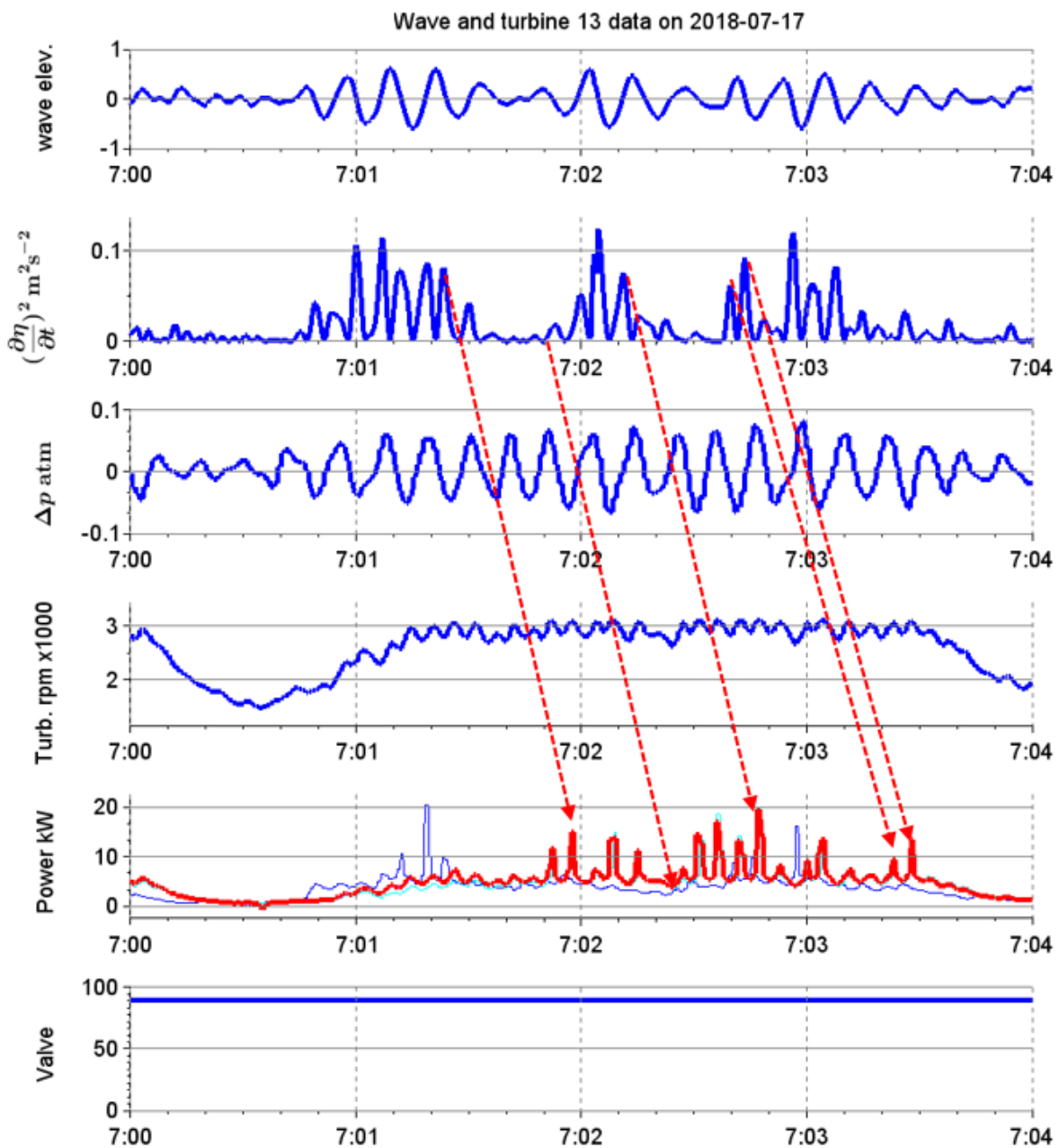


FIGURE 36: OTHER EXAMPLE OF MATCHING OF WAVE AND PLANT DATA

Should a rough approximation be needed for a particular application, a mean propagation time of 20 to 30 seconds is suggested.

4.5 WAVE STATISTICS FOR RECORDS OF LESS THAN 20 MINUTES

As discussed in Section 4.2.1, standing in the way of exploring the potentially valuable benefits of using shorter samples of WEC power performance, one important issue is whether meaningful wave statistics can be obtained using records shorter than 20 minutes (or 17 min 4 s, to be more precise). In applying the method used to try to address this, it is found that:

- ▶ The meaningful definition of the energy period for short records is far more complicated than the definition of a significant wave height for short records
- ▶ The lack of established practice and studies on the use of records shorter than 20 minutes to characterise the wavefield means that further, more rigorous work on this aspect would be useful
- ▶ However, reducing the sampling record length from three hours to as short as five minutes had little impact on two important statistics for WEC power performance assessment, the scatter diagram and the power matrix (or a proxy of it, as will be discussed later), and consequently little impact on energy yield prediction.

These findings are reported on in detail below.

4.5.1 SPECTRAL SIGNIFICANT WAVE HEIGHT

It is common practice to characterise a wavefield by its spectral significant wave height H_{m0} , which is defined e.g. in IEC-TS/62600-100 as

$$H_{m0} = 4.00 \sqrt{m_0}$$

Where m_0 is the zeroth moment of the distribution of the spectrum of a surface elevation time series. The n th moment is defined as

$$m_n = \sum_{i=1}^N S_i f_i^n \Delta f_i$$

Where S_i is the i -th spectral component, that is, the spectral density of variance in the surface elevation record associated to frequency f_i , and Δf_i is the width of the frequency band associated with frequency f_i . N is the total number of spectral components of the spectrum. In this particular case,

$$m_0 = \sum_{i=1}^N S_i \Delta f_i$$

so that m_0 is simply the total variance in the spectrum, which, from Parseval's identity, must equal the time-domain variance of the samples of wave heights in the wave records.

Hence the spectral significant wave height H_{m0} must equal four times the square root of the signal variance, or four times the standard deviation of the surface elevation. This relationship gives a straightforward way to assign a value to H_{m0} for short records based on the variance observed in the time-domain, as

$$H_{m0} = 4 \sqrt{\sigma}$$

Where σ is the standard deviation of the samples of surface height in the wave record.



Whether this is a meaningful statistic for records shorter than 20 minutes depends on the intended use. As will be shown later, for the purpose of WEC power performance assessment this definition of H_{m0} does not appear to give rise to particular complications – or at least, much less so than the energy period, as will be discussed in the next section.

As a basic consistency check for the short samples significant wave height, the relationship with time-domain statistics were examined. [19] showed that the wave heights reported by human observers was closely related to the average heights of the highest one third of the waves. Thereafter this was referred to as the significant wave height of a wavefield. It is usually noted $H_{1/3}$. It was found that for most wave records, the spectral significant wave height H_{m0} and time-domain significant $H_{1/3}$ are equal in very good approximation. However, for nearshore waves significant differences are reported and must be considered for the design of coastal structures [20].

Figure 37 shows the scatter plot of spectral significant wave height obtained from the time-domain variance (or equivalently, m_0) against the average height of the highest one-third of the waves ($H_{1/3}$) for one-hour and five-minute samples. The correspondence is good for both, though a slight tendency for larger H_{m0} may be seen for the short samples at larger wave heights. For extreme events ($H_{1/3}$ over 4 meters) it does appear the five-minute samples lead

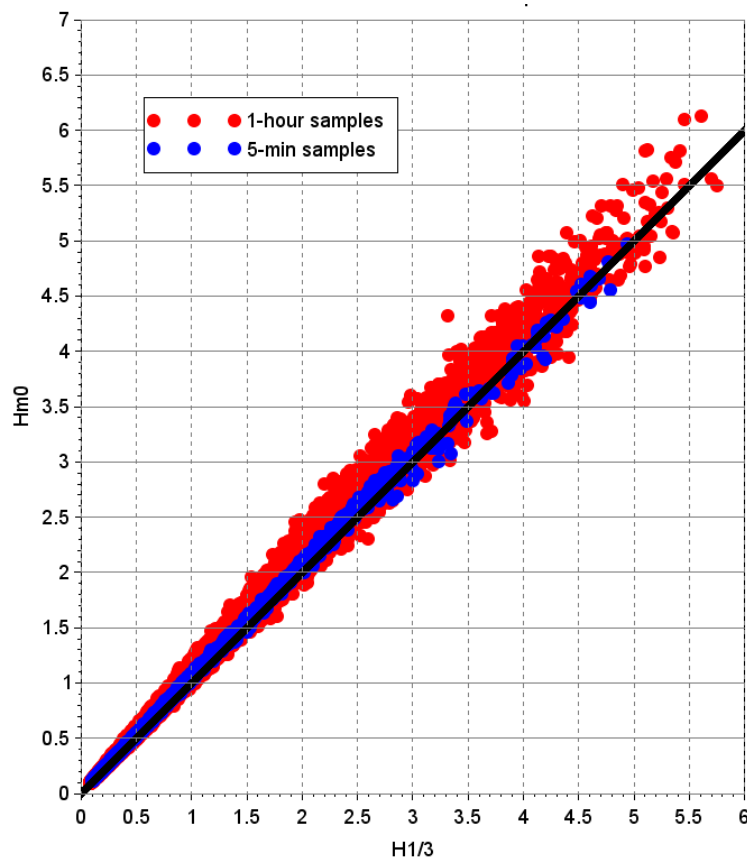


FIGURE 37: H_{m0} VS. $H_{1/3}$ FOR 1-HOUR AND 5-MINUTE SAMPLES

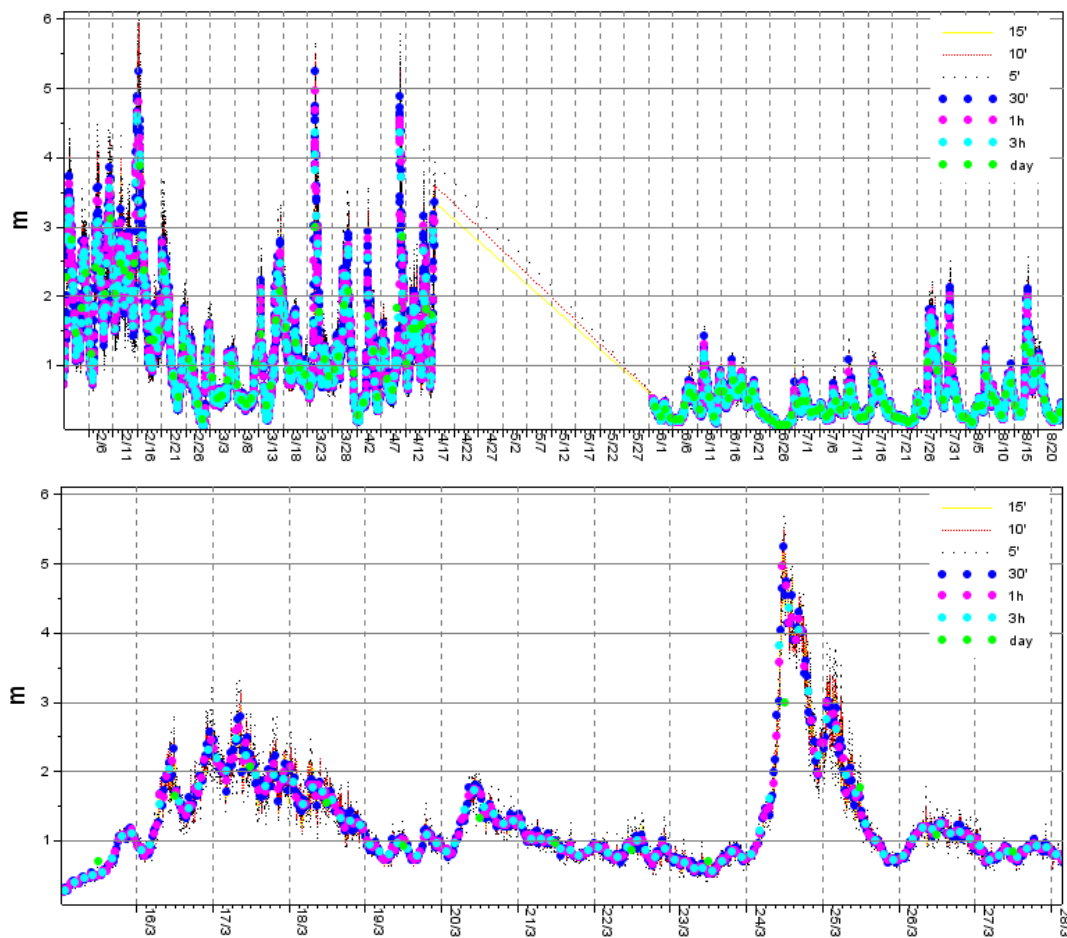


FIGURE 38: TIME SERIES OF SIGNIFICANT HEIGHTS FOR VARIOUS SAMPLE DURATIONS

to significantly higher H_{m0} , but these occur so rarely that this is not expected to impact power performance analysis for this plant, where contribution to annual yield of such extreme events is negligible.

The time series of significant wave heights obtained with this method and for sample durations ranging from 24 hours to 5 minutes is shown in Figure 38. The whole record is shown (upper panel) as well as a zoom around a storm event end March 2019. As expected, the short sample variability is higher, oscillating around the longer samples average with amplitudes of the order of half a meter. Apart from this, no striking inconsistency is found between the time series.

In summary, no particular difficulties were found in assigning a significant wave height to short duration samples, using the equivalence of variance in the spectral and time domain. The utility of the wave statistics, and in particular, the scatter diagrams obtained with this method will be discussed in the section on annual energy production.

4.5.2 ENERGY PERIOD

Together with significant wave height, energy period is the other commonly used wave statistic to which WEC power output dependence is analysed. Unlike the evaluation of significant wave height for which time domain variance, or mean of the highest third of waves could be used, for energy period, a spectral analysis is needed, which complicates the definition of meaningful values for short samples. These issues and some methods that appear to partially remediate them for this particular dataset are presented in this section.

It is worth recalling here that as discussed in Section 4.3.2.1, data from the pressure sensor on the seabed, independently of the sample duration, leads to a low occurrence of short-period sea-states. This could be related to measurement limitations or to nearshore phenomena such as refraction of longer-period waves off from the undersea canyon to the east of the plant. This does not appear to affect shorter samples more than longer samples so it is not expected to significantly change the results presented hereafter.

Energy period is defined (e.g. in IEC-TS/62600-100-Ed.1/7.5-e) as the variance weighted mean of the period of the spectral components, as:

$$T_e = \frac{m_{-1}}{m_0}$$

Where the moments of the spectral distribution m_{-1} and m_0 are defined as per the previous section. As a ratio of integrals of the spectrum, it is less sensitive to details of the spectral analysis than the peak period commonly used in marine structure design, but it still normally requires adequate record length to reduce confidence intervals on spectral component estimates.

In looking at the coherence of estimates of T_e as the time resolution is increased (and record length for the spectral analysis shortened), it was found that for this dataset it is useful to ensure only variance at wave frequencies should be used. Including spectral components outside wave frequencies resulted in shorter-sample sea-states with consistently higher T_e . It was found that using cut-off periods of between 4 and 40 cycles per second removed low-frequency variance that is more present in the longer-sample spectra than in the shorter-sample spectra. With this first fix the energy periods of samples of duration ranging from three hours down to ten minutes were found to be in acceptable agreement, inasmuch as their mean values were similar.

It was then found that the five-minute samples energy period was still consistently higher than that of longer samples. The main contributor appears to be the lack of resolution of the spectral analysis, where the Nyquist frequency interval results in too coarsely spaced periods in the range of interest.

Figure 39 is an example of this problem for a record on the morning of 18 March 2018. The spectrum obtained with 16 degrees of freedom (DOF) on a 1-hour record (upper panel) has good resolution even for long period wave. (The vertical dashed lines indicate the periods corresponding to the frequencies on the abscissa for convenience). The spectra obtained for the 12 five-minute records within this 1-hour record are on the mid and lower panels, obtained with respectively 8 DOFs and 16 DOFs spectra.

The important difference between the middle and lower panel on Figure 39 is that the 15 second component that was still in the 8 DOF spectrum has disappeared in the 16 DOF spectra, as expected from coarser Nyquist frequency interval. Consequently the variance that could project on the 15 seconds component now must project on the adjacent components near 12 seconds and 20 seconds. As a consequence, the integration of the variance to obtain m_{-1} will result in spuriously high variance assigned to periods longer than 20 seconds. This will result in a bias towards longer energy periods if the five-minute samples are analysed with 16 DOF spectra. While reducing the degrees of freedom from 16 to 8 will result in larger errors bounds for the spectral components, it is found that this is a preferable limitation than the significant bias towards long energy periods.

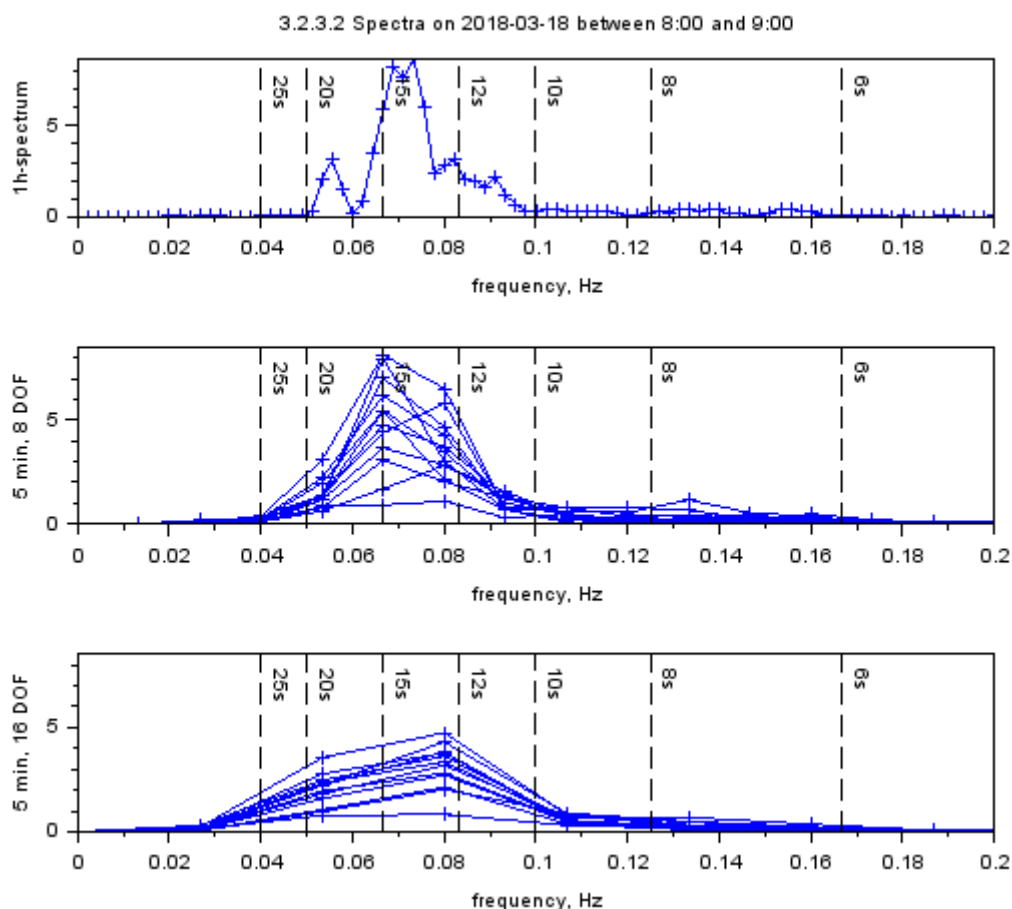


FIGURE 39: EXAMPLE OF RESOLUTION PROBLEM WITH 16 DOF SPECTRA IN SHORT SAMPLES

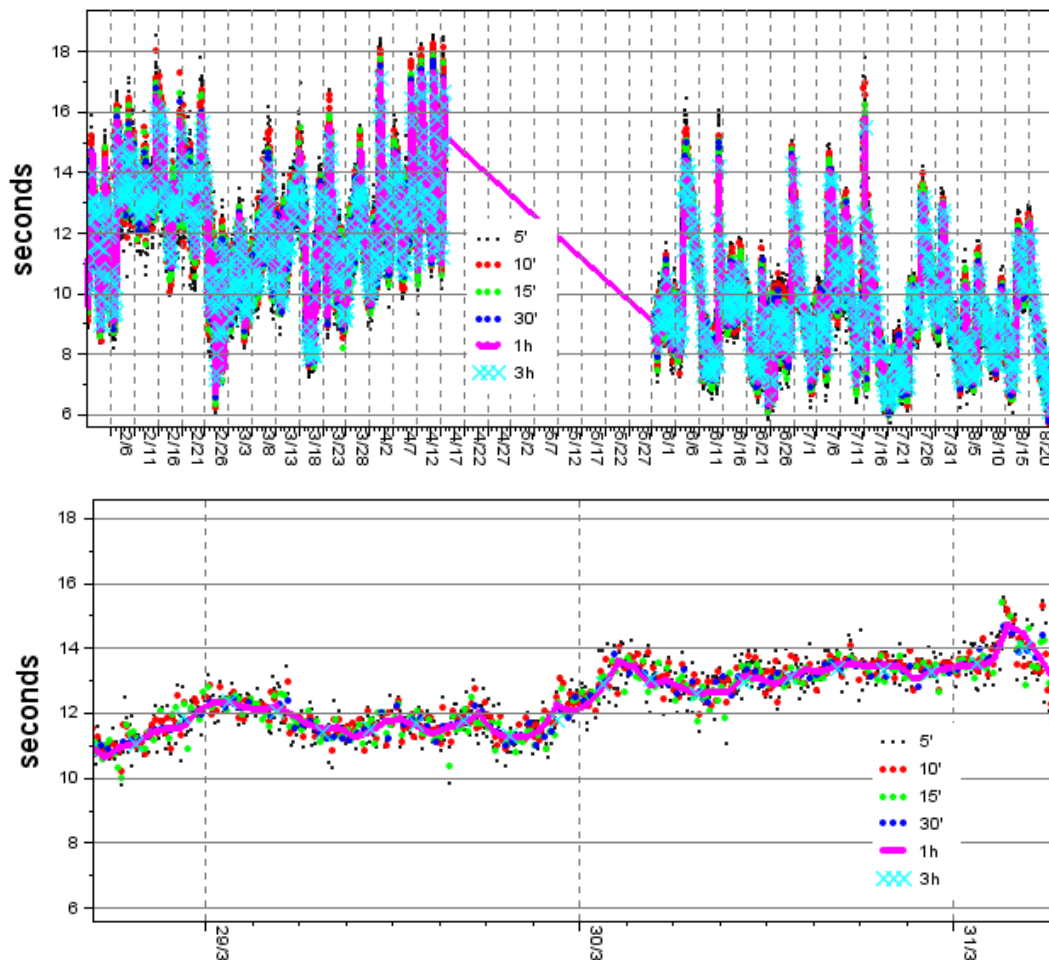


FIGURE 40: ENERGY PERIOD OBTAINED FOR THE RECORD AND ZOOM ON END MARCH

Figure 40 shows the time series of energy periods obtained with the various sample durations, with the aforementioned corrections for short samples applied. The long time series shown in the upper panel illustrate the good overall coherence of the energy periods with various samples. The zoom on end March in the lower panel shows the larger scatter for the short samples. The five-minute T_e oscillate around the hourly values with an amplitude of about 1 second.

As a basic consistency check, the relationships between the energy periods from these spectral analysis and zero-upcrossing periods from time-domain analysis were compared. The scatter plot of the energy period for one-hour and five-minute samples (with the corrections applied) vs. the mean of the zero-upcrossing period for the highest third of the waves in the samples is shown in Figure 41. While scatter is higher for the short samples (as expected from the much larger population), the means and their trends with the zero-upcrossing period are quite consistent.

In summary, certain complications were found when attempting to assign meaningful values of energy period to short samples. Simple methods were presented that appear to

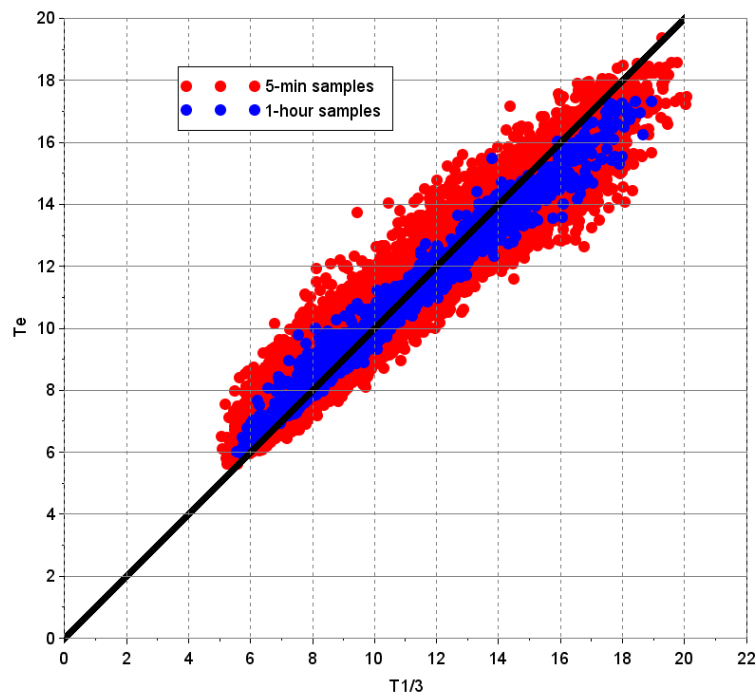


FIGURE 41: ENERGY PERIOD VS. MEAN UPCROSSING PERIOD OF THIRD OF HIGHEST WAVES

significantly reduce the problems for this dataset. As will be discussed later, a convenient metric to evaluate the utility of the resulting sea-states, for the purpose of power performance assessment, is the impact on annual energy production estimates of changing the scatter diagrams obtained with the longer samples with those obtained with shorter samples. It will be seen that for the data available for this analysis, resulting differences are within an acceptable range.

4.5.3 SCATTER DIAGRAMS OBTAINED

The scatter diagrams obtained with the wave statistics at time scales from 3 hours to 5 minutes are reported in this section. Due to the limited coverage of the data used, these diagrams are not representative of conditions near Mutriku for the whole year. However, conditions for winter, spring and summer are reasonably well sampled, so the range of wave conditions at Mutriku should be covered. Also, the earlier discussion of how the wavefield at the entrance of the OWC chambers may be significantly different from that at the pressure sensor should be borne in mind.

Table 1 and Table 2 show the scatter diagram obtained with 1-hour wave records and 5-minute wave records, respectively. Compared to scatter diagrams obtained from wave buoys at BiMEP nearby (Table 3, see OPERA/WP1 deliverables for more details), both have low occurrence of sea-states with short energy period. This absence is consistent with the bias towards longer periods, especially for shorter-period sea-states, that would be expected from the dynamic effects detailed by Henriques et al. in OPERA/D4.2 [17]. However, it could be

TABLE 1: SCATTER DIAGRAM OF HOURLY SEA-STATES AT PRESSURE SENSOR

Hs (top of bin)	>5.5																		
	5.5																		
	5													0.1	0.1				0.2
	4.5												0.1	0.1	0.2				0.4
	4											0.1	0.2	0.2					0.5
	3.5											0.1	0.5	0.3	0.1	0.1			1.1
	3											0.8	1.5	0.5	0.2	0.1			3.2
	2.5											1.4	2.6	0.6	0.1	0.1			4.7
	2				0.1	0.1	0.1	0.9	1.8	3.3	0.7	0.3	0.1	0.1					7.5
	1.5			0.2	0.6	0.8	3.0	3.3	2.7	1.5	0.8	0.4	0.2	0.1					13.5
Hs (top of bin)	1		0.1	1.6	1.6	7.5	7.0	4.7	3.3	1.7	0.3	0.1							27.9
	0.5	0.1	2.2	8.8	10.0	9.7	4.2	3.3	1.5	0.8	0.5								41.0
		0.1	2.2	10.5	12.3	18.1	14.4	12.1	11.6	12.0	4.1	1.6	0.8	0.3					100
		<4	5	6	7	8	9	10	11	12	13	14	15	16	17	18	19	20	>20
		Te (top of bin)																	

TABLE 2: SCATTER DIAGRAM OF 5-MINUTES SEA-STATES (8 DOF)

Hs (top of bin)	>5.5																		
	5.5																		
	5														0.1	0.1			0.1
	4.5													0.1	0.1	0.1			0.3
	4												0.1	0.2	0.2	0.1			0.6
	3.5												0.2	0.5	0.3	0.2	0.1		1.3
	3												0.6	1.4	0.5	0.2	0.1	0.1	2.8
	2.5												1.3	2.2	0.6	0.2	0.1	0.1	4.7
	2				0.2	0.1	0.2	0.8	1.9	2.5	0.8	0.3	0.1	0.1					7.0
	1.5			0.2	0.6	0.9	2.6	3.0	2.7	1.9	0.9	0.4	0.2	0.1					13.4
Hs (top of bin)	1		0.1	1.5	1.9	6.8	7.0	4.9	3.2	1.8	0.5	0.1	0.1						27.9
	0.5	0.1	2.7	8.5	9.8	9.6	4.8	3.2	1.6	0.9	0.4	0.1							41.7
		0.1	2.8	10.2	12.5	17.4	14.6	12.1	11.5	11.4	4.3	1.9	0.9	0.4	0.1				100
		<4	5	6	7	8	9	10	11	12	13	14	15	16	17	18	19	20	>20
		Te (top of bin)																	

TABLE 3: SCATTER DIAGRAM FROM THE BIMEP REFERENCE BUOY

Hs (top of bin)	>5.5								0.1	0.1	0.1	0.1							0.3
	5.5								0.1	0.1									0.3
	5								0.1	0.1	0.1	0.1	0.1						0.5
	4.5					0.2	0.2	0.1	0.1	0.2	0.1	0.1							0.9
	4				0.2	0.3	0.3	0.3	0.3	0.3	0.2	0.1							2.0
	3.5				0.5	0.6	0.7	0.6	0.6	0.4	0.2	0.1							3.8
	3				0.4	0.7	0.8	1.1	1.0	0.7	0.5	0.3	0.1						5.6
	2.5			0.2	1.0	1.3	1.7	2.2	1.8	1.5	0.9	0.3	0.1						10.9
	2			1.0	2.5	2.4	3.2	3.2	2.8	1.8	0.5	0.2							17.7
	1.5		0.6	3.4	4.7	6.0	5.4	4.1	2.4	0.9	0.3	0.1							27.8
Hs (top of bin)	1	0.3	2.3	6.0	6.7	5.0	3.3	1.7	0.6	0.2	0.1								26.4
	0.5	0.1	0.8	1.1	0.9	0.6	0.2												3.8
		0.4	3.7	11.7	16.2	16.7	15.6	13.7	9.8	6.3	3.2	1.4	0.6	0.1	0.1				100
		<4	5	6	7	8	9	10	11	12	13	14	15	16	17	18	19	20	>20
		Te (top of bin)																	

explained by other nearshore phenomena, such as refraction, diffraction or attenuation of waves. One candidate would be the general topographic configuration, with an underwater canyon to the east of the plant from which long period waves would be refracted off towards the plant. At any rate, again, while a possible bias in the Te estimates would be a problem for

TABLE 4: SCATTER DIAGRAM OF 5-MINUTE SEA-STATES AT SENSOR (16DOF)

Hs (top of bin)	>5.5																		0.1		
	5.5																		0.2		
	5														0.1	0.1					
	4.5													0.1	0.1	0.1			0.3		
	4												0.1	0.1	0.2	0.1	0.1		0.6		
	3.5												0.4	0.4	0.2	0.1	0.1		1.3		
	3											0.2	1.1	1.0	0.3	0.2	0.1		2.8		
	2.5											0.6	1.9	1.5	0.4	0.1	0.1	0.1	4.7		
	2					0.1	0.1	0.1	0.6	1.2	2.5	1.5	0.4	0.2	0.1	0.1			7.0		
	1.5					0.1	0.6	0.7	2.0	3.0	2.5	2.2	1.2	0.6	0.3	0.1	0.1		13.5		
1				0.1	1.3	1.6	5.6	7.2	5.0	3.5	2.2	1.0	0.3	0.1	0.1			27.9			
0.5				2.3	7.8	9.2	9.7	5.0	3.5	2.0	1.1	0.6	0.2	0.1				41.6			
				2.3	9.3	11.5	16.1	14.4	12.2	10.0	11.4	7.3	2.7	1.4	0.8	0.4	0.1		100		
			<4	5	6	7	8	9	10	11	12	13	14	15	16	17	18	19	20	>20	
			Te (top of bin)																		

many applications, for evaluating the impact of using short samples for power performance assessment, there are no obvious reasons why this should affect the main conclusions.

Another aspect that is apparent is that the shorter sample statistics cover more cells of the scatter diagram. (This is clear at Mutriku, comparison with the hourly sea-states at the BiMEP buoy may give a different impression, but that's another sensor in another, deeper location). For about half of the energy period bins, the five-minute scatter diagram has one more bin of significant wave height populated. Further, these matrices only show frequency of occurrence over 0.05% (rounded up to 0.1% in the display). In the matrices of the number of occurrence (not shown), the larger coverage of (H_s, T_e) for the short sample is far more striking. This will also be more visible in the power matrices presented in the following section.

This feature could have been expected from the time series of wave statistics from samples of different durations that were shown in the previous section. As it turns out, this may be one of the chief advantages in complementing post-processing of open-sea performance data with a shorter sample analysis. This will be discussed in more details later.

To complete the earlier discussion on obtaining meaningful estimates of the energy period for short samples, the scatter diagram obtained using 16 degrees of freedom for the spectra on the 5-minute records is shown in Table 4. It exhibit what appears to be a bias towards longer energy periods for all cells above 15 seconds (compare the occurrence of sea-states with energy period over 16 seconds with those in Table 1 Table 2). This is quite consistent with the problems expected from insufficient spectral resolution discussed in the previous section.

The scatter diagrams obtained for other sample durations are also shown for completeness. The significance of the differences between these scatter diagrams is discussed in the next section.

TABLE 5: SCATTER DIAGRAM OF 30 MINUTES SEA-STATES AT SENSOR

Hs (top of bin)	>5.5																	
	5.5																	
	5										0.1							0.2
	4.5									0.1	0.2	0.1						0.4
	4									0.1	0.2	0.2	0.1					0.5
	3.5									0.2	0.4	0.3	0.1	0.1				1.1
	3									0.8	1.4	0.5	0.3	0.1	0.1			3.2
	2.5							0.1		1.3	2.7	0.4	0.1	0.1				4.8
	2				0.1	0.1	0.1	0.8		2.2	2.9	0.7	0.3	0.2	0.1			7.3
1.5				0.2	0.6	0.8	3.2	3.0	2.8	1.7	0.6	0.4	0.1	0.1			13.6	
1		0.1	1.6	1.5	7.6	7.2	4.9		3.3	1.6	0.3	0.1					28.1	
0.5	0.1	2.4	8.6	10.1	9.5	4.3	3.1		1.4	1.0	0.4	0.1					40.8	
		0.1	2.5	10.4	12.3	18.0	14.8	11.8	12.0	11.8	3.6	1.8	0.7	0.3				100
	<4	5	6	7	8	9	10	11	12	13	14	15	16	17	18	19	20	>20
	Te (top of bin)																	

TABLE 6: SCATTER DIAGRAM OF 15-MINUTES SEA-STATES AT SENSOR

[illegible]

TABLE 7: SCATTER DIAGRAM OF 10-MINUTE SEA-STATES AT SENSOR

Hs (top of bin)	>5.5																	
	5.5																	
	5										0.1	0.1					0.2	
	4.5									0.1	0.1	0.1					0.3	
	4									0.1	0.2	0.2	0.1				0.5	
	3.5									0.1	0.5	0.2	0.2	0.1			1.2	
	3									0.5	1.5	0.6	0.2	0.1	0.1		3.0	
	2.5							0.1		1.3	2.5	0.6	0.2	0.1	0.1		4.9	
	2				0.1	0.1	0.2	0.8		1.8	2.8	0.8	0.3	0.1	0.1		6.9	
	1.5			0.2	0.6	0.9	2.7	3.1		2.7	2.0	0.9	0.3	0.2	0.1		13.6	
1		0.1	1.5	1.8	7.0	7.1	5.0		3.3	1.7	0.5	0.2				28.0		
0.5		2.5	8.5	9.8	9.8	4.4	3.2		1.6	1.0	0.5	0.1				41.3		
			2.5	10.2	12.3	17.7	14.3	12.1	11.3	12.0	4.3	1.8	0.9	0.4			100	
	<4	5	6	7	8	9	10	11	12	13	14	15	16	17	18	19	20	>20
	Te (top of bin)																	

4.5.4 SIGNIFICANCE OF DIFFERENCES IN SCATTER DIAGRAMS OBTAINED

The one-hour sea-states and five-minutes sea-states (resp. Table 1 and Table 2) appear rather similar in structure but differences will be better appreciated in Table 8, which shows the cell-to-cell relative differences (positive indicate higher occurrence in the 5-minute matrix). The relative difference is only shown for cells with an occurrence higher than 0.8% in the 1-hour matrix, which together account for over 91% of the record. Cells that occur less frequently may be under-sampled in the hourly record and differences between methods may be large but may not be statistically relevant. Differences are less than 10% for the most frequent sea-states, but there are differences of over 15% or even 20% in some of these cells. A tendency towards lesser occurrence of sea-states with large H_{m0} for longer period sea-states, more of low H_{m0} at these long periods and generally higher occurrence of short-period sea-states is visible in the record of five-minute samples statistics.

The significance of these differences may be appreciated by first comparing to the differences between scatter diagrams obtained with standard sampling duration, and second, evaluating the impact of these differences on key aspects of power performance assessment, such as Annual Energy Production (AEP). The latter is perhaps the most relevant to this analysis.

Table 9 Table 10 show these relative differences for the 3-hourly and half-hourly sea-states respectively. For this dataset, the statistics of H_s and T_e obtained from five-minutes samples at energy periods less than 13 seconds do not differ more from those obtained with standard sample durations of 3-hour, 1-hour and 30 minutes than those standard method differ between themselves. For longer energy periods, however, the relative differences become more significant for the five-minute samples.

Results on the impact of these differences on power performance assessment and in particular on AEP will be presented in the following sections. These suggest impacts of only a few percent

TABLE 8: RELATIVE DIFFERENCE BETWEEN THE 1-HOUR AND 5-MINUTE SCATTER DIAGRAMS

Hs (top of bin)	>5.5																
	5.5																
5	4.5																
	4																
3.5	3																
	2.5																
2	2																
	1.5																
1	1																
	0.5																
		<4	5	6	7	8	9	10	11	12	13	14	15	16	17	18	
		Te (top of bin)															

TABLE 9: RELATIVE DIFFERENCES OF SCATTER DIAGRAM OF 3-HOURLY AND HOURLY SEA-STATES

Hs (top of bin)	>5.5																	
	5.5																	
	5																	
	4.5																	
	4																	
	3.5																	
	3																	
	2.5																	
	2																	
1.5																		
1																		
0.5																		
	<4	5	6	7	8	9	10	11	12	13	14	15	16	17	18			
	Te (top of bin)																	

TABLE 10: RELATIVE DIFFERENCES OF SCATTER DIAGRAMS OF HALF-HOURLY AND HOURLY SEA-STATES

Hs (top of bin)	>5.5																	
	5.5																	
	5																	
	4.5																	
	4																	
	3.5																	
	3																	
	2.5																	
	2																	

on power production estimates, which for many applications will be well within the range of other sources of uncertainty such as interannual variability and intra-site variability in the wavefield.

In conclusion, for this dataset, it appears that samples significantly shorter than twenty minutes can provides wave statistics that are sufficiently stable to be useful for the purpose of power performance assessment. It was necessary to filter out non-wave frequency variance as for longer samples, low-frequency noise impacted the T_e estimates. For sample of duration shorter than five minutes, it is found that reducing the number of degrees of freedom in the spectral analysis is necessary to avoid a significant bias in T_e .

4.6 PLANT OPERATING DATA WITH SHORT SAMPLES

Certain characteristics of the time series of plant operating data with samples of various durations are presented in this section. As for wave statistics, it is presumed that a trade-off must be made between having sufficient resolution in time (short samples) to resolve key

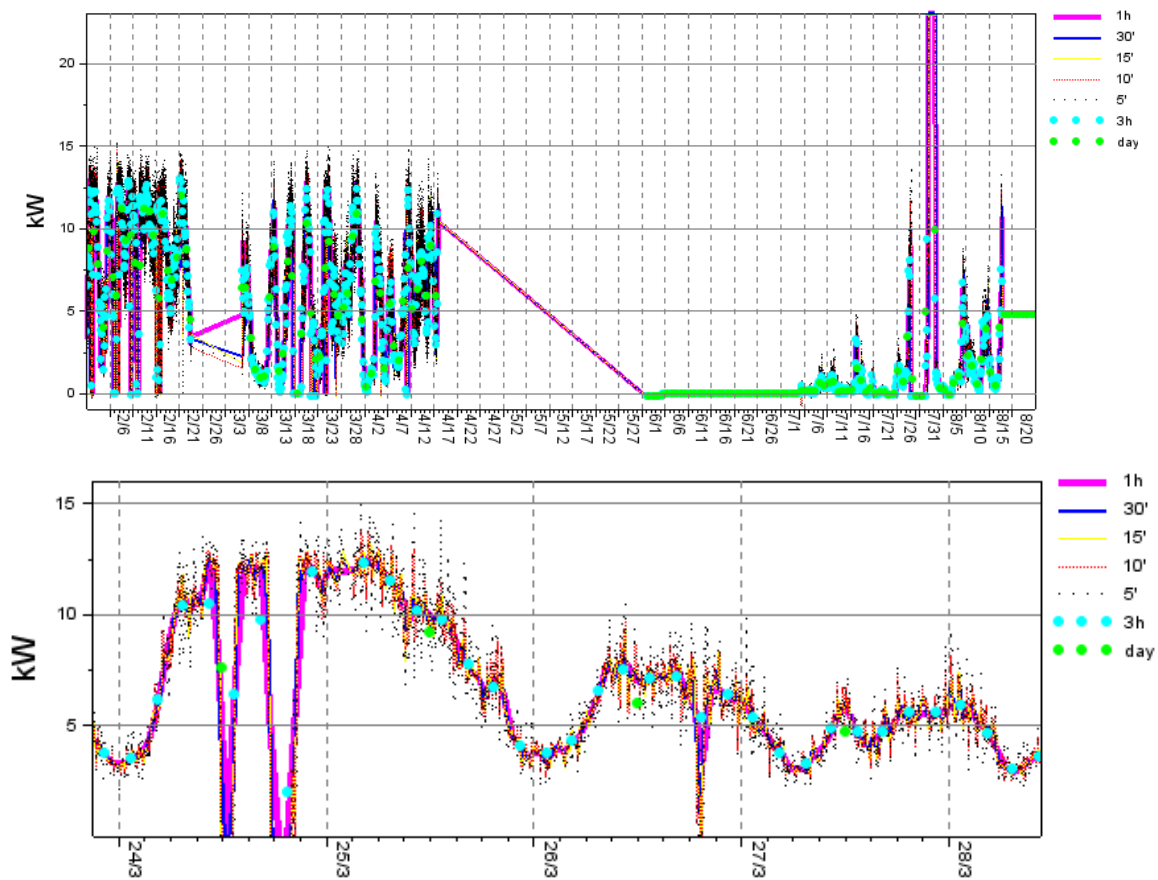


FIGURE 42: TIME SERIES OF TURBINE 13 POWER OUTPUT AVERAGED OVER VARIOUS SAMPLE DURATIONS

plant behaviour, vs. the increase in sample variability and lack of reliability of e.g. estimates of mean power for a short sample. However, much less guidance is available for these data than for wave data. On the other hand, the processing used here is much easier for plant data, where only mean value over the sample duration is needed. It is recalled that in contrast, for wave statistics spectral analysis must be done even for short samples. For this reason particular difficulties from using shorter samples are not expected as was the case for wave data.

Figure 42 shows the time series of power output averaged in samples with duration ranging from 24 hours to five minutes, for the whole dataset (upper panel) and zooming in on a few days late March 2018. Gaps in coverage are visible end February 2018, and then mid-April to June 2018. Also, a problematic period in the power record is apparent in June, where turbines output is registers are exactly zero. It was assumed this was due to some problem in the data collection and the June data was not used in the analysis that follows. Another period that is excluded are the last few days of July and first few days of August, where Turbine 13 output climbs at 23 kW before shutting down and rising again.

Such events would have to be accounted for in an assessment of the plant power performance as they impact turbine availability, but for the purpose of assessing a method for power

performance assessment, it is less of a problem. It also considerably simplifies the analysis by reducing scatter and accelerating convergence in mean. It is noted, however, that the methods examined herein may be less effective when data includes many problematic records that, for example, augment the number of samples necessary for means to converge.

4.7 POWER MATRICES

This section reports on the joint statistics of turbine power output, conditioned on the significant wave height and energy mean period obtained from the record at the pressure sensor. As discussed earlier, the wavefield at the entrance of a chamber of the plant may be significantly different from that above the pressure sensor 200 m upwave. In fact it appears to be significantly different between chambers spaced only a few meters. These matrices are thus not properly speaking power matrices, as defined e.g. in IEC-TS/62600-100. A power matrix relates a WEC mean power output to the statistics of the wavefield *at* the WEC itself. The matrices presented here relate the power output to the closest available wave measurement. A spatial transfer model would be necessary to evaluate statistics *at* the WEC from the measurements, but at least 3 months of data at the entrance of the breakwater chamber would be necessary, following IEC specifications (which, also, explicitly exclude application to shoreline devices).

Another important difference with power matrices as per IEC-TS/62600-100 is that as per Clause 9.2 (in Edition 1), the power matrix is to be obtained via a capture length matrix. This process was not followed here due to the additional uncertainty introduced by the calculation of the energy flux for this shoreline device. The deepwater approximation for the energy flux is not applicable. The shallow water energy flux may be calculated assuming linearity, but the group velocity will be much lower at the entrance of the plant than at the wave measuring instrument (as it goes with the square root of depth). The possibility to reduce intra-cell variance with a capture length matrix instead of a power matrix is discussed further in Section 4.11.

It should also be mentioned that in this analysis all periods where data was not available from the plant sensors, or when they appear to malfunction, were discarded. This reduces the influence of spurious data on the results and is acceptable when the objective is to assess methods for power performance assessment. However, should the objective be instead performance assessment, these periods where data from the Mutriku plant appear problematic should be considered more carefully as they could be correlated to times where some of the turbines are not available for power production, the occurrence of which obviously should be considered when assessing power production in normal conditions. The matrices presented herein should thus be considered indicative of the upper bound of power matrices that would result from a comprehensive performance assessment. At any rate, data

TABLE 11: 1-HOUR SAMPLES POWER MATRIX

Hs (top of bin)	>5.5																		
	5.5																		
	5													4.4	2.3				
	4.5												7.3	2.8	4.9				
	4											12.3	4.2	8.0	8.1				
	3.5										12.2	9.8	4.3	11.7	8.6	6.7			
	3									9.6	11.1	10.0	9.7	8.5	4.6				
	2.5								10.7	9.2	10.2	10.9	4.3	7.7					
	2					12.3	11.6	11.4	9.4	9.2	8.2	6.2	8.2	6.2	4.8				
	1.5				10.0	8.4	5.9	7.2	6.6	6.5	6.0	5.6	6.4	4.0	3.1				
1				3.4	3.2	3.5	3.3	2.9	2.4	1.8	2.3	2.1							
0.5				0.1	0.3	0.5	0.6	0.8	0.9	0.7	0.5	0.4	0.1						
	<4	5	6	7	8	9	10	11	12	13	14	15	16	17	18	19	20	>20	
	Te (top of bin)																		

TABLE 12: 5-MINUTE SAMPLES POWER MATRIX

Hs (top of bin)	>5.5														6.1	1.4									
	5.5														4.9	4.3									
	5													7.7	6.8	4.2	4.1	7.9							
	4.5													8.1	6.4	6.1	5.1	6.4							
	4													10.4	10.3	5.8	5.5	7.8	6.7	10.4					
	3.5													11.8	10.5	10.0	7.8	9.4	8.3	6.4					
	3													10.6	10.3	10.3	9.6	9.9	8.9	7.4	5.6				
	2.5													11.1	12.4	10.0	9.6	9.8	9.7	9.1	7.4	6.4	5.2		
	2													11.4	11.3	8.2	9.3	9.5	8.7	8.6	7.8	8.0	7.2	5.4	4.5
	1.5													10.2	8.2	6.1	6.9	6.8	6.8	6.3	5.9	5.9	4.8	3.7	4.0
1													0.8	3.0	3.3	3.7	3.5	3.3	2.6	2.2	2.4	2.6	2.5	2.3	
0.5													0.2	0.3	0.5	0.6	0.8	0.9	0.7	0.7	0.5	0.3	0.1		
		<4	5	6	7	8	9	10	11	12	13	14	15	16	17	18	19	20	>20						
		Te (top of bin)																							

coverage from the pressure sensor is nearly 100% during the period considered, and plant data for Turbine 13 is consistently available except for the month of June.

These distinctions with normal terminology and the reasons for this method of estimation should be borne in mind. Nonetheless, the term “power matrix” will be used hereafter for convenience.

Table 11 and Table 12 show the power matrices obtained for Turbine 13 from the hourly records and from the five-minutes samples respectively. An immediately visible difference is that the five-minute matrix has many more cells populated. This is due to the fact that, as was seen in the scatter diagrams presented in the previous section, the five-minutes wave statistics oscillate around the longer samples' values, and have higher extremes. (This effect of wider coverage of the (H_s, T_e) space appears more pronouncedly than in the scatter diagrams because only cells with occurrence higher than 0.1% were shown there). The total number of power vs. (H_s, T_e) records is also about 12 times higher (although the issue of independence of samples should be considered, as discussed in following sections. This

possibility to populate more cells of the power matrix with performance data, though from short samples, may at least in some case be a useful complement, if not preferable, to the interpolation or numerical modelling results that must be used otherwise to populate cells that occur too infrequently in the longer samples wave statistics.

Matrices obtained with half-hourly, quarter-hourly and ten-minute samples are also shown for completeness. Other than the cell coverage being higher for matrices using shorter samples, there are no striking differences in the mean power estimates for each cell. But the main criterion for whether differences are significant is arguably their impact on the evaluation of annual energy production. This will be looked at in the next section.

4.8 IMPACT ON ENERGY PRODUCTION ESTIMATES

One of the main outputs of power performance assessment is prediction of energy yield, a basic parameter for valuation of wave energy projects. Therefore an important criterion on whether the use of shorter samples can provide useful information is whether yield prediction agrees with that obtained with samples of longer duration. This provides a useful metric to evaluate the relevance of the differences in power matrices or scatter diagrams obtained with various sample durations.

The data available for this study does not adequately sample the annual cycle of wave climate so it cannot be expected to provide accurate energy yield prediction. Data do cover winter, spring and summer conditions so the range of conditions expected at Mutriku should be reasonably well represented. In particular, the power matrix should be populated with data on a reasonable range of the (H_s, T_e) space. The method to calculate Annual Energy Production (AEP) in a real performance assessment would be the same as that used in this analysis, except a longer dataset would be used to better assess the scatter diagram and the average year's wave climate.

Thus, it is reasonable to expect that results concerning the impact of using shorter sample durations would be of relevance to a more comprehensive AEP calculation. For simplicity the power productions calculated will be referred to as AEP, though again the autumn season is not sampled and other limitations such small spatial scale variability of the wavefield must be considered for a device operating in complex nearshore topography, as discussed in previous sections.

Table 16 Table 17 show AEP estimates obtained for Turbine 13 with 1-hour samples and the 5-minute samples respectively. AEP estimates are within 0.3% of each other. Unfortunately this is not a validation of the short-sample analysis, but simply a reflection of the fact that we have summed the same time series of power output from Turbine 13, just in smaller groupings for the short-samples. This is due to the fact that the time series of sea-states that were used to make the power matrix is exactly the same as that used to make the scatter diagram used

TABLE 13: 30-MINUTE SAMPLES POWER MATRIX

Hs (top of bin)	>5.5																			
	5.5														4.5					
	5												12.4	5.3	3.2					
	4.5											12.3	7.0	3.8	4.5					
	4										12.5	11.9	4.7	8.1	4.7					
	3.5										11.1	8.7	6.3	8.6	8.2					
	3								12.1	10.2	10.8	9.8	11.0	8.6	5.2					
	2.5								11.4	9.2	10.1	10.3	7.1	8.6	5.7					
	2				11.9	12.2	9.9	9.7	9.8	8.7	8.5	6.5	8.3	6.8	4.6					
	1.5				9.8	8.4	5.9	7.2	6.8	6.5	5.8	5.9	6.0	3.5	3.4					
1				2.2	3.2	3.6	3.3	3.0	2.3	1.8	2.1	2.0	3.8							
0.5		0.2	0.1	0.3	0.5	0.6	0.8	0.9	0.7	0.5	0.4	0.1								
		<4	5	6	7	8	9	10	11	12	13	14	15	16	17	18	19	20	>20	
		Te (top of bin)																		

TABLE 14: 15-MINUTE SAMPLES POWER MATRIX

Hs (top of bin)	>5.5																		
	5.5													6.8					
	5											6.1	4.8	5.1					
	4.5									12.8	7.3	5.0	4.2						
	4									12.6	9.0	4.5	6.4	6.1					
	3.5									12.2	8.9	7.1	9.9	10.2	6.5				
	3								11.8	10.2	10.5	9.9	10.2	9.1	6.5				
	2.5								10.8	9.3	10.2	9.8	8.5	7.3	6.2				
	2				12.3	11.8	9.3	11.5	9.6	8.6	8.3	7.1	8.2	6.1	4.7				
	1.5				10.2	8.0	6.2	7.0	6.8	6.8	6.0	6.0	5.6	3.9	3.5				
1			1.0	2.9	3.2	3.6	3.4	3.1	2.4	1.9	1.9	3.3	2.3						
0.5			0.1	0.3	0.5	0.6	0.8	0.9	0.7	0.5	0.5	0.1	0.1						
		<4	5	6	7	8	9	10	11	12	13	14	15	16	17	18	19	20	>20
		Te (top of bin)																	

TABLE 15: 10-MINUTE SAMPLES POWER MATRIX

Hs (top of bin)	>5.5																		
	5.5																		
5																			
4.5																			
4																			
3.5																			
3																			
2.5																			
2																			
1.5																			
1																			
0.5																			

to obtain AEP (by multiplying element by element by the power matrix). Differences can only emerge when the time series of sea-states is different from that used to populate the power matrix. This is normally the case when power performance is evaluated in one location, e.g. as described IEC-TS/62600-100. A longer interannual time series of sea-state statistics is

TABLE 16: ENERGY PRODUCTION (MWH) WITH THE 1-HOUR POWER MATRIX AND SCATTER DIAGRAM

Hs (top of bin)	>5.5																		
	5.5																		
	5																		0.1
	4.5																		0.2
	4														0.1				0.3
	3.5												0.4	0.1	0.1				0.8
	3											0.7	1.4	0.5	0.2				2.8
	2.5											1.1	2.3	0.6					4.1
	2											1.5	2.4	0.4	0.2				5.6
	1.5					0.1			0.1	0.7									
Capacity factor 19.19 %	1				0.2	0.4	0.4	1.9	1.9	1.5	0.8	0.4	0.2						7.9
	0.5				0.5	0.5	2.3	2.1	1.2	0.7	0.3								7.5
	0.5				0.2	0.4	0.5	0.3	0.3										1.8
	Capacity factor				0.9	1.4	3.3	4.4	4.1	5.7	7.7	2.2	0.9	0.4	0.1				31.1
Te (top of bin)																			

TABLE 17: ENERGY PRODUCTION FROM THE 5-MINUTE POWER MATRIX AND SCATTER DIAGRAM

Hs (top of bin)	>5.5																		
	5.5																		
	5																		0.1
	4.5																		0.2
	4													0.1					0.4
	3.5												0.2	0.4	0.2	0.2			1.0
	3												0.5	1.2	0.4	0.2			2.5
	2.5												1.1	1.9	0.6	0.1			3.9
	2												1.5	1.9	0.5	0.2			5.3
	1.5												1.6	1.0	0.4	0.2			7.9
Capacity factor 19.24 %	1					0.2	0.5	0.5	1.6	1.8	1.6	1.0	0.4	0.2					8.0
	0.5					0.4	0.6	2.2	2.2	1.4	0.7	0.3	0.1						1.9
	0.5					0.2	0.4	0.5	0.3	0.2	0.1								
	Capacity factor					0.8	1.6	3.3	4.3	4.3	5.7	7.1	2.4	1.1	0.5	0.2			31.2
Te (top of bin)																			

available for the location than that available for the testing period. For evaluation of yield in another location, e.g. with IEC-TS/62600-102 the scatter diagram will also be different.

In this case there is no long time series of wave climate available at Mutriku. To get a meaningful evaluation of the impact of differences in the power matrices in power production, the scatter diagram for the BiMEP reference buoy is used. There are obvious limitations to using the wave climate at this buoy deployed at some 70 m depth to calculate energy production for this shoreline WEC. However, it does provide a realistic scatter diagram to evaluate how important the differences in power matrices obtained with various sample durations are, in terms of mean annual energy production. However, because the power matrix of the five-minute samples is much more populated than that of the one-hour sample, and that for all cells of the one-hour matrix that are not populated the production must be assumed to be zero, simply calculating energy production element by elements leads to significantly higher production with the five-minute matrix, of some 20% (not shown). This is

TABLE 18: ENERGY PRODUCTION IN BIMEP USING POWER MATRIX OF 1-HOUR SAMPLES

Hs (top of bin)	>5.5																		
	5.5																		
	5																		
	4.5																		
	4									0.2									0.2
	3.5									0.4	0.2								0.7
	3									0.4	0.3								0.8
	2.5									1.4	0.7	0.2							2.5
	2				3.4	3.3	2.9	1.5	0.4	0.1									11.5
	1.5			5.3	3.9	2.1	1.5	0.5	0.2										13.6
Capacity factor 20.09 %	1			1.5	0.9	0.5	0.2												3.2
	0.5																		
				6.8	8.3	5.9	4.5	3.4	2.2	1.1	0.3	0.1							32.6
		<4	5	6	7	8	9	10	11	12	13	14	15	16	17	18	19	20	>20
		Te (top of bin)																	

TABLE 19: ENERGY PRODUCTION IN BIMEP WITH POWER MATRIX OF 5-MINUTE SAMPLES

Hs (top of bin)	>5.5																		
	5.5																		
	5																		0.0
	4.5																		0.0
	4										0.1								0.2
	3.5										0.4	0.2							0.7
	3										0.4	0.3							0.8
	2.5										1.3	0.7	0.2						2.4
	2					3.1	2.3	2.3	1.5	0.4	0.1								9.8
	1.5				5.3	3.9	2.2	1.4	0.5	0.2									13.6
Capacity factor 18.89 %	1				1.3	1.0	0.6	0.2											3.1
	0.5																		0.0
				0.0	6.7	8.0	5.1	3.9	3.4	2.1	1.0	0.3	0.1	0.0					30.6
		<4	5	6	7	8	9	10	11	12	13	14	15	16	17	18	19	20	>20
		Te (top of bin)																	

mainly a reflection of the fact that the five-minute matrix is far more populated – arguably a good thing. To obtain meaningful comparisons, the elements of the five-minute power matrix that are zero in the one-hour matrix must also be set to zero.

Table 18 and Table 19 show the energy productions obtained for the one-hour samples and the five-minute samples with this method. The difference of two MWh amounts to a slightly less than 6% relative difference. Using 30-minute, 15-minute and 10-minute samples results in slightly lesser differences in AEP, just below 5%. This is consistent with previous results that suggest the five-minutes samples do differ slightly more than longer samples. However, it should be mentioned that the 30 minutes samples fare worse by this metric, at -4.4% compared to the 1-hour samples, than the 15 minutes samples, at -2.97. The 3-hours sample fare the worst, at -7.3%, but that is dominated by the effect of unpopulated cells in the 3-hours power matrix compared the one-hour power matrix, where production must be assumed to be zero. Considering the limitation of the dataset, it appears to be a valid

TABLE 20: AEP (MWH) WITH 1-HOUR POWER MATRIX AND 5-MINUTE SCATTER DIAGRAM

Hs (top of bin)	>5.5																		
	5.5																		0.0
	5																		
	4.5																		0.1
	4										0.1		0.1						0.4
	3.5										0.2	0.4	0.1	0.2					1.0
	3										0.5	1.3	0.5	0.2					2.5
	2.5							0.1			1.0	2.0	0.6						3.9
	2				0.2		0.2	0.7			1.6	1.8	0.4	0.2					5.2
	1.5			0.2	0.5	0.5	1.6	1.7			1.6	1.0	0.4	0.2					7.7
1			0.4	0.5	2.1	2.0	1.3			0.7	0.3	0.1						7.5	
0.5			0.2	0.4	0.5	0.3	0.2			0.1								1.9	
Capacity factor 18.66 %			0.0	0.9	1.6	3.1	4.2	4.0	5.6	7.0	2.2	1.1	0.4	0.1					30.3
	<4	5	6	7	8	9	10	11	12	13	14	15	16	17	18	19	20	>20	
	Te (top of bin)																		

conclusion that no statistically significant increase in the AEP difference is found for the five-minutes samples compared to the more standard 30 minutes samples.

AEP also provides a convenient metric to evaluate the significance of the differences in the scatter diagrams obtained with the various sample durations. AEP can be calculated with the one-hour power matrix combined with the scatter diagrams of the other sample durations. In this way the differences in AEP resulting from the differences in scatter diagrams only can be calculated, with a realistic power matrix.

Table 20 shows the AEP calculated with the one-hour power matrix and the 5-minute samples scatter diagrams at Mutriku. Compared to AEP obtained with the one-hour power matrix and one-hour scatter diagram, AEP decreases by -2.7%. And for this calculation a monotonic increase in the AEP change with reduction in sample duration is seen with AEP with the 30-minute, 15-minute, and 10-minute scatter diagrams at -0.15%, -0.6% and -1.7% respectively. This suggest a consistently increase bias in the scatter diagram as sample duration is reduced beyond usual durations for sea-state statistics. However, it also suggests that these changes, if consistent, have little impact on the calculation of power production. It is reasonable to expect that resulting from interannual variability and intra-site variability, for example, will be far more significant.

It is worth noting that using the 5-minute power matrix with the 1-hour scatter diagram results in slightly lesser agreement, with AEP 3.2% higher. Likewise, using the 1-hour power matrix with the 5-minute scatter diagram reduces AEP by 2.8%. These differences are still very acceptable and indicate that at least for this dataset, the scatter diagrams obtained with 5-minute samples still provide an acceptable estimate of the scatter diagram. It may be worth noting at any rate that they are not inconsistent with what would be the effect of a bias towards longer energy periods, of which some possible signs and potential causes were

discussed in the previous sections, if this bias were also to be more pronounced for shorter samples.

As conclusion, the results of annual energy production presented in this section show that for this dataset, power performance assessment, and in particular, annual energy production estimates, are impacted by the order of 5% when changing the sample duration from one-hour to five-minutes. This may not be statistically significant, and changes of the same order are obtained when using standard sampling durations of 30 minutes. Changes to the scatter diagram are lesser, below 3%, and suggest scatter diagrams for short samples are quite accurate for power performance calculation.

4.9 SAMPLE DURATION AND DISPERSION IN PERFORMANCE DATA

As discussed earlier, an initial motivation for this study was to investigate if the scatter in power performance data could be reduced by relating WEC power output to wave characteristics at time scales finer than the standard 20 minutes of sea-state statistics. Summarising our results, we were not successful in using the finer time-scale wave characteristics to better predict the WEC behaviour at short time-scales. However, the error on the mean, that is, on the value to be reported in a cell of the power matrix, can be expected to be lesser using short samples, due to the larger number of measurements it makes available. This is subject to conditions of independence that will be examined in the next section. Results in this section are mostly on the dataset available at Mutriku. Certain results are also reported for the IDOM Oceantec WEC operating at BiMEP.

4.9.1 MUTRIKU DATA

4.9.1.1 SAMPLE VARIABILITY

The sample standard deviation obtained for the one-hour samples of power performance for Turbine 13 at Mutriku is shown on Table 21. (Only cells with more than 5 samples are shown). The ratio of the standard deviation obtained with the five-minute over that obtained with the one-hour samples is shown on Table 22. For almost all the cells, sample variability is significantly higher for the five-minute sample, with an average of 51% higher for the cells shown.

Sampling variability is expected to increase for shorter samples. And at least with the methods that are presented here, this effect could not be compensated by relating power output to shorter-term wave statistics in some improved way. This doesn't rule out that future analysis, that would for example identify better predictability patterns at shorter time scale, may not be successful in doing so.

TABLE 21: STANDARD DEVIATION OVER MEAN VALUE FOR CELLS OF THE 1-HOUR POWER MATRIX

Hs (top of bin)	>5.5																		
	5.5																		
	5												1.20	1.77					1.48
	4.5										.71	1.73	1.00						1.15
	4									.03	1.18	.62							.46
	3.5								.07	.44	1.33	.10	.26						.37
	3								.43	.20	.36	.45	.25						.28
	2.5								.47	.24	.16	1.41	.18						.41
	2				.03	.02	.01	.33	.27	.37	.67	.34	.48	.19					.27
	1.5			.08	.43	.26	.24	.30	.33	.50	.30	.19	.21	.06					.26
1			1.08	.78	.55	.60	.61	.64	.82	.62	.35							.67	
0.5		2.32	1.30	1.26	1.15	.84	.50	.55	.59	.93								.94	
		2.32	.82	.63	.49	.42	.35	.39	.40	.70	.64	.52	.06					.53	
	<4	5	6	7	8	9	10	11	12	13	14	15	16	17	18	19	20	>20	
	Te (top of bin)																		

TABLE 22: RATIO OF SAMPLES STANDARD DEVIATIONS, 5-MINUTE TO 1-HOUR MATRIX

Hs (top of bin)	>5.5																			
	5.5																			
	5													1.09						1.09
	4.5												1.17	1.16	1.13					1.15
	4												1.20	1.15						1.17
	3.5											1.01	0.99	4.17						2.05
	3										0.92	1.68	1.27	0.95	1.89					1.34
	2.5										0.94	1.33	1.99							1.42
	2						7.79			1.08	1.49	1.05	0.88	1.13		2.40				2.26
	1.5					1.95	0.94	1.54	1.31	1.25	1.38	1.08	1.65	2.43	2.75					1.63
1					0.90	1.00	1.14	1.16	1.26	1.32	1.25								1.15	
0.5				1.08	1.05	1.08	1.08	1.06	1.33	1.31	1.79	1.35							1.24	
			1.08	1.30	2.70	1.25	1.18	1.23	1.23	1.31	1.31	1.73	1.92	2.40					1.51	
		<4	5	6	7	8	9	10	11	12	13	14	15	16	17	18	19	20	>20	
		Te (top of bin)																		

4.9.1.2 RMS ERROR ON THE MEAN

For unbiased, normally distributed measurements, the Root Mean Square (rms) error on the mean is the standard deviation of the samples divided by the inverse of the square root of the number of measurements:

$$\sigma_{mean} = \frac{\sigma_{samples}}{\sqrt{N_{sample}}}$$

The rms error on the mean of cells of the power matrix for the one-hour samples that would be obtained if these measurements were normally distributed is shown in Table 23 (rms error normalised by the mean value for each cell). Scatter is rather high for all cells, with a mean value of 53% of the mean for the cells shown. There are 2396 hourly samples, but the dispersion in performance measurements within one cell still results in significant rms error to be expected on the mean.

TABLE 23: RMS ERROR OM CELLS OF 1-HOUR POWER MATRIX IF NORMALLY DISTRIBUTED

Hs (top of bin)	>5.5																				
	5.5																				
	5											54%							54%		
	4.5										32%	77%	41%						50%		
	4										42%	23%							33%		
	3.5									10%	40%	4%							18%		
	3								8%	3%	8%	17%	11%						9%		
	2.5								6%	2%	3%								4%		
	2							1%			8%	3%	3%	15%	10%			9%		7%	
	1.5					3%	10%	5%	3%	3%	3%	7%	6%	7%	9%					6%	
1					38%	12%	5%	5%	5%	7%	14%								12%		
0.5				31%	9%	10%	10%	8%	5%	10%	14%	38%							15%		
				31%	17%	9%	6%	6%	5%	6%	8%	23%	28%	20%	9%				14%		
		<4	5	6	7	8	9	10	11	12	13	14	15	16	17	18	19	20	>20		
		Te (top of bin)																			

TABLE 24: RATIO OF RMS ERROR ON MEAN OF 5-MIN TO 1-HOUR POWER MATRICES

Hs (top of bin)	>5.5																			
	5.5																			
	5												0.45						0.45	
	4.5												0.47	0.36	0.47				0.43	
	4												0.37	0.36					0.37	
	3.5											0.29	0.29	0.97					0.51	
	3										0.31	0.51	0.37	0.25	0.76				0.44	
	2.5										0.29	0.42	0.56						0.42	
	2				2.11					0.34	0.41	0.35	0.23	0.35		0.93			0.68	
	1.5				0.63	0.25	0.44	0.41	0.38	0.40	0.27	0.47	0.58	0.88					0.47	
1				0.21	0.27	0.34	0.32	0.36	0.39	0.33								0.32		
0.5				0.29	0.31	0.30	0.32	0.29	0.40	0.36	0.53	0.37						0.35		
				0.29	0.39	0.73	0.37	0.34	0.37	0.36	0.39	0.39	0.47	0.70	0.93				0.45	
	<4	5	6	7	8	9	10	11	12	13	14	15	16	17	18	19	20	>20		
	Te (top of bin)																			

Table 24 shows the ratio of the expected rms error of the five-minute samples to the one-hour samples, were they conditions of independent, normally distributed measurements be satisfied. The much larger number of measurements for the five-minute samples (28 740 samples) results in significantly lower expected error on the mean value of the power matrix. On average, the rms error would be less than half of that in the hourly power matrix cell.

It will be seen in the following section that at least for the five-minute samples, conditions of independence of successive samples are not fulfilled. More advanced analysis would be necessary to determine what are the expected errors in the means of the one-hour and five-minute samples. Table 24 however serves to illustrate that despite the significantly higher sample variability for short samples, the error on the mean value in the power matrix cells may be lesser, due to the corresponding increase in the number of samples.

4.9.2 BIMEP DATA

This discussion of scatter in performance data is now completed with data from the Marmok floating WEC, operated by Oceantec (now IDOM) at the Biscay Marine Energy Platform (BiMEP). More information on this WEC can be found in relevant deliverables of the OPERA Project or from the IDOM Oceantec website. Borja de Miguel of IDOM kindly provided the standard deviations of measurements for the power matrix of twenty-minute, one hour, and three hour samples.

Table 25 shows the standard deviations, normalised to the mean power for each cell, for the one-hour samples. Table 26 shows the ratio of standard deviation for the twenty-minute samples to the that of the one-hour samples (>1 means the twenty-minute samples have more scatter). Table 27 shows the same ratio for the three-hour to the one-hour samples. Only sea-states that occurred at least five times during the testing period reported are shown. Due to various issues such as incomplete coverage from the wave measuring buoy, upper ranges of the power matrix were not sufficiently populated during the particular stretch reported upon therein.

For those sea-states that occurred at least five times, the twenty-minute samples usually have higher standard deviation than the one-hour samples, with an average increase of 12%. The three-hour samples have slightly lesser standard deviation, though the difference, at 4% on average, may be well within uncertainty. Thus, for this testing period, samples of power performance for this floating WEC also exhibit higher variability with shorter samples, in agreement with the conclusions at Mutriku. These differences, while less than those shown in the previous section for Mutriku, are likely to be significantly higher for even shorter samples.

Again, for normally distributed measurements, the increase in number of samples for the twenty-minute samples relative to the one-hour samples (or one-hour samples relative to three-hour samples), should be more than compensate for the slight increases in standard deviation, in terms of expected rms error on the mean. So that as far as reducing the confidence intervals in the power matrix cells, using shorter samples may still be a good strategy. However, this is subject to conditions of independence that will be discussed for Mutriku in the next section.

4.10 SAMPLE DURATION AND TESTING TIME NEEDED

This section reports methods, their assessment and potential caveats in using short sample duration to reduce the open-sea testing time necessary to obtain reliable estimates of power performance. Some of the conditions that were found to be necessary to best use short samples for this particular dataset are reported. As discussed earlier, the reduction in necessary testing time is one of the three main potential benefits of using short samples that

TABLE 25: 1-HOUR SAMPLES STANDARD DEVIATIONS OVER MEAN VALUE, OCEANTEC MARMOK

Hs (top of bin)	3									0.42	0.33		0.38
	2.5			0.24	0.27	0.09	0.14	0.35	0.41	0.17			0.24
	2		0.41	0.33	0.26	0.22	0.20	0.19	0.18	0.22			0.25
	1.5	0.28	0.53	0.43	0.31	0.27	0.30	0.44	0.50				0.38
	1	0.21	0.60	0.50	0.44	0.41	0.51	0.31	0.18				0.40
	0.5	0.29	0.38	0.30	0.37								0.34
		0.26	0.48	0.36	0.33	0.25	0.29	0.32	0.32	0.27	0.33		0.32
		5	6	7	8	9	10	11	12	13	14	15	16
		Te (top of bin)											

TABLE 26: MARMOK, RATIO OF 20-MINUTE OVER 1-HOUR SAMPLES STANDARD DEVIATION

Hs (top of bin)	3									0.74	0.98		0.86	
	2.5			0.97	1.11	2.15	1.31	0.75	1.06	1.68			1.29	
	2		1.02	1.25	1.14	1.04	1.26	1.17	1.28	1.11			1.16	
	1.5	0.97	1.02	1.04	1.12	1.16	1.07	1.15	0.88				1.05	
	1	1.16	1.08	1.06	1.05	1.07	0.99	1.12	1.26				1.10	
	0.5	0.93	0.99	1.39	0.99								1.08	
		1.02	1.03	1.14	1.08	1.36	1.16	1.05	1.12	1.17	0.98			1.12
		5	6	7	8	9	10	11	12	13	14	15	16	
Te (top of bin)														

TABLE 27: MARMOK, RATIO OF 3-HOUR TO 1-HOUR SAMPLES STANDARD DEVIATIONS

Hs (top of bin)	3														
	2.5							0.29						0.29	
	2	1.25	1.05	1.20	0.80	0.98	0.87	1.04							1.03
	1.5	0.89	1.09	0.87	0.91	0.97	1.10							0.97	
	1	0.92	1.02	1.11	0.77	1.02	0.94	0.82							0.94
	0.5	0.64	1.12	1.30	1.05									1.03	
		0.78	1.07	1.14	0.97	0.91	0.96	0.93	1.04	0.29				0.96	
		5	6	7	8	9	10	11	12	13	14	15	16		
Te (top of bin)															

are reported upon. (The other two are reduction of error on the mean with obtaining performance data over a wider range of (H_s, T_e)).

The rate of convergence in mean (or mean square) of the measurements of power output, and how it may vary with sample duration and sample size is examined. It was seen in the previous section that, (1) the standard deviation of the individual samples of power output during a particular combination of H_s and T_e increases when the sample duration is reduced, but that (2) the standard deviation of the mean (i.e., the expected rms error on the estimate of the mean) for shorter samples may still be lower due to the increase in number of samples.

For this to be true several properties are required for the sample distribution. One of them is the independence of samples. Short samples may be less independent than longer samples

because, say, more of them are taken during a time where the wave spectrum has a particular shape, or the tide is at a certain level, or wave direction is more correlated, etc. This would decrease the real degrees of freedom of the sample mean and could reduce or reverse the expected reduction in the scatter of the mean values in the power matrix. The analysis reported in this section shows that this is the case to some extent, but that this effect can be reduced significantly and, in selected applications, possibly removed altogether by ensuring sufficient separation in time between the short samples.

It is useful to first focus the analysis on a few selected cells of the power matrix. Two cells are particularly appropriate as they represent very different sea and plant operating conditions but both contribute importantly to the annual energy production (see Table 16):

Storm cell $2 < H_s < 2.5$ and $13 < T_e < 14$

Mean regime cell $0.5 < H_s < 1$ and $9 < T_e < 10$

The first one is a local maximum in energy production due to a good trade-off between large incoming wave energy flux and plant production vs relatively frequent occurrence. It will be referred to as “storm cell”. The second one is a local maximum in energy production essentially because the high frequency of occurrence compensates, in terms of annual energy production, for a small plant production. It will be referred to as the “mean regime” cell hereafter.

Times series of Turbine 13 mean power during storm cell and mean regime cell sea-states are shown in Figure 43. Dash-dotted lines correspond to the final estimate of the mean for the samples of the same colour. These final estimates are quite similar for the various sample durations for these cells. Scatter in mean power measurements is significantly higher for the shorter samples, as expected from the previous section’s discussion. The general impression is one of surprisingly high scatter in mean power output considering that these are data for the same cell of the scatter diagram in the upwave pressure sensor data. The next section will report on some of the reasons identified for this high intra-cell dispersion.

The convergence in mean with number of samples is shown for the same cells in Figure 44. The number of samples for the estimate of the mean to converge near its final value is clearly many times larger for the short samples. This increase is far more than that expected from the larger sample variance alone. Successive short sample measurements appear to be much more correlated than successive hourly measurements. The results is that in terms of testing time needed to converge near the final estimate of the mean, there are no gains from using the shorter samples (not shown). Other cells yield similar results. Hence, it appears that simply reducing the sampling duration does not bring any benefits in terms of reducing necessary testing period.

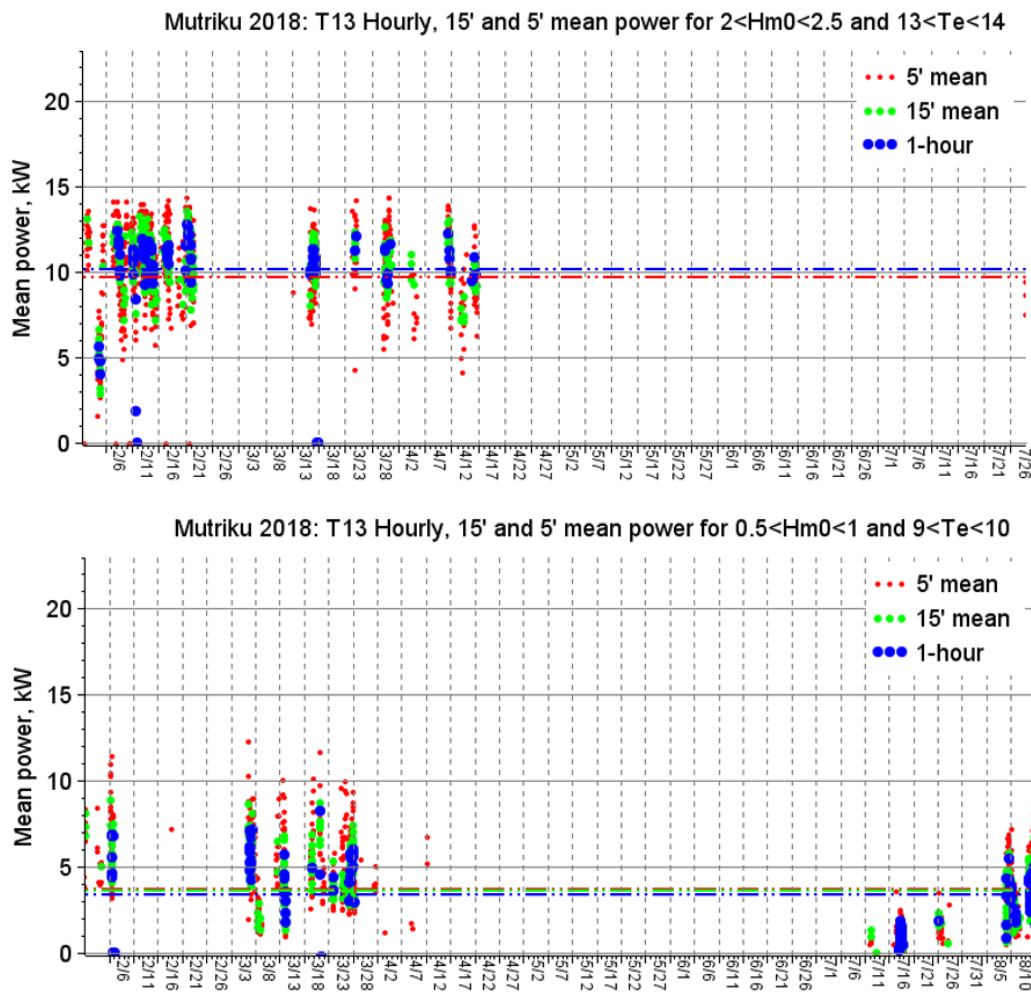


FIGURE 43: TIME SERIES OF POWER OUTPUT FOR THE STORM AND MEAN REGIME CELLS

If correlation between successive samples is the problem, it is worth examining if requiring a minimum time spacing between short samples may alleviate this problem. This would not have any application in terms of reducing necessary testing time to obtain a power matrix. It may, however, have applications in terms of reducing the necessary sampling duration for each device configuration. For example, control algorithms such as those evaluated in OPERA could be cycled through much faster if shorter sampling were to yield acceptable performance assessments.

Figure 45 shows the convergence in mean for five-minute samples without requirement of spacing (red), five-minute samples with requirements of at least one-hour spacing (green), and the one-hour samples (blue). The gains in terms of rapidity of convergence are quite substantial. The five-minute samples converge about as fast as the one-hour samples when required to be spaced apart at least one hour. The spacing requirement thus appears to work in reducing correlation between successive measurements. Unfortunately, the final estimate of the mean for the 1-hour spaced five-minute samples is now some 10% off from the

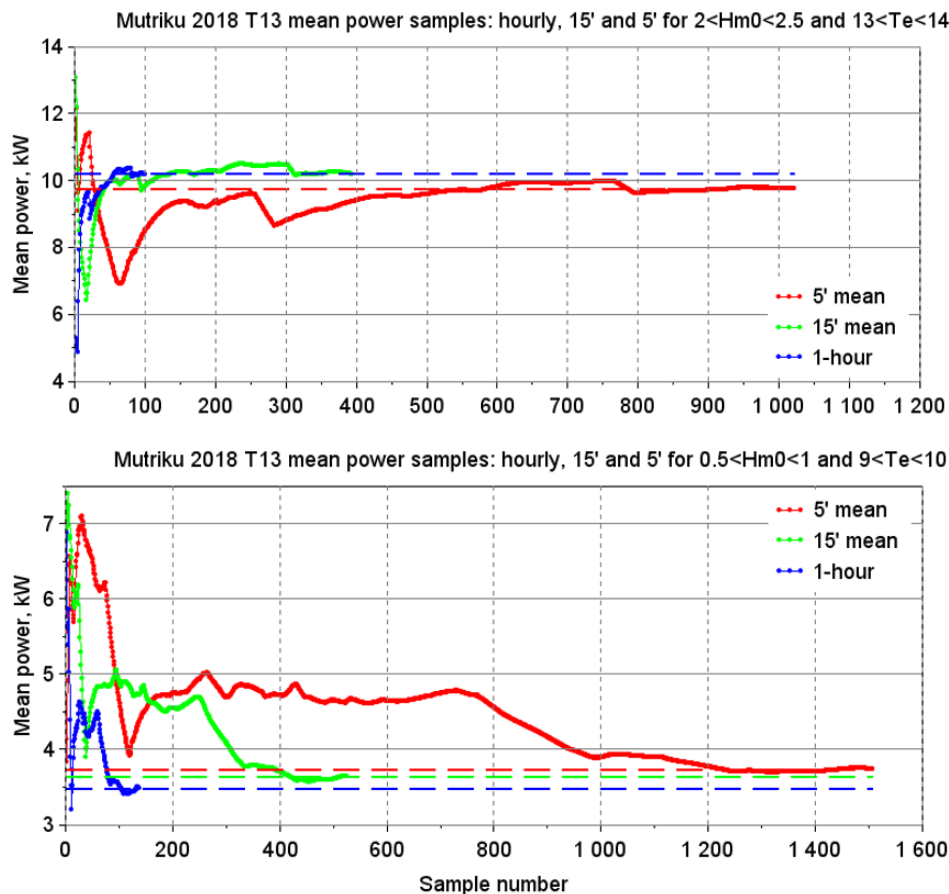


FIGURE 44: CONVERGENCE IN MEAN WITH THE NUMBER OF SAMPLES

estimates of the mean from the one-hour or the non-spaced five-minute samples. Similar problems are found for other cells. The exact reasons for this were not investigated. It may be due to the combination of large sampling variability and large reduction in the number of five-minute samples when requiring that they be at least one hour apart.

In summary, the results reported in this section suggest that the gains in terms of rms error on the mean from using shorter samples is minimal. Possibly because of higher correlation for successive short samples. The number of samples necessary to converge to the mean may be significantly reduced by requiring that short samples be spaced at least one hour from each other. However, this results in what appears to be larger rms error on the mean, presumably due to the significant reduction in the number of short samples. The potential benefits from applying this method to more rapidly testing various device control or configuration, and best trade-off between reduced accuracy and reduced testing time, will depend on the details of each application.

4.11 CAUSES OF THE HIGH SCATTER IN PERFORMANCE DATA

The time series of power in Figure 43 shows that even for the same cell of the scatter diagram, power output for the WEC may vary by as much as 100% for the five-minute samples. The

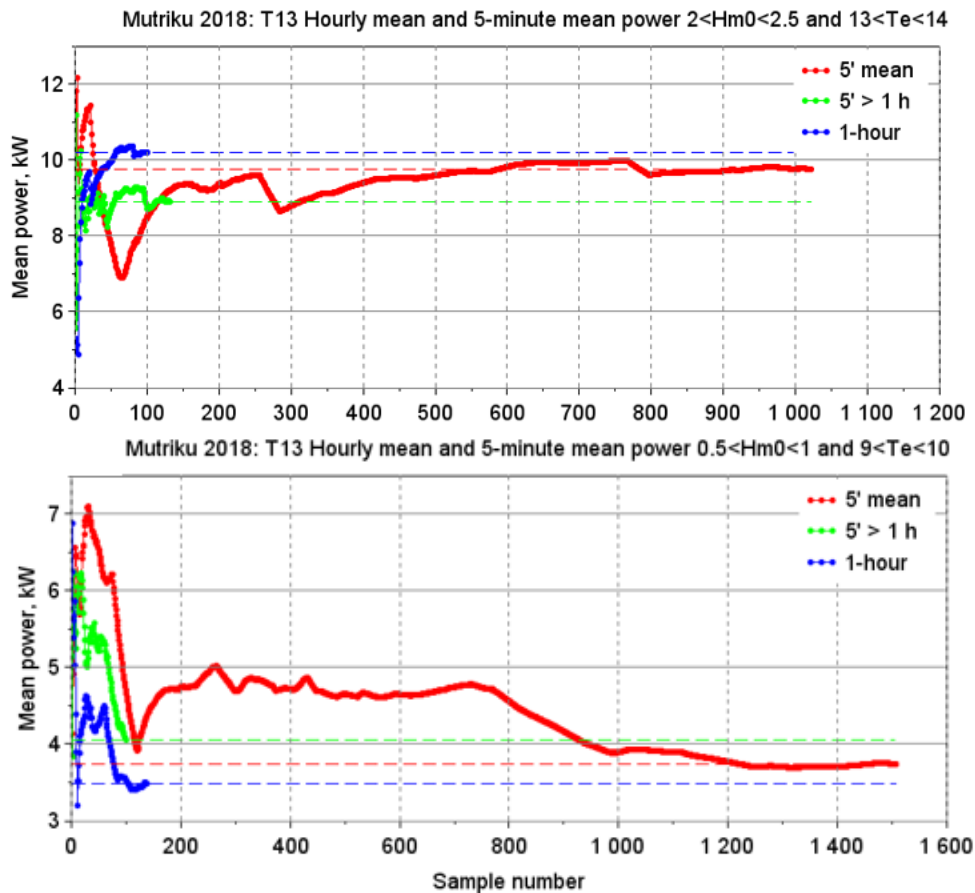


FIGURE 45: CONVERGENCE TO THE MEAN WHEN REQUIRING ONE-HOUR SPACING

hour-long samples have slightly less but still surprisingly high scatter. It is worth assessing likely reasons for this as they may impact conclusions regarding the possible use of shorter samples. Main findings are reported in this section.

As summary, some (perhaps about half) of the intra-cell variance in sample power output can be explained by small variations in the statistics of the incoming wave field across a same (H_s, T_e) cell. So it may be reduced by normalising power measurements such as in the capture length matrix or by adding dimensionality to the power matrix. However, it appears some of the intra-cell scatter is due to other causes, which may relate to details of the plant control algorithms or physics or misrepresentation of the incoming wavefield by the statistics of the pressure sensor. The latter could be due, for example, to long-shore variability in the wavefield or slight changes in wave direction.

4.11.1 EFFECT OF TIDES

On very low tides, the seabed at the foot of the Mutriku plant uncovers. This suggests that the effect of tides on a shoreline plant like Mutriku be significant. Tidal height is thus a good candidate explanation for some of the scatter in plant operating data for a same (H_s, T_e) sea-state.

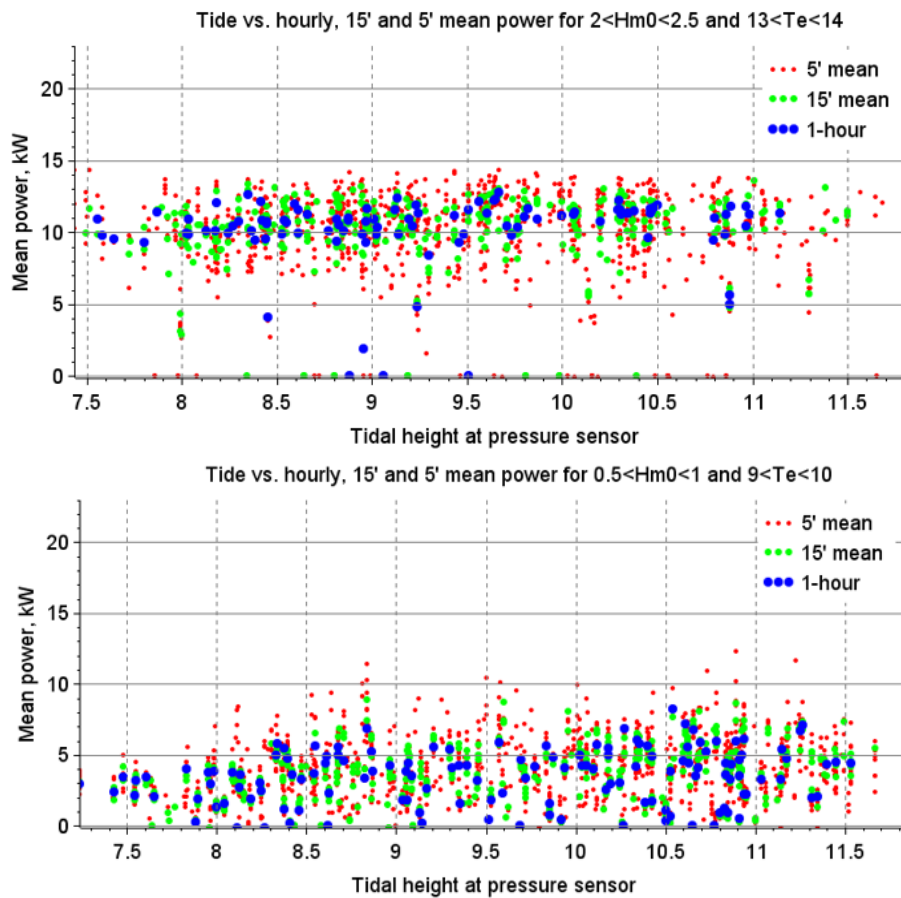


FIGURE 46: TIDAL HEIGHT AND TURBINE 13 POWER FOR THE STORM AND MEAN REGIME CELLS

Figure 46 shows the power output vs. mean tidal height during each sample for the storm (upper panel) and mean regime (lower panel) cells of the power matrix. As discussed earlier, these two cells are representative of two different types of high contributors to the annual energy output and are a convenient way to examine dependencies to variables others than (H_s, T_e) in the power matrix. A very slight positive correlation between tidal height and power output may be seen for both cells, possibly more pronounced for the mean regime cell. However, it is clear from Figure 46 that very little of the scatter in performance data appears correlated with mean tidal height. This is the case for other cells and for any of the sample durations.

Clearly this investigation is far from sufficient to accurately assess the effects of tides on power production at Mutriku. Nonetheless, it appears unlikely that tidal height could explain much of the scatter in performance data within a same cell of the power matrix.

4.11.2 EFFECT OF VARIATION OF WAVE HEIGHT AND PERIOD ACROSS A CELL

The scatter plots of each sample's mean power output vs. H_{m0} for the storm cell and mean regime cell are shown in Figure 47. Correlation is high for the mean regime cell, where output

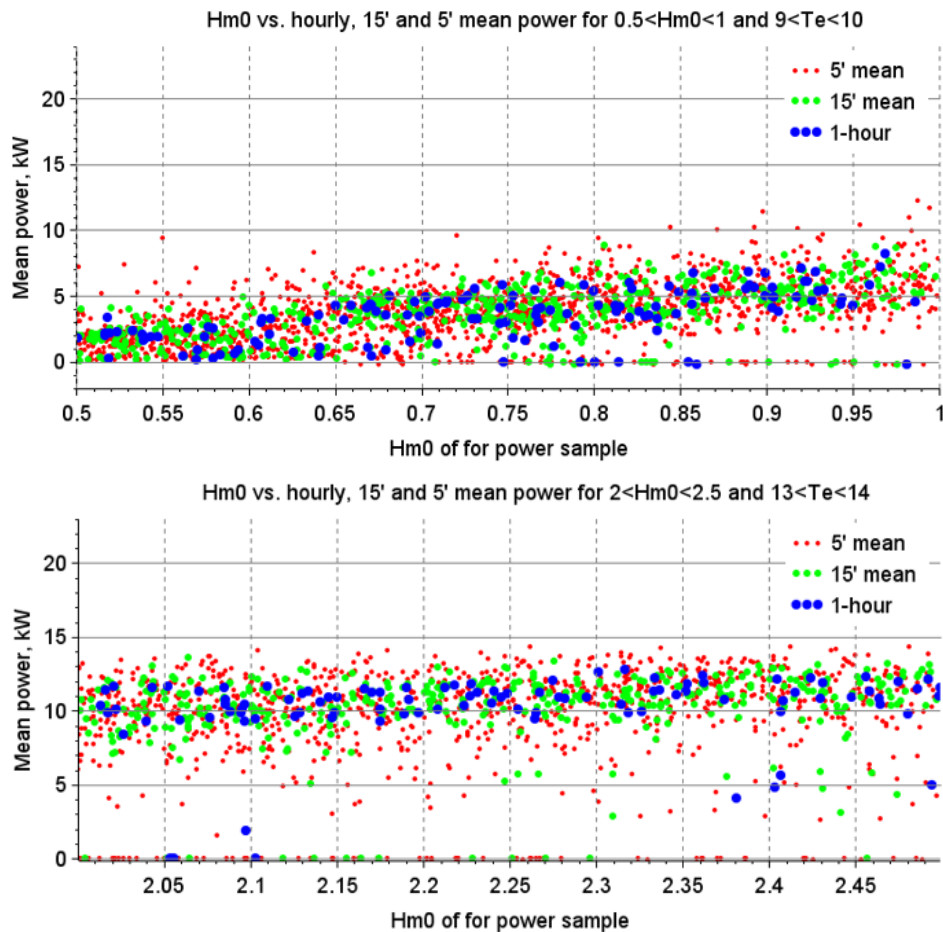


FIGURE 47: EFFECT OF CHANGE IN HM0 ACROSS ONE CELL ON TURBINE 13 OUTPUT

risks from a near-zero to slightly above 5 kW. The effect is not significant for the storm cell. A stronger effect may have been expected for the low wave heights of the mean regime cell, since the relative change in H_{m0} , and hence in the energy flux, across the cell is much higher there.

The strong impact of H_{m0} for small wave height suggests that the standard half a meter resolution in the power matrix is insufficient for low wave heights for the Mutriku data. Possibly this is the case for many shoreline devices, and possibly also for floating WECs. Edition 1 of IEC-TS/62600-100 does not require that low wave height cells have higher resolution in H_{m0} than other cells. It may be worth consideration, though, again, TS100 excludes shoreline devices from its scope.

Correlation of power output for the storm and mean regime cell with other readily available parameters for each sample was also investigated. It is found that output at low wave heights correlates positively and significantly with $H_{1/10}$, the mean of the highest 10% of the waves (not shown). No strong influence of the energy period of samples is found. However, and somewhat surprisingly since energy period has little influence, the mean zero-upcrossing period may also predict some of the variability within cells at large H_{m0} (Figure 48), though the correlation is less within cells of small wave heights.

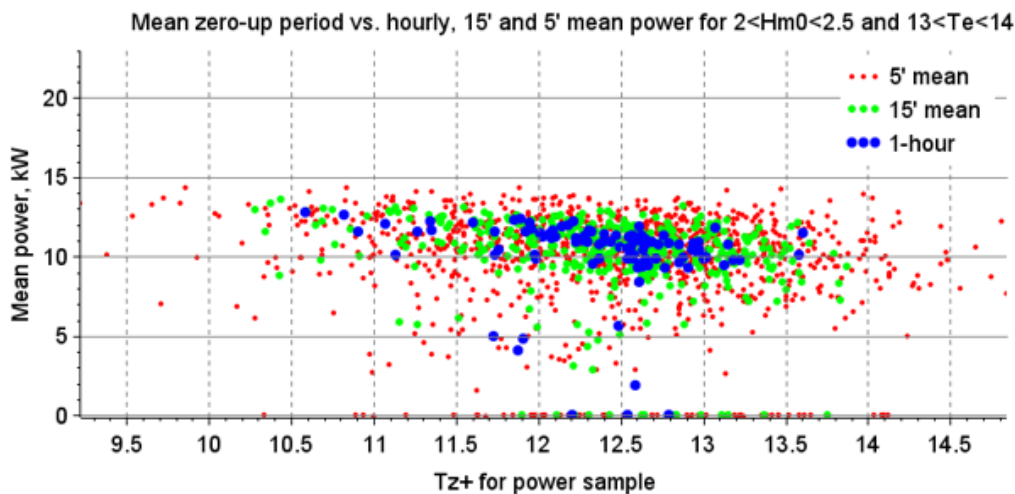


FIGURE 48: CORRELATION OF MEAN POWER TO ZERO-UPCROSSING PERIOD WITHIN THE STORM CELL

4.11.3 CAPTURE LENGTH MATRIX AND REDUCTION IN INTRA-CELL VARIABILITY

It was shown above that some of the large scatter in output within cells of the power matrix appears related to slight changes in wave statistics across cells. In the capture width matrix, the variation of the energy flux across a cell is accounted for by dividing mean power by the energy flux calculated for the significant wave height and energy period for each sample. (Note that to obtain this reduction in dispersion the energy flux must be calculated with the wave statistics of each sample rather than using a single average value of the energy flux for all the sample that fall in a cell).

As briefly discussed earlier, one difficulty in calculating capture width at Mutriku is assigning the correct value of the energy flux. The deepwater approximation is not applicable. Assuming linear shallow water waves, another simple formula for the energy flux can be obtained for the water column above the wave measuring instrument. However, even assuming rays straight from the sensor to the chamber, the energy flux at the chamber entrance must be calculated with a lower depth, slower group velocity, and possibly different wave height. Also, the linear approximation is problematic in front of the plant due to the wave height becoming of the same order as the water depth.

There are thus a few complications that must be addressed in calculating the capture width for a shoreline device. A rigorous analysis of the potential benefits of using a capture width matrix instead of a power matrix in power assessment would involve deriving an acceptably accurate form for the energy flux.

It may be however that normalising sample mean power by approximate formula of the energy flux may also be useful to reduce scatter in measurements. More generally, other operations using other wavefield variables unrelated to the energy flux may also be useful to reduce intra-cell dispersion. The energy flux has the desirable property that it also makes

physical sense to divide power output by it. But if any operation on the measured power reduces sampling variability, thus providing better estimates of mean power for each cell and of annual energy production from a given testing period, it would still be interesting even if does not make physical sense. The benefits in terms of accuracy of the yield prediction is the same. What is important for this to be used is that the variables which operate on the mean power can be accurately for each sample, and that they be available in long time series to be used for annual energy production calculation. The method used would be the same as for the real capture length matrix, both to calculate mean values for each cell and to predict yield.

To see if such benefits in reduced intra-cell scatter and more accurate mean estimation could be obtained with other normalisations than that of the capture length matrix, mean power for each sample was normalised by various formula including:

- $H_{m0}^2 T_e$ for each sample, which mimics the formula for energy flux in the deepwater limit
- $\sqrt{D} H_{m0}^2$, which mimics the formula for energy flux of shallow water waves, where D is a representative water depth obtained from the mean water level during the sample
- various combinations of dividing sample mean power by H_{m0} , H_{m0}^2 or H_{m0}^2/T_e as well as time-domain variables such as $H_{1/10}$, T_{zup} and mean period of highest one third of waves.

It was found that none of them significantly changed the mean of the sample variability across the entire power matrix, but that one certain ranges of cells the difference could be important. One of them, the shallow water energy flux approximation, was found to significantly increase variability.

As illustration Table 28 shows the mean values found when dividing sample mean power by $H_{m0}^2 T_e$, and the ratio of sample standard deviation to that in the corresponding cell of the power matrix, normalised to the mean value in each cell is shown in Table 29. Table 28 is thus a form of the capture length matrix. Obviously the deepwater energy flux is not applicable at Mutriku but it doesn't matter when the objective is reduction in sample variability. Both tables are for the five-minute samples are shown for illustration. The dispersion is quite similar between the power matrix data and that of the capture length data approximated in this way, with many cells having ratios close to one in Table 29. However, for lower wave heights except for very short energy periods, there is reduction of about 15% and up to 30% in sample variability. The average of change for all cells (not accounting for frequency of occurrence or contribution to annual energy production) is negligible (+2%). It may be that this is still a useful method to reduce variance for those cells that matter most to power production, depending on the details of the site and WEC characteristics. Similar behaviour is observed for the various matrices obtained with the various proxies listed above, except for the shallow water energy flux, where variability increases significantly.

TABLE 28: TURBINE 13 OUTPUT NORMALISED BY DEEPWATER ENERGY FLUX (5-MINUTE SAMPLES)

Hs (top of bin)	>5.5																		
	5.5																		
	5																		
	4.5																		
	4										0.1	0.1							
	3.5									0.2	0.2	0.1	0.1	0.1					
	3									0.3	0.2	0.2	0.2	0.2	0.1	0.1			
	2.5						0.7			0.6	0.4	0.3	0.3	0.3	0.2	0.2	0.1	0.1	
	2				1.2	1.0		0.7	0.7	0.6	0.5	0.4	0.4	0.4	0.3	0.2		0.2	
	1.5				1.9	1.3		1.0	1.0	0.9	0.7	0.6	0.5	0.5	0.4	0.3		0.3	0.2
1				0.8	1.3	1.5	1.4	1.2	1.0	0.7	0.6	0.5	0.6	0.4	0.4				
0.5			0.1	0.4	0.7	1.0	0.9	1.0	1.0	0.7	0.6	0.4	0.2						
		<4	5	6	7	8	9	10	11	12	13	14	15	16	17	18	19	20	>20
		Te (top of bin)																	

TABLE 29: RATIO OF STANDARD DEVIATION TO THAT IN POWER MATRIX CELLS, 5-MINUTE SAMPLES

Hs (top of bin)	>5.5													1.00	1.00				1.00
	5.5													1.00	1.00				1.00
	5												1.00	1.00	1.01	1.00	.99		1.00
	4.5												1.00	1.00	1.00	1.00	.92		.99
	4												1.05	1.00	1.01	1.01	.99		1.01
	3.5										1.19		1.02	1.02	1.02	1.02	1.00	1.10	1.05
	3									1.02	1.03	1.04	1.03	1.02	1.03	1.11	1.19		1.06
	2.5					.83				1.07	1.04	1.04	1.03	1.03	1.05	1.01	.98		1.01
	2				1.37	1.16			1.07	1.03	1.07	1.04	1.06	1.02	1.07	1.01	1.07	1.88	1.15
	1.5				1.38	1.04		1.15	1.02	.98	1.02	1.02	1.04	.96	.97	1.28	1.60		1.12
	1				1.03	.62	.80	.93	.84	.83	.80	.78	.72	.72	.67	1.18			.83
	0.5				1.38	1.34	1.19	.88	.88	.92	.86	.89	.96	.92	.76	.80			.98
		<4	5	6	7	8	9	10	11	12	13	14	15	16	17	18	19	20	>20
		Te (top of bin)																	

In summary, the definition of the capture length matrix for Mutriku would require more advanced analysis. Normalising sample mean power by various sea-state variables associated with each sample indicate that intra-cell sampling variability may be somewhat reduced at low wave height, relative to the power matrix. The reduction, if any, would not be sufficient to explain the very high intra-cell variability observed, but may have some advantages in terms of more accurate mean yield prediction, depending on the details of a site wave climate and WEC response.

4.11.4 EXAMPLE OF DETAIL OF INTRA-CELL VARIABILITY

As illustration of a high intra-cell difference in power output, two time series of 5-minute samples of WEC operating data and incoming wave field at the pressure sensor is shown for the “storm cell”, one of the largest contributors to mean annual energy production. These two samples are characterised by very different mean power despite being in the same (H_s, T_e) cell. Relevant sample data are summarised in the table below, where J is the deepwater energy flux that would correspond to the significant wave height and energy period, and T13 is the mean power output for Turbine 13 during the sample.

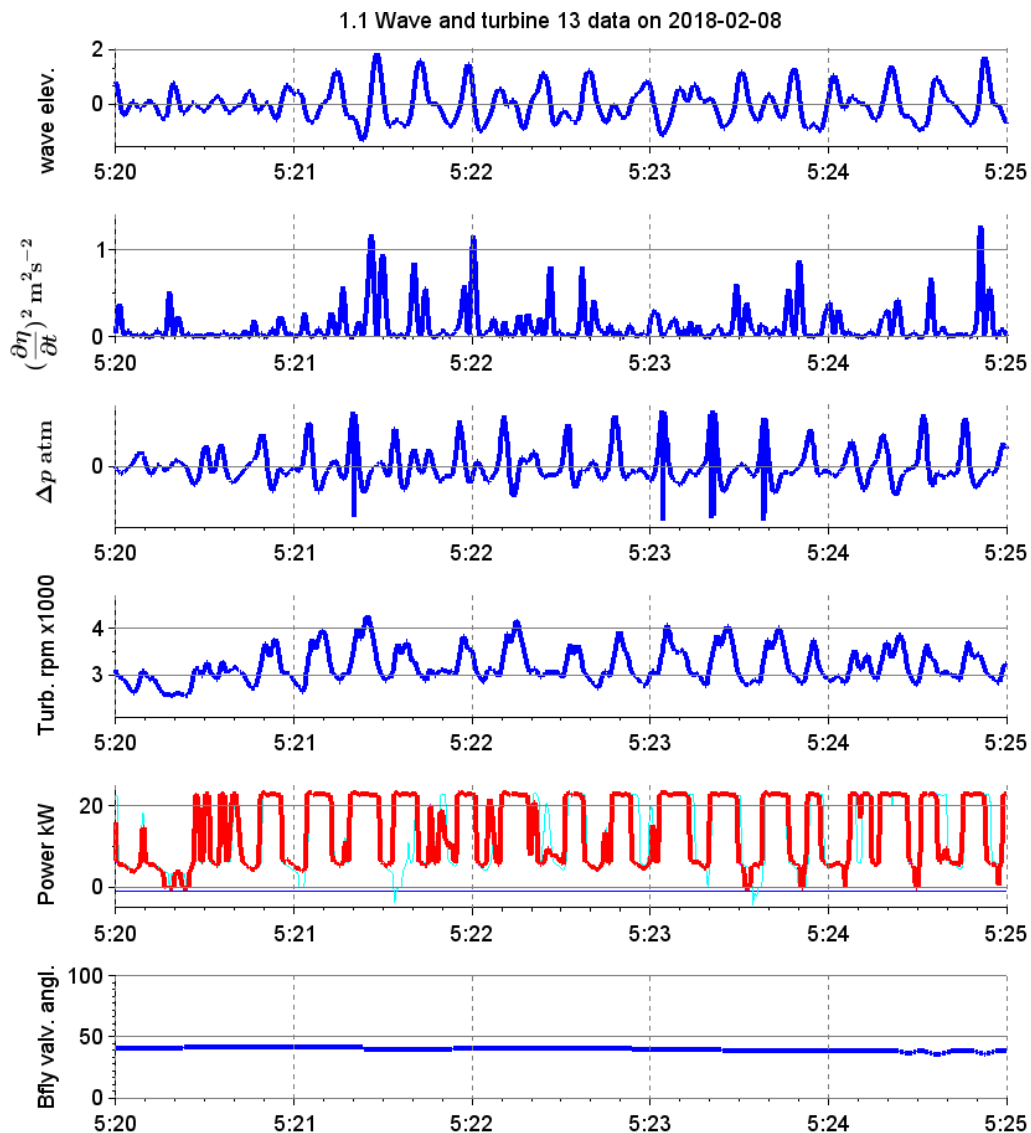


FIGURE 49: WAVE AND PLANT DATA FOR ENERGETIC STORM CELL SAMPLE

	Date			Begin	End	Hm0	Te	J	T13
Energetic sample	2018	2	8	5:20	5:25	2.44	13.95	40.70	14.08
Low energy sample	2018	2	8	16:00	16:05	2.11	13.27	29.04	7.45

While both samples fall in the same cell of the scatter diagram or power matrix, the energy flux in deepwater would be some 30% less in the lower sample. Assuming the energy flux at Mutriku is proportional to H_{m0}^2 , as in the shallow water approximation, it would also be 25% lower. Energy production is slightly over half of that of the other sample.

Time series of wave and plant data are shown for the energetic sample are shown in Figure 49 and that for the low energy sample in Figure 50. The turbine power response amplifies the difference in the incoming wavefield (second panel from the bottom, red is Turbine 13 and thin blue and cyan lines are Turbines 7 and 15). In the energetic sea-state it must be cropped

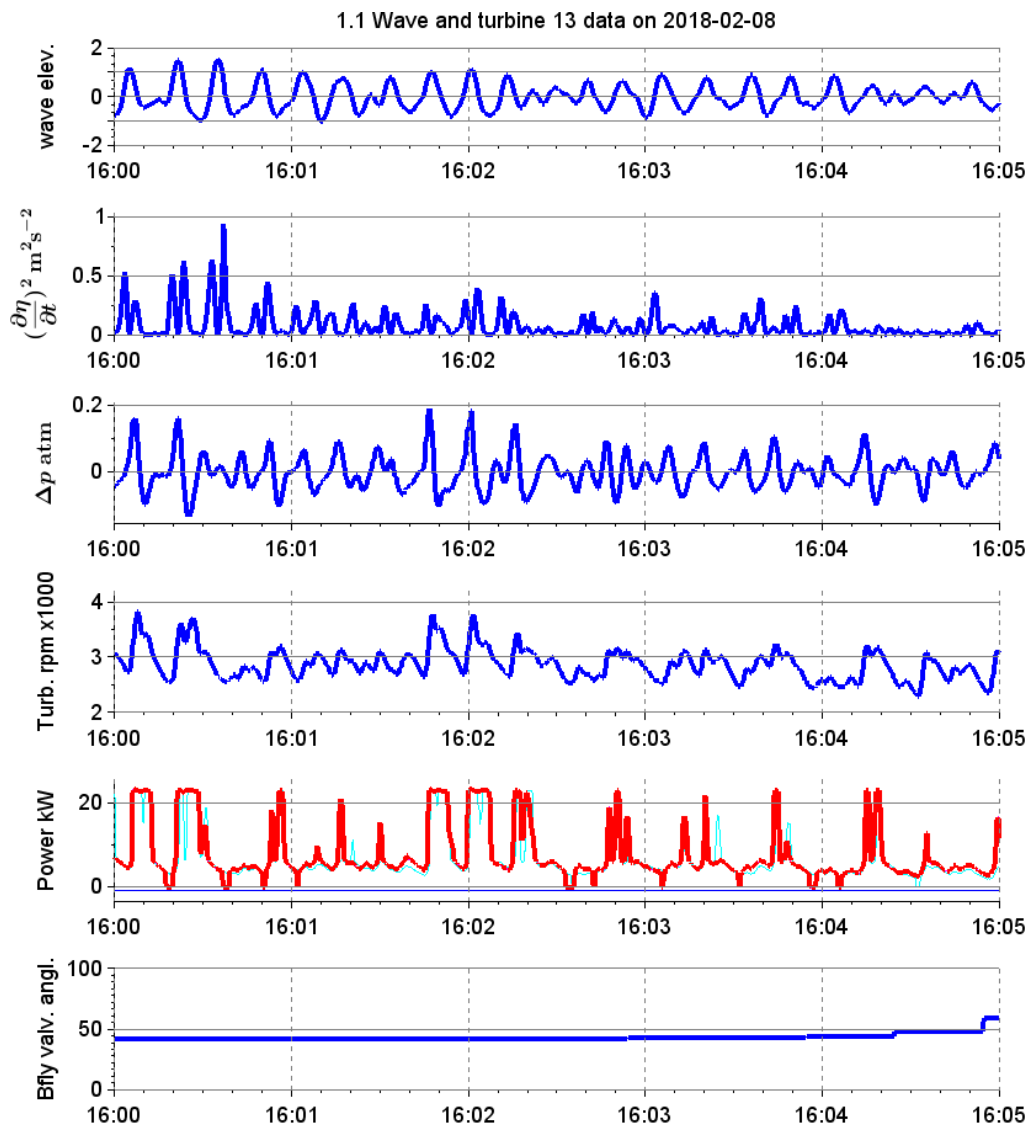


FIGURE 50: WAVE AND PLANT DATA FOR LOW ENERGY STORM CELL SAMPLE

at 23 kW (for a nominal capacity of 18.5 kW) for nearly half of the time. For the low energy sample, Turbine 13 output also reaches this maximum value some of time, but for a much lesser part of the sample duration.

These two examples show that some of the intra-cell variance is readily explained by the variation in wave statistics across cell. This type of scatter may be reduced by using a capture length matrix, or with one of the methods outlined in the previous section. Over half of difference in output between the two samples may be simply proportional to the difference in the energy flux. The remaining difference may be related to details of the plant response, control, or possibly to limitations in the measurement of the incoming wavefield. For example, longshore variability, or small changes in direction, may contribute to some of the intra-cell standard deviation.

4.12 SUMMARY AND PRACTICAL IMPLICATIONS

The results of analysing the data for winter, spring and summer 2018 from EVE's wave power plant at Mutriku compel further investigating the potential value of conducting certain power assessments with sample duration shorter than the minimum of twenty minutes currently required in IEC-TS/62600-100. There are several potential advantages that may be expected from this approach:

1. Reduced test-time thanks to faster convergence to final values of power matrix cells, since number of samples per hour of testing is up to four times higher. However, this is subject to certain conditions such as independence of short samples, which appear to be important for this dataset.
2. Reduced standard deviation on the estimate of the mean (or reduced rms error in the values of the power matrix), again subject to conditions of independence of samples.
3. Better coverage of the (H_s, T_e) space in the power matrix, because the short-term statistics change faster, and have more pronounced extremes, as is expected for samples that average a lesser number of waves.

Of these three potential benefits, it is found that that third one, on larger coverage of the (H_s, T_e) space, appears to be the most robust. In addition, it can easily be implemented in post-processing existing datasets of testing at sea.

4.12.1 ISSUES OF POTENTIAL INTEREST TO THE IEC GROUP OF EXPERTS

IEC-TS/62600-100 and IEC-TS/62600-102 are some of the IEC technical specifications where the results presented are of potential interest. An important caveat on the relevance of these results is that neither of these technical specifications cover the case of shoreline device, which is what most of this analysis as focused on. Bearing in mind this limitation, some of the following issues are worth mentioning.

It may be of interest to the sector that future editions of TS100 and TS-102 provide a unified framework for using short samples to populate a larger range of the power matrix. It was shown that short sampling may be particularly useful to better predict yield at a second location where the scatter diagram is significantly different from that of the test-site. However, it was found that particular care is necessary to obtain meaningful wave statistics beyond 15 minutes resolution. These include sufficiently small frequency interval to reduce bias on the energy period, which may necessitate reducing the number of degrees of freedom of the spectral analysis. Another important caveat is the higher correlation between successive short samples than for longer samples.

For this shoreline device, it was found that the 0.5 m resolution in significant wave height (H_s) is insufficient at low wave height. This is because incoming wave energy increase manifold between the low H_s side and high H_s side of the same cell. Despite the low hourly energy production, due to their high frequency of occurrence these cells contribute significantly to annual energy production. Reducing bias there by increasing the resolution in wave height may thus be beneficial for more accurate yield prediction.

Results suggest intra-cell standard deviation may be reduced appreciably in certain cells by using, rather than a power matrix, a capture width matrix or similar matrices where each sample mean power is normalised or operated upon by various wave statistics pertaining to this sample. A representative energy flux is more difficult to define for this shoreline device than in the deepwater. But simple operations such as normalising by the deepwater energy flux appear to reduce intra-cell variance by some 10-30% at low wave heights.

4.12.2 SUMMARY FOR WEC DEVELOPERS

As far as practical applications of these results for WEC developers, two particular situations can be thought of where the results presented may be used. The first is the case where open-sea testing is over, or largely underway; the second is for a case where open-sea testing is still at the planning stage.

4.12.2.1 APPLICATION TO EXISTING DATASETS OF POWER PERFORMANCE

In this first case, no change is required to the experimental setup and data collection protocol. It is essentially adding short-sample analysis to the post-processing of the open-sea testing data, in complement to standard 20-minute or longer sample analysis.

It is required, however, that wave and plant data are available that contain the original data allowing for shorter sampling. This is expected to be almost always the case for plant operating data. For wave instrument data also, it is usually the case nowadays that raw measurements of pressure, acceleration, or GPS data is registered at 2 Hz someplace onboard, though it usually isn't transmitted in real time. The short-sample analysis may then be used as a complement to the standard analysis in the post-processing.

A particular interest could be the possibility to obtain performance data on (H_s, T_e) combinations that occur too infrequently in the hourly or 20-minute statistics, but that, as was seen in previous sections, may occur more frequently in the 10- or 5-minutes statistics. This could be interesting, for example, when evaluating power production at a second location based on testing at a first location. Some (H_s, T_e) that occur infrequently at the test site may be important contributors to the annual energy flux at the second location. In this case the short-sample statistics may provide some performance data for these cells, to complement or replace interpolation or modelling results.

A second area of interest would be when adding dimensions to the power matrix in the post-processing. For example, considering the effect of spectral shape, tides, etc. The more dimensions are added to the power matrix, the more the number of samples per cell will decrease. To have meaningful averages in each cell, short-sample analysis may prove particularly useful when exploring WEC performance across added dimensions to the power matrix.

A third potential use in post-processing would be when comparing the performance of control strategies. Again, short samples will cover a wider range of the (H_s, T_e) plane, and this can be done in a shorter testing period than with longer samples. A comparison over a larger variety of sea conditions may thus be possible. In this and other applications it is important to consider the issue of independence of measurements, which may require a minimum time-spacing between short samples (see Section 4.8).

4.12.2.2 APPLICATION AT THE PLANNING STAGE OF OPEN-SEA TESTING

It was shown that to obtain faster convergence of means when using samples shorter than twenty minutes, it is important to decorrelate successive samples by requiring that they be spaced in time. One hour appeared to be sufficient with the data analysed here, shorter separations may be possible. However, results suggest that other problems may arise such as larger errors in final estimates. A likely reason this is the reduction in number of samples, which makes the problem of higher sampling variability for short samples more severe, in terms of rms error on the mean. In this case, this may be resolved in a testing period longer than the few months of data available to this analysis. Despite these issues that need further investigation, and, above all, more open-sea operating data, it is worth reporting the possibility that further benefits may be available to developers who will consider short-sampling at the planning stage for open-sea testing of various WEC configurations.

Sufficient separation of successive short samples will be easily achieved when, for example, testing various control strategies. In OPERA, seven control strategies were tested at EVE's wave power plant in Mutriku. A method was successfully implemented so they can be remotely or automatically switched via the Internet, as detailed in e.g., [17]. It should thus have little additional cost or complication to cycle through these seven strategies in short implementations of five minutes each, instead of twenty minutes or one hour each. This would provide for the necessary separation of short samples. Another potential advantage is that different control strategies would be compared on sea conditions that are more similar, including in ways that are not apparent when looking at only (H_s, T_e) , such as spectral shape, tides, currents, etc. (This may result, however, in higher correlation between successive samples).

The chief advantage, however, would be an up to 75% reduction in the testing time necessary to compare the performance of the various control strategies, using five minutes samples

instead of twenty minutes samples. This could have important implications both for reducing the cost of testing and for accelerating the improvements to WEC controls and power performance in general.

However, the analysis identifies a number of potential caveats in using short samples of power performance, including: obtention of meaningful estimates of the energy period, increase in sampling variability, and independence of samples. The previous sections present some methods to account for these issues, that appear to work for this particular dataset, in that differences in annual yield prediction using five-minute or one-hour samples are of the same order as those obtained with various standard sample durations (hourly, half-hourly, three-hourly).

5. YIELD PREDICTION FOR SCALED PROTOTYPES FROM OPEN-SEA TESTING

In this section, general comments are provided on scaling power performance from an open-sea testing of a prototype device to a commercial device at a different location which may involve device scaling to adapt to the commercial site scatter diagram. The OPERA project did not produce open-sea test data or numerical modelling which can be used to generate comments on this topic. Therefore, all information provided in this section is based on experience in the OPERA team from OPERA project or previous WEC development activities. This may be used in the development of TS102 where device scaling is not described.

In the development path of a WEC design, scaled physical testing using the Froude scaling methods is generally used on the device main design parameters. This method was proven accurate, especially using relatively small scaling factors, which is the case between a prototype and a commercial device. There are however several aspects of scaling to be considered as they can affect the device power performance and energy yield:

- **Froude scaling limitations**

There are device specific parameters which cannot be scaled using Froude scaling, such as air compressibility and viscous forces. In OWC devices such as the MARMOK-A-5 and the Mutriku wave power plant, turbine design and air compressibility cannot be scaled with this method. Air compressibility influences the air flow through the air turbine and can influence the power performance and/or the optimal turbine control strategy.

When a parameter cannot be scaled using the Froude scaling method, additional numerical modelling is required.

- **Structural design**

The detail design at the commercial scale cannot be directly derived from the prototype design using Froude scaling, which only provides the device general dimensions and weights required at each scale considered. It is important to ensure the structural integrity of the device, its stiffness and fulfil all Froude scaling requirements. Deviations may introduce variations in the device performance.

- **Control system**

The detail design at the commercial scale cannot be directly derived from the prototype design using Froude scaling, which only provides the device general dimensions and weights required at each scale considered. The control and automation system may not need any modifications. This does not affect the device operation and performance but does not follow the Froude

scaling requirements. While it can be an issue for large scaling factors, it may not have any impact on small scaling factors as dealt with in this section.

- **Electrical PTO**

The electrical PTO needs to be fully designed for the new scale in order to guarantee similar power performances. In some cases, with small scaling factors, the same electrical PTO can be used but its efficiency is most likely to be reduced when the most common sea states occur.

In summary, small changes in device dimensions may be beneficial to ensure the optimised prototype design remains optimised at a commercial location. This would allow accurate prediction in energy yield from an open sea scaled prototype. However, scaling requirements are difficult to fulfil, and a substantial amount of work is needed. Guidelines to carry out this work would be beneficial in TS100.

6. REFERENCES

- [1] International Electrotechnical Commission (IEC), IEC-TS62600-102: Marine Energy - Wave, tidal and other water current converters - Part 102: Wave Energy converter power performance assessment at a second location using measured assessment data. Edition 1.0, 2016-08, 2016.
- [2] International Electrotechnical Commission (IEC) , IEC-TS62600-100: Marine Energy - Wave, tidal and other water current converters - Part 100: Electricity producing wave energy converters - Power performance Assessment. Edition 1.0, 2012-08, Geneva: IEC, 2012.
- [3] M. Ojanguren and J. L. Aguiriano, "MARMOK-A-5 Brief Description," Oceantec, 2016.
- [4] International Electrotechnical Commission (IEC), IEC-TS62600-101: Marine Energy - Wave, tidal and other water current converters - Part 101: Wave energy resource assessment and characterization. Edition 1.0, 2012-08, 2015.
- [5] Esgemar, S. A., Campaña de Sísmica de Reflexión en El Área de BiMEP, Arminza (Vizcaya) - Informe de resultados, 2017.
- [6] EMEC, *Wave Test Site*, Orkney, 2014.
- [7] D. Mollison, "Wave climate and the wave power resource," in *Hydrodynamics of Ocean-Wave Energy Utilization, Proceedings of the IUTAM Symposium*, Lisbon, Portugal, 1985.
- [8] D. Woolf, "Sensitivity of power output to wave spectral distribution," Seapower Ltd., 2002.
- [9] M. S. Longuet-Higgins, "The statistical analysis of a random moving surface.," *Phil. Trans. R. Soc. Lond. A* 249, pp. 321-387, 1957.
- [10] D. E. Cartwright and M. S. Longuet-Higgins, "The statistical distribution of the maxima of a random function," *Phil. Trans. R. Soc. Lond. A* 237, pp. 212-232, 1956.



- [11] J.-B. Saulnier, A. Clement, A. F. O. Falcao, T. Pontes, M. Prevosto and P. Ricci, “Wave groupiness and spectral bandwidth as relevant parameters for the performance assessment of wave energy converters,” *Ocean Engineering*, pp. 130-147, 2011.
- [12] K. Doherty, “Temporal and Spectral Ocean Wave Characteristics and their Influence on WEC Performance (in Draft),” Kenneth Doherty Consultancy, 2015, 2015.
- [13] OPERA, “Tracking metrics for wave energy technology performance,” Grant Agreement No 654444, 2019.
- [14] Y. Goda, Random seas and design of maritime structures, World Scientific Publishing Company, 2010.
- [15] C. T. Bishop and M. A. Donelan, “Measuring waves with pressure transducers,” *Coastal Engineering*, vol. 11, no. 4, pp. 309-328, 1987.
- [16] C. H. Tsai, M. C. Huang, F. J. Young, Y. C. Lin and H. W. Li, “On the recovery of surface wave by pressure transfer function,” *Ocean Engineering*, vol. 32, no. 10, pp. 1247-1259, 2005.
- [17] F.-X. Faÿ, A. Pujana, P. Ruiz-Minguela, J. Kelly, M. Mueller, J. Henriques, L. Gato, A. Carrelhas, B. Lopes and E. Aldaiturriaga, “OPERA D4.2: Shoreline OWC wave power plant control algorithms,” H2020 OPERA Project Deliverable. , 2018.
- [18] I. Txarterina, “Wave by wave assessment of power production to reduce uncertainty in IEC-TS/62600-100,” Dissertation for MSc., Heriot-Watt University , Orkney, 2017.
- [19] H. U. Sverdrup and W. H. Munk, “Wind, sea and swell: theory of relations for forecasting,” US Hydrographic Office, HO Pub. 601 (1947): 1-44, 1947.
- [20] F. Thompson and C. Vincent, “Significant wave height for shallow water design,” *Journal fo Waterway, Port, Coastal and Ocean Engineering*, pp. 828-842, 1985.
- [21] J. Berque, “OPERA Technical Note: Processing of Winter-Spring 2018 pressure sensor data at Mutriku,” H2020 OPERA Project. , 2018.